Surface Modification of Ceramic Membranes with Thin-film Deposition Methods for Wastewater Treatment

Dissertation by

DANIYAL JAHANGIR

Submitted in Partial Fulfillment of the Requirements for the
Degree of
Doctor of Philosophy

King Abdullah University of Science and Technology
Thuwal, Kingdom of Saudi Arabia

November, 2017

EXAMINATION COMMITTEE PAGE

The dissertation of Daniyal Jahangir is approved by the examination committee.

Committee Chairperson: Prof. TorOve Leiknes
Committee Members: Prof. Pascal Saikaly, Prof. Zhiping Lai, Prof. Jean-Philippe Croué

ABSTRACT

Surface Modification of Ceramic Membranes with Thin-film Deposition Methods for Wastewater Treatment

Membrane fouling, which is caused by deposition/adsorption of foulants on the surface or within membrane pores, still remains a bottleneck that hampers the widespread application of membrane bioreactor (MBR) technology for wastewater treatment. Recently membrane surface modification has proved to be a useful method in water/wastewater treatment to improve the surface hydrophilicity of membranes to obtain higher water fluxes and to reduce fouling.

In this study, membrane modification was investigated by depositing a thin film of same thickness of TiO_2 on the surface of an ultrafiltration alumina membrane. Various thin-film deposition (TFD) methods were employed, i.e. electron-beam evaporation, sputter and atomic layer deposition (ALD), and a comparative study of the methods was conducted to assess fouling inhibition performance in a lab-scale anaerobic MBR (AnMBR) fed with synthetic municipal wastewater. Thorough surface characterization of all modified membranes was carried out along with clean water permeability (CWP) tests and fouling behavior by bovine serum albumin (BSA) adsorption tests. The study showed better fouling inhibition performance of all modified membranes; however the effect varied due to different surface characteristics obtained by different deposition methods. As a result, ALD-modified membrane showed a superior status in terms of surface characteristics and fouling inhibition performance in AnMBR filtration tests. Hence ALD was determined to be the best TFD method for alumina membrane surface modification for this study.

ALD-modified membranes were further characterized to determine an optimum thickness of TiO_2-film by applying different ALD cycles. ALD treatment significantly improved the surface hydrophilicity of the unmodified membrane. Also ALD-TiO_2 modification was observed to reduce the surface roughness of original alumina membrane, which in turn enhanced the anti-fouling properties of modified membranes.

Finally, a same thickness of ALD-TiO_2 and ALD-SnO_2 modified membranes were tested for alginate fouling inhibition performance in a dead-end constant-pressure filtration system. This is the first report on the application of SnO_2-modified ceramic

membrane for testing its alginate fouling potential; which was determined to be nearly-same for both modified membranes with a negligible amount of difference. This revealed SnO_2 as a potential future anti-foulant to be tested for membrane modification/fabrication for application in water/wastewater treatment systems.

Keywords: Surface modification; Ceramic membrane; Thin-film deposition; Atomic layer deposition; TiO_2; SnO_2; Anaerobic MBR; Membrane fouling.

ACKNOWLEDGEMENTS

I owe a great many thanks to many people who helped and supported me during the writing of this doctoral thesis report.

Firstly, I would like to record deepest thanks to my supervisor, Prof. TorOve Leiknes, for his supervision, advice, and guidance from the very early-stage of this research as well as giving me extraordinary experiences throughout the work. Above all and the most needed, he provided me unflinching encouragement and support in various ways. His truly scientific intuition has made him as a constant oasis of ideas and passion in research domain, which exceptionally inspires and enriches my growth as a student and a researcher. His involvement with discussions and suggestions has triggered and nourished my intellectual maturity.

I express my profound gratitude to the King Abdullah University of Science and Technology (KAUST), for the award of PhD Scholarship. This opportunity enabled me to pursue my higher education in a technological challenging atmosphere of a reputed university of Saudi Arabia. The professional management of this scholarship program was a great source of motivation for me to do research in a stimulating yet conducive environment. The efforts made by KAUST helped me in expanding my frontiers of knowledge to the next level.

I would also make use of this opportunity to say thanks to my PhD committee members, Prof. Pascal Saikaly, Prof. Zhiping Lai and Prof. Jean-Philippe Croué for their advice and sincere support. It really helped me out to accomplish this task.

Last but not the least; I would also thank all fellows in my research group and in Water Desalination and Reuse Center (WDRC) - KAUST, as without their sincere support this thesis would have been a distant reality. I also extend my heartfelt thanks to my family, friends and well-wishers.

Daniyal Jahangir
KAUST ID: 130964

TABLE OF CONTENTS

LIST OF ABBREVIATIONS

AFM	Atomic Force Microscopy
ALD	Atomic Layer Deposition
AnMBR	Anaerobic Membrane Bioreactor
AS	Activated Sludge
BF	Biofilm
BSA	Bovine Serum Albumin
CAPEX	Capital Expenditures
CFV	Cross-Flow Velocity
CIP	Clean-In-Place
COD	Chemical Oxygen Demand
CVD	Chemical Vapor Deposition
CWP	Clean Water Permeability
DOC	Dissolved Organic Carbon
EDS	Energy Dispersive Spectroscopy
EPS	Extracellular Polymeric Substances
HRT	Hydraulic Retention Time
KAUST	King Abdullah University of Science and Technology
MBE	Molecular Beam Epitaxy
MBR	Membrane Bioreactor
MF	Microfiltration
MLSS	Mixed Liquor Suspended Solids
MWCO	Molecular Weight Cut-off
NF	Nanofiltration
OLR	Organic Loading Rate
OPEX	Operating Expenses
PAC	Powdered Activated Carbon
PE	Polyethylene
PLD	Pulsed Laser Deposition
PSD	Particle Size Distribution
PVD	Physical Vapor Deposition
PVDF	Polyvinylidine Fluoride
RO	Reverse Osmosis
SEM	Scanning Electron Microscopy
SRT	Solids Retention Time
TEM	Transmission Electron Microscopy
TFC	Thin-Film Composite
TFD	Thin-Film Deposition
TMP	Trans-membrane Pressure
TOC	Total Organic Carbon
TSS	Total Suspended Solids
UF	Ultrafiltration

LIST OF FIGURES

LIST OF TABLES

This dissertation is dedicated to my parents, teachers & friends for their endless and unparalleled support and encouragement.

CHAPTER: 1
INTRODUCTION

1.1 Background of the study

Around 1.1 billion people worldwide face water shortfall and scarcity. It is highly critical that increased use of water by humans does not only reduce the water availability for drinking purposes, industrial and agricultural development but has a profound effect on aquatic ecosystems. The population growth coupled with urbanization and industrialization has resulted in an increasing demand for water as well as serious consequences on the environment. Additionally, the water stress regions have imbalance between water resources and its use which have been known as a major risk to the global economy. However, with the current state of affairs, corrective measures still can be taken to avoid the crises to worsen. One way to overcome this paucity and efficiently use the limited water resources is treatment of wastewater produced due to rapid global urbanization. Wastewater treatment for reclamation and reuse has gained considerable attention in recent years, with research continually increasing towards new advanced wastewater treatment processes [1].

With the current need for more efficient and reliable processes for wastewater treatment, membrane bioreactors (MBR) technology has gained considerable attention. MBRs are now considered an established wastewater treatment process, competing directly with the conventional processes such as activated sludge systems. MBRs represent a promising technology as biomass is separated from the treated water by filtration through a membrane which eliminates the operational and ecological issues associated with conventional processes. Also, no sedimentation is required hence reducing the footprint [2]. However, keeping in view the high operational cost associated with aerobic MBRs due to aeration, anaerobic membrane bioreactors (AnMBRs) have now gained remarkable interest in both research and commercial community.

AnMBR technology combines the advantages of anaerobic processes and membrane technology, among which the most cited are; excellent effluent quality, smaller footprint, biomass retention, low sludge production and net energy production [3, 4]. Due to these advantages AnMBR is evolving as one of the most important new systems for advanced wastewater treatment. AnMBRs have mostly been used for treatment of industrial wastewaters but there is a growing interest to also use the technology for municipal wastewater. Moreover, most of the membrane modules in AnMBRs are based on microfiltration (MF) or ultrafiltration (UF) membranes having the configuration of flat sheet, hollow fiber or tubular systems. Additionally, the membrane materials such as polymers, ceramics and metals used for AnMBRs have their own merits and demerits. Recently ceramic membranes are gaining attention and preferred owing to their unique characteristics such as high resistance to abrasion, corrosion, concentration polarization and fouling as they can be backwashed/cleaned effectively [5].

Use of ceramic membranes instead of polymeric membranes for wastewater treatment applications is growing as they are easy to clean, can have lower fouling rates and greater life span as compared to polymeric membranes. Moreover, application of ceramic membranes can reduce the number of pre-treatment steps involved in the water/wastewater treatment processes. Hence, the global water scarcity problem has resulted in increased demand of ceramic membranes for separation purposes, among which 55% accounts for (waste)water treatment applications. The market size of ceramic membranes is expected to reach around $5.1 billion by 2020 [6]. However, researchers are still continuously making more efforts to produce highly efficient ceramic membranes for water/wastewater treatment applications.

1.2 Problem statement

The deposition or adsorption of foulant materials on the surface or within membrane pores, is known as membrane fouling, which still remains one of the bottlenecks that hamper the widespread application of MBR technology for wastewater treatment. Membrane fouling eventually leads to flux decline, high energy consumption and shorter life span of the membrane that results in reduced process efficiency and an overall increase in operational cost. Moreover, due to the complex nature of the foulants and diversity of operational conditions, membrane materials and wastewater strength / compositions in different investigations, the membrane fouling phenomena in AnMBRs is not yet been fully understood. Recently, membrane surface modification has proved to be a useful method in water/wastewater treatment processes to improve the surface hydrophilicity of membranes to obtain higher water fluxes and to reduce fouling. The basic objective of this study was to modify the surface of ultrafiltration (UF) alumina membranes by TiO_2 employing various thin-film deposition (TFD) methods to conduct a comparative study of the anti-fouling performance of the modified membranes in a lab scale AnMBR filtration system.

1.3 Motivation statement

Several methods have been previously reported on applying surface modification of membranes in order to enhance their performance in water/wastewater treatment systems. Some of these methods include: dip coating, spin coating, spray coating, interfacial polymerization, plasma polymerization, grafting etc. However, there are few reports on detailed studies of applying different thin-film deposition methods (e.g. sputter, e-beam evaporation, pulsed laser deposition, atomic layer deposition

etc.) for membrane surface modification for use in water/wastewater treatment systems. The motivation for this study, Surface Modification of Ceramic Membranes By Thin-film Deposition Methods for Wastewater Treatment, was therefore to determine the surface features and respective filtration performance of modified membranes using different thin-film deposition methods.

1.4 Research questions

Based on a literature survey, the following research questions where formulated:

Question 1: Which would be the preferred TFD method for membrane surface modification of a ceramic (alumina) membrane for lab-scale AnMBR filtration?

Question 2: Using the chosen preferred TFD method, which significant characteristics/features of the thin-film need to be measured and optimized for application in AnMBR filtration?

Question 3: Can alternative metal-oxides be used for surface modification of alumina substrate using the chosen TFD method to obtained improved desired surface features?

1.5 Hypothesis

Based on the literature survey and research questions formulated, the following hypotheses are proposed to be verified / tested in this PhD research:

1. Surface modification of an alumina membrane with TiO_2 employing various TFD methods will increase the membrane surface hydrophilicity.

2. A more hydrophilic and less rough surface compared to an unmodified alumina membrane will result in less adhesion/adsorption of a model protein foulant, i.e. bovine serum albumin (BSA).
3. Different surface characteristics of the modified membrane can be observed as a function of the different TFD method applied.
4. Based on literature survey, the atomic layer deposition (ALD) method is expected to be the preferred method for surface modification of alumina membranes.
5. Surface modification of alumina membranes will show different anti-fouling potentials when alternative metal-oxides are applied in the thin-film layer.

1.6 Research phases

To address all the research questions and to verify the hypotheses, this PhD research was conducted in the following three phases:

1. Surface modification of alumina membrane with different thin-film deposition methods and application in AnMBR for fouling control

In the first phase of this study, a UF alumina membrane surface was modified by coating a thin layer of TiO_2 using different thin-film deposition (TFD) methods to improve the fouling inhibition features of the membrane. For water treatment applications, TiO_2 is a well-known membrane surface coating material to increase its hydrophilicity [7]. Hence, thin-film of same thickness of TiO_2 was deposited over the alumina membrane surfaces via atomic layer deposition (ALD), sputter and electron-beam (e-beam) physical vapor deposition methods. Basic objective of this phase was to characterize the surface characteristics (hydrophilicity, roughness etc.) and to conduct a comparative study of fouling inhibition performance of all these modified

membranes in a lab-scale AnMBR for wastewater treatment. Thorough surface characterization such as water contact angle measurement, atomic force microscopy (AFM), scanning electron microscopy (SEM), energy dispersive spectroscopy (EDS) along with clean water permeability (CWP) and bovine serum albumin (BSA) adsorption tests were conducted for unmodified and all modified membranes. The comparative analysis of all the membranes modified with different TFD methods resulted in a better performance of the membrane modified by ALD method, which was chosen as the preferred method and later used to compare the fouling inhibition potential of modified membranes in filtration tests.

2. Surface modification of alumina membranes with different ALD-TiO_2 cycles for fouling control in AnMBR system

In the second phase of this PhD research, only ALD was used for surface modification of the alumina membrane with a TiO_2 thin film. In this phase, different thicknesses of ALD-TiO_2 film were coated over the alumina membrane and various surface properties of ALD-modified membranes were characterized, including thin-film thickness measurement, surface hydrophilicity and roughness. Basic objective of this research was to conduct a comparative study of fouling inhibition performance between ALD-modified and unmodified alumina membranes in the lab-scale AnMBR filtration test. In order to determine the potential of these membranes, effect of ALD-TiO_2 cycles on membrane surface hydrophilicity, surface roughness, BSA adsorption, CWP and EPS was studied.

3. Comparative study of alginate fouling inhibition potential of alumina membrane modified with ALD-TiO_2 and ALD-SnO_2

In the third and last phase of this study, the alumina membrane surface was modified with an alternate metal-oxide (*i.e.* SnO_2) using the chosen ALD method and compared with ALD-TiO_2 to test their respective fouling inhibition potential for alginate filtration in a dead-end constant-pressure filtration set-up. As alginate is reported a major foulant compound in (waste)water treatment systems, therefore, in this study, alginate was employed as a model foulant to test the fouling inhibition potential of each modified membrane [8]. It is important to mention here that to the best of our knowledge, no study has been reported so far on the application of SnO_2-modified membranes in water-based membrane filtration tests. CWP tests were conducted for the unmodified alumina membrane and the ALD-TiO_2 and ALD-SnO_2 modified membranes. Thorough surface characterization, *i.e.* thin film thickness measurement, mean water contact angle measurement, roughness measurement, SEM and EDS analysis, were carried out for all membranes. This research phase revealed the potential of SnO_2 as an anti-foulant, however, in future, further tests and research are needed assess its application in water/wastewater treatment systems.

CHAPTER: 2
LITERATURE REVIEW

2.1 Advanced wastewater treatment with membrane bioreactor (MBR) systems

2.1.1 Introduction to MBR systems

World has been witnessing a continually growing water stress since the last few decades, both in terms of water shortage and water quality, which has resulted in alternative water management needs and an merging focus on efficient use of water resources and non-conventional water sources such as wastewater reclamation [9]. Water treatment and reuse technologies have emerged from simple sedimentation, flocculation etc., to highly engineered methods of wastewater reclamation [10]. A large majority of water treatment plants use the conventional activated sludge (CAS) system, which only fulfills the quality of water to be discharged but is not suitable to be reused for other purposes. Thus, in order to be reused it is necessary to apply complementary treatments. The addition of ultrafiltration (UF) membranes is a possible solution, which has now advanced so much for biological treatment of wastewater and emerged as a new technology, known as membrane bioreactors (MBR). The combination of membranes with a more compact and energy saving bioreactor has received considerable attention as a promising technology for advanced wastewater treatment [11]. Schematics of two typical configurations of MBR systems (submerged and side-stream) are shown in Figure 2-1.

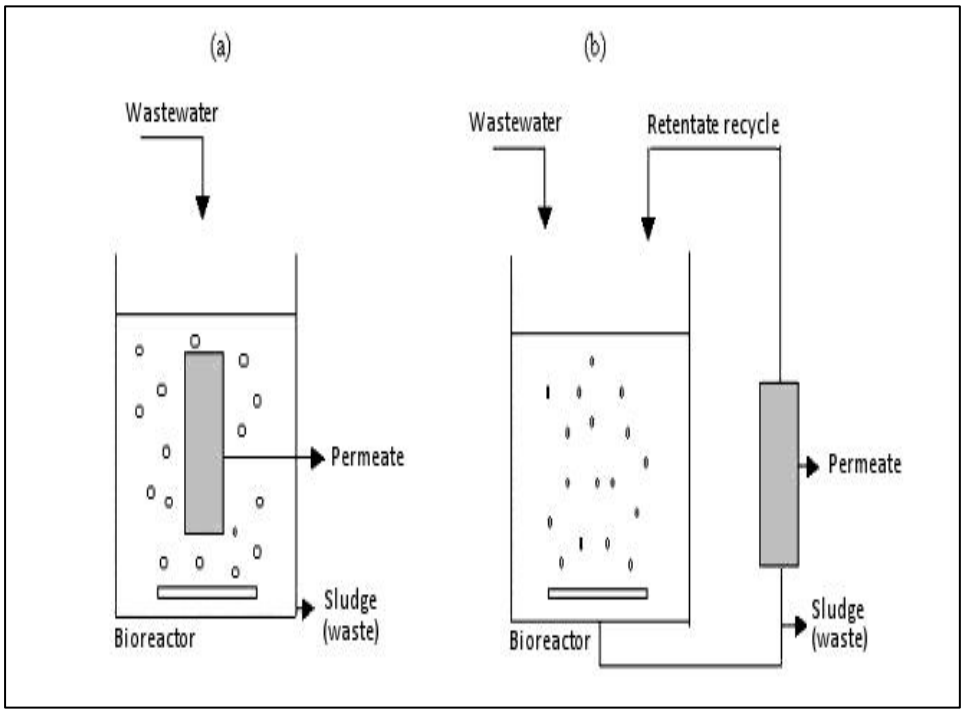

Figure 2-1: Configuration of MBR systems (a) submerged configuration (b) side-stream configuration [12]

2.1.1.1. Advantages and disadvantages of aerobic MBR systems

MBRs offer more advantages over the conventional processes in all aspects, including compactness, quality of water and reliability. As compared to CAS, MBR technology provides higher efficiency, smaller footprints and reduces the need of maintenance and attendant operation. High mixed liquor suspended solids (MLSS) can be used in MBRs owing to their superior solids separation method and independence on sludge settleability, which promotes efficient water treatment. Also, solids and liquids can be independently managed in MBRs, as opposed to CAS where sludge age and hydraulic loads are directly linked to the sedimentation step. Some other advantages often attributed to MBR systems include simple operation, low sludge generation, modular construction and no need of disinfection.

Despite of all the advantages of MBR systems, there are still some issues with this technology, which need further remediation to increase the effectiveness of the process. Some major constraints of MBR systems are:

- High capital equipment and operating costs.
- Sensitivity to upstream treatment processes.
- High energy consumption due to aeration.

Although great steps have been taken to reduce the energy demand in commercial aerobic MBRs, current research activities have moved towards investigating anaerobic processes applied in MBR systems to reduce the energy consumption by eliminating the need of aeration in the bioreactor. Due to its unique advantages, anaerobic MBR (AnMBR), which combines anaerobic process and membrane technology, is attracting remarkable interest in both industrial and research sector.

2.1.2 Anaerobic MBR systems

An anaerobic MBR (AnMBR) system can be simply defined as a biological treatment process which uses membranes for solid-liquid separation without the use of oxygen. The schematic of a typical cross-flow AnMBR system is shown in Figure 2-2. AnMBR has evolved as an important alternative system for advanced wastewater treatment because it combines energy production and pollution control. Moreover, because of no oxygen requirement along with lower sludge yield of AnMBRs, the costs of aeration and sludge handling are considerably lower as compared to the aerobic counterpart. Also, AnMBR is preferred to conventional anaerobic technologies, which have biomass retention dilemma. Biomass retention is one of the main concerns as there is a need of high SRT for biogas production by methanogens. In comparison to aerobic treatment, the total biomass production is low. In

conventional anaerobic systems biomass retention can be a challenge owing to the comparatively poor biomass settling properties of anaerobic sludge [13]. All this has resulted in the use of membranes with anaerobic biological reactor which can provide retention of microorganisms.

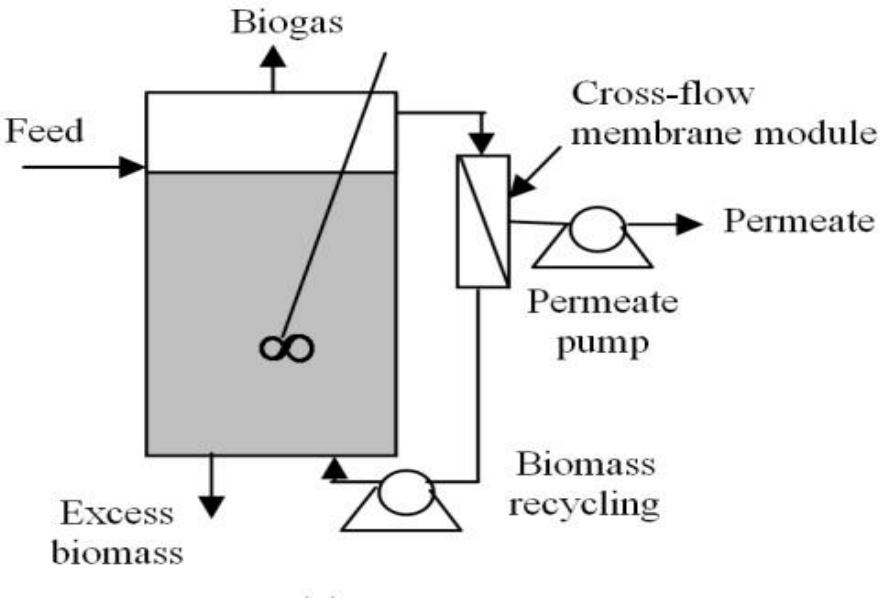

Figure 2-2: Schematic of anaerobic membrane bioreactor (AnMBR) [14]

2.1.2.1. Comparison of aerobic MBR and AnMBR

A comparison of the features of AnMBR and aerobic MBR is summarized in Table 2-1. It can be seen that AnMBR has advantages of low sludge production, less energy consumption, high effluent quality and smaller footprint. Moreover, no use of oxygen has decreased the cost associated with aeration in MBRs as well as the lower production of sludge, thereby reducing sludge handling problems as well as cost. The overall result is decreased operation and maintenance costs as compared to aerobic MBRs.

Table 2-1: Comparison of aerobic MBR and AnMBR [15]

Feature	Aerobic MBR	AnMBR
Energy requirement	High	Low
Sludge production	High	Low
Bioenergy recovery	No	Yes
Nutrient requirement	High	Low
Organic loading rate	High to moderate	High
Organic removal efficiency	High	High
Effluent quality	High	High
Foot print	Low	Low
Biomass retention	Total	Total
Alkalinity requirement	Low	High to moderate
Temperature sensitivity	Low	Low to moderate
Start-up time	<1week	<2 weeks
Mode of treatment	Total	Total or pretreatment

2.1.2.2. Membrane materials and modules for AnMBR

The membrane materials which have been used for AnMBRs can be classified into three major categories: polymeric, inorganic (ceramic) and metallic. All of these membrane materials have their own merits and demerits. Polymeric membranes are used commercially for AnMBRs as they are less expensive. Most of the polymeric membranes used are of Polyvinylidene difluoride (PVDF) and polyether sulfone (PES) [16]. Metallic membranes have also been used in AnMBR showing better fouling recovery, performance and endurance to high temperature and oxidation [17, 18]. Ceramic membranes provide high resistance to abrasion, corrosion, concentration polarization and fouling as they can be backwashed and cleaned effectively [5, 19].

Most membrane modules employed in AnMBRs are based on microfiltration (MF) or ultrafiltration (UF) membranes having the configuration of either flat sheet, hollow fiber or tubular systems. Hollow fiber membrane modules (polymeric) are most commonly used due to their low cost and high packing density. However, flat sheet configuration has also gained interest due to their easy maintenance and good stability. Tubular membrane modules also have the same advantages as flat sheet

module but have several disadvantages such as high pumping cost, low packing density and high capital cost. Table 2-2 summarizes the different membrane materials and modules used in AnMBR systems.

Table 2-2: Various membrane materials and module configurations studied in AnMBR

Membrane material	Module configuration	Nominal pore size (μm)	Reference
Polyvinylidene difluoride(PVDF)	Hollow fiber	0.04	[20]
Polyvinylidene difluoride(PVDF)	Hollow fiber	100 kDa	[21]
Polyvinylidene difluoride(PVDF)	Flat sheet	70 kDa	[22]
Polyvinylidene difluoride(PVDF)	Tubular	0.03	[23]
Polyvinylidene difluoride(PVDF)	Tubular	0.1	[24]
Polyether sulfone (PES)	Flat sheet	20-70 kDa	[25]
Polyether sulfone (PES)	Tubular	20 kDa	[26]
Polyethylene (PE)	Flat sheet	0.4	[27]
Polyethylene (PE)	Hollow fiber	0.4	[28]
Polypropylene (PP)	Hollow fiber	0.45	[29]
Polysulfone (PSf)	Tubular	0.2	[30]
Ceramic	Tubular	40 kDa	[31]
Ceramic	Tubular	0.2	[32]
Metal	Tubular	1	[18]

2.1.2.3. Application of AnMBR in various wastewater treatment

As described earlier, AnMBR has been studied extensively for wastewater treatment owing to the rapidly growing water scarcity related issues. Both industrial and municipal wastewater can be treated by AnMBR. However, there are number of investigations which used synthetic wastewater, as AnMBR feed, for research purpose. A comprehensive summary of AnMBR performance for various wastewaters is given in Table 2-3.

Rapid industrialization has resulted in increased wastewater, mainly coming from food-processing, tannery, pharmaceuticals, textile and petroleum industries. AnMBRs have been used to treat the wastewater from industries which often have high organic loads. Studies have shown that food-processing industries have high particulate and

organic strength wastewater; hence, the characteristics of food-processing industrial wastewater render to be much more suitable to be treated with AnMBR. The AnMBR process has also been recently used for the treatment of municipal wastewater as it provides low sludge production, high efficiency and energy production. Several reports in the development of anaerobic MBR systems commonly use synthetic wastewater to study different aspects of membrane fouling and system performance [3]. Different substrates have been used to make feed which includes starch, peptone, molasses, yeast, volatile fatty acids and glucose.

Table 2-3: Summary of AnMBR performance for various wastewaters

Type of wastewater	Configuration	Membrane characteristics	Operating conditions	Influent	Effluent	Ref.
Synthetic (Tapioca Starch wastewater)	External	Hollow fiber UF Membrane Pore size: 0.03–0.15 µm	HRT=10 d Temp=30 °C OLR=1.76 kg COD/m^3/d	COD=20.15 g/L	COD=675–780 mg/L (>95%)	[33]
Synthetic (Meat extract + Peptone)	Immersed (Submerged)	Flat-sheet PE membrane, Pore size: 0.40 µm	HRT=6 h SRT=150 d MLVSS=2.6±0.15 g/L Temp=35±1 °C Flux=10 L.m^{-2}.h^{-1}	COD=0.45± 0.02 g/L	CODs=18±9 mg/L (95%)	[34]
Synthetic (Whey + Sucrose)	Immersed (Submerged)	Flat-sheet membrane, Pore size: 0.40 µm	SRT=30–40 d MLVSS=5.50–20.40 g/L OLR=1.45–13.0 kg COD/m^3/d Temp=35±1 °C Flux=2–5 L.m^{-2}.h^{-1}	not reported	not reported	[35]
Synthetic (Glucose + Peptone + Yeast Extract)	External	Tubular MF membrane Zirconia pore size: 0.140 µm PP pore size: 0.20 µm	HRT=6.5 d Temp=54–56 °C OLR=4 kg COD/m^3/d	COD=27.05 g/L Kj–N=1.29	CODt= not reported (78.5–84%)	[36]
Synthetic (Glucose)	External	Hollow fiber PE membrane Pore size: 0.4 µm	MLSS=3.5 g/L	COD=0.8 g/L	not reported	[37]
Industrial (Cheese Whey)	External	MF pore size: 0.20 µm	HRT=1 day/4 d SRT= 29.7-78.6 d MLVSS= 6.4-10 g/L OLR= 19.8 kg COD/m^3/d Temp= 37±2°C	COD=68.5± 3.4 mg/L BOD_5=37.7± 2.85 mg/L Kj-N = 1.1 ± 0.01 TP=0.5±1.8	COD= not reported (98.5%) BOD_5 < 100 mg/L (99.2%) TSS= not reported	[38]

				Å TSS=1.35±0.05 mg/L pH=6.5	(100%)	
Industrial (Diluted tofu processing waste)	External	Hollow fiber MF membrane	Flux =139 $L.m^{-2}.h^{-1}$ HRT=4 h RNA conc.= 150–200 mg/L Temp=60±0.1°C pH=5.5 Flux=4.3 $L.m^{-2}.h^{-1}$	COD=26.5±2.2 mg/L TSS=23±4 mg/L pH=1	Carbohydrate content 2 g/L	[39]
Industrial (Olive-mill Wastewater)	External	Ceramic tubular UF 25 kDa MWCO	HRT=16.7 h MLSS=1.0–2.4 g/L Temp=35±2 °C Flux= 80–450 $L.m^{-2}.h^{-1}$	COD=350–500 mg/L SS=1.0–1.5 mg/L pH=6.51–7.81	COD < 30 mg/L (>95%) TN=9–9.85 (15–20%) pH=6.9-7.3	[40]
Industrial (Petrochemical wastewater)	Immersed (Submerged)	Kubota flat panel membrane Pore size: 0.45 μm	HRT=32 h SRT=175 d MLSS>30 g/L OLR=14.5 kg $COD/m^3/d$ Temp=37.1 °C	COD=19 pH=7	COD=610 (98%)	[41]
Industrial (Textile wastewater)	Immersed (Submerged)	Hollow fiber MF membrane Pore size: 0.40 μm	HRT=24 h pH=6.8–7.2 Temp=35 °C Flux=1.8–14.4 $L.m^{-2}.h^{-1}$ PAC dose=1.7 g/L	COD=730–1100 mg/L	COD= not reported (90%) Color= not reported (94%) Turbidity=8 NTU	[42]
Municipal	Immersed (Submerged)	Flat-sheet MF PVDF 140 kDa MWCO	HRT=10 h MLSS=6.41–9.31 g/L OLR=~1 kg $COD/m^3/d$ Temp=30±3 °C Flux=11 $L.m^{-2}.h^{-1}$	COD=425±47 mg/L TP=4.3±0.5 SS=295±33 mg/L pH=7.5±0.4	COD=50±10 mg/L (88±2%) TP=3.8±0.7 (~0%) SS < 0.8 mg/L (>99%) pH=7±0.2	[22]
Municipal	Immersed (Submerged)	Flat-sheet dynamic membrane, Dacron mesh	HRT=8 h MLSS=6–20 g/L OLR= ~0.9 kg $COD/m^3/d$ Temp=10–15 °C Flux=65 $L.m^{-2}.h^{-1}$	COD=302.1±87.9 mg/L NH_4^+–N=40±8.5 TN=59±10 SS=120±23 mg/L pH=7.3±0.3	COD=120.8±34.0 mg/L (57.7±4.6%) SS=0–15 mg/L pH=7–7.5	[43]
Municipal	External	Tubular UF membrane 40 kDa MWCO	HRT=3 h SRT=100 d Temp=25 °C Flux=7 $L.m^{-2}.h^{-1}$	CODt=645±103 mg/L CODs=385±63 mg/L TSS=140±18 mg/L $MPN_{Fecal\ coliforms}=10^6$/100 mL	CODt=104±12 mg/L (87%) CODs=104±12 mg/L (73%) BOD=32±5 mg/L TSS < 1 mg/L $MPN_{Fecal\ coliforms}=0$ (100%)	[31]
Dilute Municipal Wastewater	External	PVDF; pore size: 0.1 μm, 200 kDa MWCO	HRT=12-48 h SRT=19-217d OLR=0.03-0.11kg $COD/m^3/d$	CODs=38-131 mg/L pH=7.5	CODs=18–37 mg/L (55–69%) pH=6.6±0.1	[44]

			MLSS=1-7 g/L Temp=25.0 °C pH=6.4±0.2			
Domestic wastewater	External	Hollow fiber, MF, Pore size: 0.2 µm	HRT=6 h MLSS=14-80 g/L OLR=2.15 kg COD/m^3/d Temp=25.0 °C Flux=7.5 L.m^{-2}.h^{-1}	COD_t=540 mg/L	CODs=65 mg/L (88%)	[45]

2.1.3 Membrane fouling in AnMBR

The critical issue limiting the commercial and widespread application of AnMBRs in wastewater treatment is membrane fouling. System efficiency could be decreased by membrane fouling because of increased maintenance cost and time and energy requirements for membrane cleaning. Interaction between sludge suspension components and membrane material leads to membrane fouling. AnMBR has different sludge characteristics as the suspension is different from aerobic MBR sludge. There are different types of fouling that can take place, individually or simultaneously, resulting in a cake-layer developing on the membrane surface and/or membrane pore blocking, which ultimately will decrease its performance. These fouling types include:

- Organic fouling (due to dissolved organic matter, proteins, polysaccharides etc.)
- Inorganic fouling or scaling (due to Fe, Mn, struvite etc.)
- Particulate fouling (due to colloids etc.)
- Biofouling (due to attachment of microbes and microbial products)

A set of approaches and techniques is available to better understand the fouling in AnMBR systems [46]. Physical and chemical methods can be used to clean the fouled membranes. However, sometimes irreversible fouling still exists even after completion of cleaning circuits as shown in Figure 2-3.

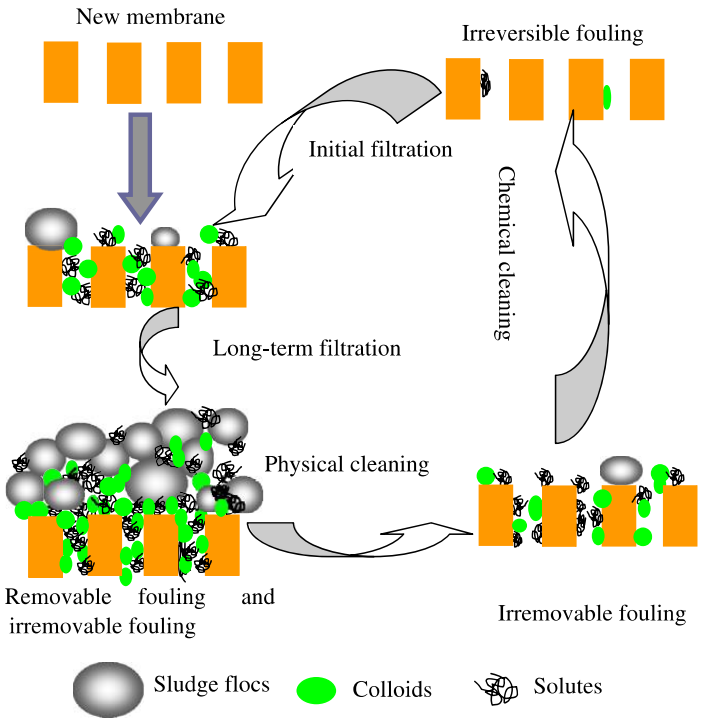

Figure 2-3: Fouling and cleaning circuits by physical and chemical ways [47]

2.1.3.1. Membrane fouling mechanism

Various membrane fouling mechanisms have been proposed based on their relative contribution to overall membrane fouling. These include adsorption of soluble components, depositions of solids as a cake layer, spatial changes to foulant composition, cake layer consolidation, pore plugging and clotting by colloidal particles and biofilm formation [48, 49].

Various reviews of membrane fouling in MBR systems encompassing fouling mechanisms have been presented in the literature [47, 50-52]. MBR systems are generally operated under constant-flux conditions with convection of foulants towards the membrane surface. Since the fouling rate increases roughly with flux [53], sustainable operation dictates that MBRs should be operated at modest fluxes and preferably below the critical flux. Even sub-critical flux operation may lead to fouling

according to a two-stage pattern [54]: a low trans-membrane pressure (TMP) increase over an initial period (stage 2) followed by a rapid increase after a certain critical time period (stage 3). Prior to these two filtration stages, a conditioning period is generally observed (stage 1). An illustration is shown in Figure 2-4 to describe the phenomenon on each stage.

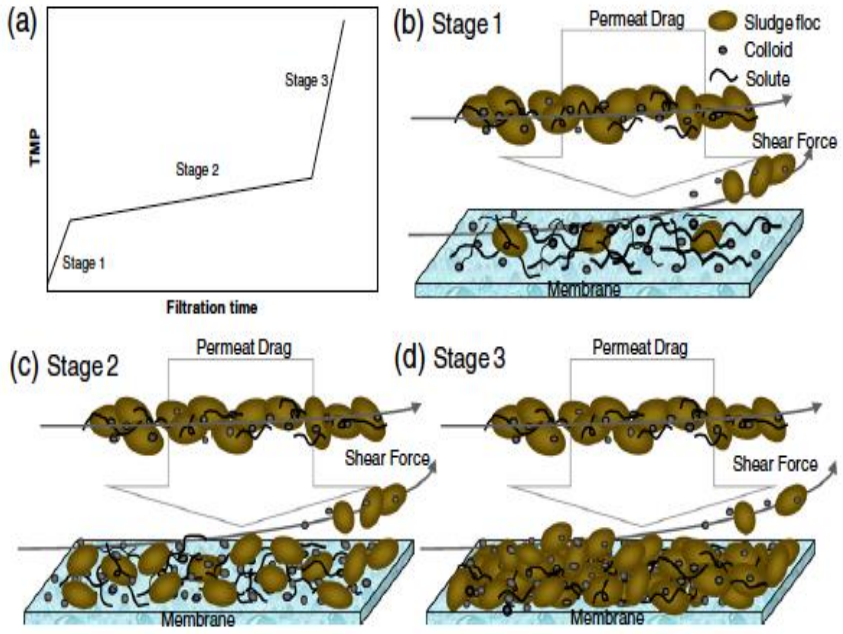

Figure 2-4: Schematic illustration of membrane fouling mechanism with (a) effect on trans-membrane pressure (TMP) at (b) stage 1 (c) stage 2 and (d) stage 3 [15]

2.1.3.2.Parameters affecting membrane fouling

Interactions between the sludge suspension and the membrane material lead to membrane fouling. Subsequently, all the parameters related to both of these components will directly affect the behavior and rate of membrane fouling. Mainly, sludge characteristics, membrane surface characteristics, feed characteristics and operational conditions affect the fouling rate in MBR systems. Major parameters that have a direct effect on membrane fouling include the hydrodynamic conditions,

particle size distribution (PSD), extracellular polymeric substances (EPS) and soluble microbial products (SMP) etc. In contrast, some other parameters affecting the membrane fouling are solids retention time (SRT), organic loading rate (OLR), hydraulic retention time (HRT) and pH etc. [25, 32].

2.1.4. Membrane fouling control in AnMBR

Strategy development for membrane fouling control is a main purpose of this study. Depending on the parameters affecting membrane fouling, such strategies in AnMBR systems can be broadly classified into the following groups:

- Feed pretreatment.
- Optimization of operational conditions.
- Modifying sludge properties.
- Membrane surface modification.

A brief explanation of each of the above-mentioned membrane fouling control method is given below:

2.1.4.1. Feed pretreatment

Characteristics of the feed wastewater can have an important effect on membrane fouling. Most of the industrial waste streams contain solid contaminants and high pH which not only damage performance, but also reduce the lifespan by causing severe membrane fouling.

Cake layer on membrane surface has been found to be mostly rich in Al, Mg, Si, Ca, and Fe due to the presence of inorganic matter in feed [55]. Pretreatment procedures such as filtration [56], pH adjustment [38] and establishment of local

wastewater limits standards can be used to remove excess quantities of these materials to avoid severe fouling.

2.1.4.2. Optimization of operational conditions

The main operational parameters affecting membrane fouling are the hydrodynamic conditions (*i.e.* HRT, cross-flow velocities (CFV), air-scouring etc.), flux, water properties (*i.e.* pH, temperature, salinity etc.), biomass concentration, SRT. Better hydrodynamic conditions can be achieved by increasing the time, flow velocity and gas scouring intensity in AnMBRs to control membrane fouling; however, changing such conditions could interrupt the sludge flocs, releasing high EPS content and producing small-size particles which can enhance membrane fouling [32, 57].

2.1.4.3. Modifying sludge properties

The feed and concentrate properties in AnMBRs can be modified by the addition of additives, such as coagulants, adsorbent agents, chemical agents and suspended biofilm carriers. Proper additives for fouling control can act through various phenomena including coagulation, adsorption of SMP, cross-linking of flocs and/or a combination of these [58]. Some novel measures have also been developed such as using powdered activated carbon (PAC) as “flux enhancers” in MBRs.

2.1.4.4. Membrane surface modification

To control membrane fouling, surface modification for hydrophilic improvement of the membrane has been a commonly-used method. Surface grafting, plasma treatment, surface blending and surface coating, etc. are used to introduce polar

organic functional groups onto the membrane surface. Polar organic functional groups can increase the antifouling ability of membrane due to their hydrophilicity, ability to resist protein adsorption, flexible long chains and large exclusion volume [59].

Commercial thin-film composite (TFC) nanofiltration membranes are prepared by coating commercially available Polyvinylidene difluoride (PVDF) ultrafiltration (UF) membrane with the graft copolymer PVDF-graft-polyoxyethylene methacrylated (PVDF-g-POEM) in attempt to reduce the membrane fouling. It was found that these new TFC-UF membranes exhibited no irreversible fouling in a 10 d dead-end filtration of BSA, sodium alginate and humic acid at concentrations of 1000 mg/L and above [60].

Moreover, TiO_2-embedded polymeric membranes prepared by a self-assembly process also have drawn considerable attention. When applied for activated sludge (AS) filtration, it was found that adsorbed foulants on the TiO_2 embedded membrane surface were more readily dislodged by shear forces than those on neat polymeric membranes due to the increased hydrophilicity of the membrane [61, 62]. Hence, membrane surface modification has found to be widely used for fouling control in MBR systems.

2.2 Ceramic membranes

2.2.1. Introduction to ceramic membranes

Ceramic membranes are composite membranes which consist of several layers of single or more, same or different ceramic materials. Generally, ceramic membranes have a macroporous support, mesoporous intermediate layer(s) and a microporous or a dense top layer. Critical parameters that indicate the performance of a ceramic membrane are its permeability and separation factor. Typically, the permeation and

separation of a porous ceramic membrane is governed by surface porosity, pore size and membrane thickness, whereas this principle is more complex for a dense membrane. The separation mechanisms and corresponding applications according to ceramic membrane's pore size are given in Table 2-4.

Table 2-4: Category of ceramic membranes [63]

Type	Pore size	Mechanism	Applications
Macroporous	> 50 nm	Sieving	UF, MF
Mesoporous	2 – 50 nm	Knudsen diffusion	UF, MF, Gas separation
Microporous	< 2 nm	Micropore diffusion	Gas separation
Dense	-	Solution diffusion	Gas separation, RO

Alumina, Titania, Zirconia and Silica etc. (or a composite of these materials) are commonly used materials for making ceramic membranes. A schematic representation of an asymmetric composite membrane is shown in Figure 2-5. It can be seen that the function of first layer is separation, the role of the middle layer(s) is to bridge the differences in pore size between the support layer and the first layer while the bottom layer is used to provide mechanical support.

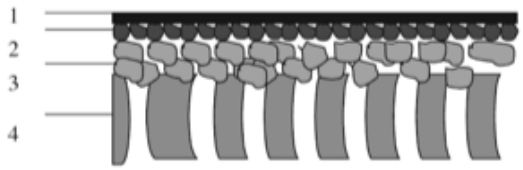

1. Modified separation layer (Dense or <2 nm)
2. Separation layer (2–50 nm)
3. Intermediate layer(s) (50–1000 nm)
4. Porous support (1–15 μm)

1 + 2 + 3+ 4	nanofiltration or gas separation membranes
2 + 3 + 4	ultrafiltration membranes
3 + 4	microfiltration membranes

Figure 2-5: Schematic of an asymmetric composite membrane [63]

Multiple steps are required to prepare such ceramic membrane as shown in Figure 2-5.

- Firstly, a support layer is made for providing mechanical strength to the membrane.
- Then a single or more layers (intermediate) are coated over the support layer.
- And finally a microporous (or dense) layer is made for the separation purpose.

Each of the above-mentioned steps requires high temperature sintering treatment, which makes the fabrication of ceramic membranes very expensive. Hence combining these multiple steps into a single step is required to reduce the membrane fabrication cost. Li *et al.* (2006) demonstrated that a phase inversion process can be used to combine this 3-step fabrication process into one step. Figure 2-6 shows the SEM image of an asymmetric dense ceramic membrane prepared by Li *et al.* (2006) using such method [52]. Figure 2-6 illustrates that the porous support of the same ceramic material is integrated with a dense and thin skin layer, which confirms that this ceramic membrane was prepared in one step.

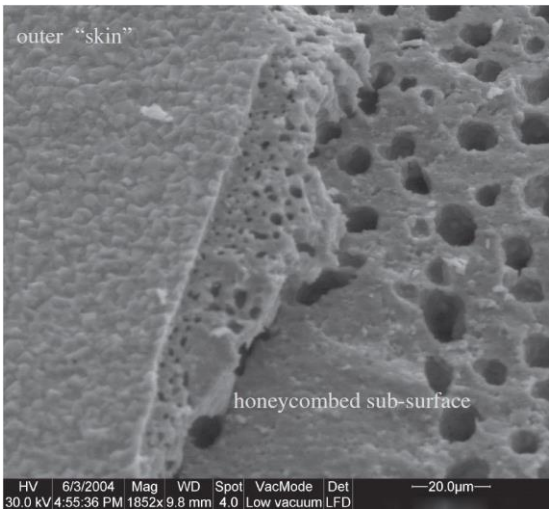

Figure 2-6: SEM image of a layered ceramic membrane [52]

Most commercial ceramic membranes are assembled as plate-and-frame or as a tubular module using membrane tubes. Multichannel monolithic membranes have been developed to give more separation area per unit volume of membrane element. Such monolithic elements can be combined to form modules. An alumina monolithic element is shown in Figure 2-7 [64].

Hsieh (1996) reported the following surface area to volume ratios:

- 30–250 m^2 / m^3 for tubes,
- 130–400 m^2 / m^3 for multichannel monolithics and
- 800 m^2 / m^3 for honeycomb multichannel monolithics [65]

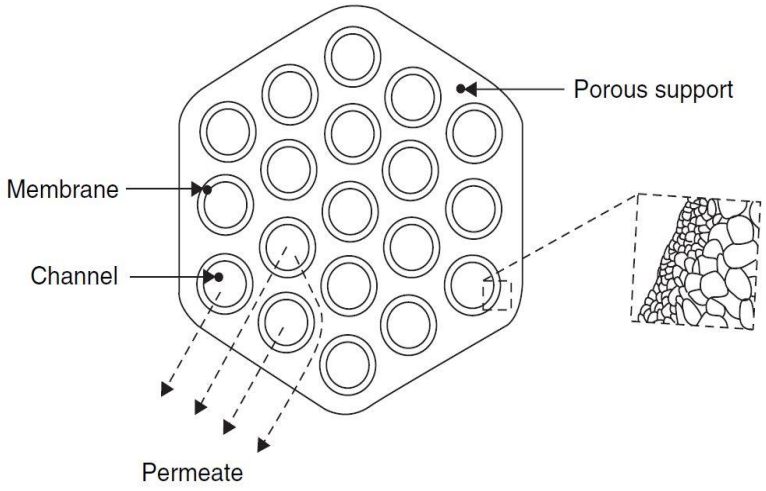

Figure 2-7: Cross-section of a monolithic multichannel membrane element [64]

2.2.1.1. Advantages and limitations of ceramic membranes

Major advantages of ceramic over polymeric membranes are summarized below [66]:

1. Resistance to extreme pH and temperature
2. Chemically inert
3. Mechanical strength
4. Long and reliable lifetime
5. Subject to more extreme backwashing and regeneration methods
6. Relatively less interaction between ceramic material and biomass: the biofouling is minimized
7. Narrow and well-controlled pore size distribution
8. High porosity and hydrophilic surface
9. Geometric simplicity
10. Ceramic membranes can be applied to difficult wastewater
11. Reduced operating expenses

Potential limitations of ceramic membranes are:

1. High capital cost
2. Physical weight
3. Lack of operational experience

2.2.2. Preparation of ceramic membranes

Ceramic membrane fabrication involves the following steps and the general flow sheet is shown in Figure 2-8 [63]:

1. Particle suspensions formation.

2. Particle suspensions are packed into a membrane precursor with a certain shape (tube, flat sheet or monolith).
3. Heat treatment of membrane precursor at high temperatures (Sintering).

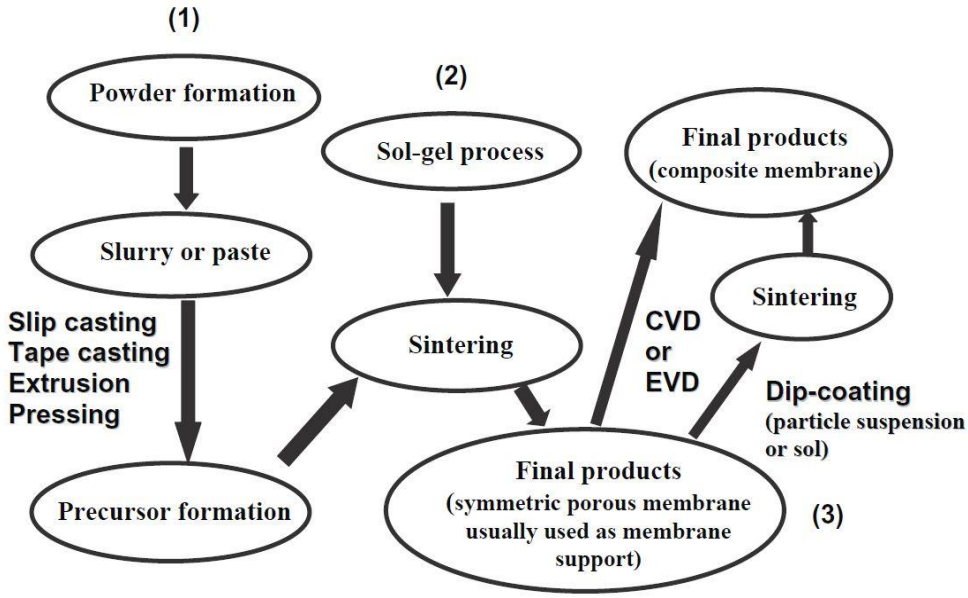

Figure 2-8: General flow diagram for fabrication of ceramic membranes [63]

Methods such as slip casting, tape casting, extrusion and pressing are used to shape the particle slurry (suspension) into a membrane precursor. A coating step such as dip-coating, sol-gel, chemical vapor deposition (CVD), followed by a high temperature sintering process can be used to produce composite membranes. Brief details of the above-mentioned methods are given below.

2.2.2.1. Slip casting

Slip casting is a commonly-used technique in membrane fabrication. As shown in Figure 2-9(a), in this method a powder suspension is poured into a porous mold. Capillary suction force extracts the solvent of suspension into the mold's pores. A gel

layer (or layer of particles) is formed on the mold surface when the slip particles are consolidated. Tiller and Tsai (1986) discussed the theory of slip casting on comprehensive basis and presented a method for selection of optimum pore diameter of mold [67]. The pore size range of the fabricated membranes falls in the range of 3-6 nm.

2.2.2.2. Tape casting

Tape casting is a very famous method for the formation of flat sheet ceramic membranes. The basic principle of tape casting method is illustrated in Figure 2-9(b). Elements of this process are:

- A drying zone
- A moving carrier
- A reservoir for powder suspensions
- A stationary casting knife

In this method, the powdered suspension is poured into a reservoir behind the casting knife. The carrier to be cast upon is set in motion. Thickness of the cast layer is determined by the knife gap between the knife blade and carrier. Solvent is evaporated from surface and the wet cast layer passes into a drying chamber. A dry membrane precursor is left behind on the surface of carrier.

The thickness range is few millimeters for the membranes prepared by this specific method [68]. However, Sahibzada *et al.* (2000) used this method to prepare a membrane with thickness around 5 μm [69].

2.2.2.3. Pressing

Ceramic membrane discs are usually fabricated using the pressing method. The schematic for this method is shown in Figure 2-9(c). An applied force consolidates a suspension of particles into a dense layer. This method has been frequently employed for development of ceramic membranes with high permeability for hydrogen and/or oxygen. Powders are pressed into a compacted disc by means of a special press machine that applies more than 100 MPa pressure. Diameter of the disc is a few centimeters and the thickness is normally around 0.5 mm.

2.2.2.4. Extrusion

Extrusion is used to produce ceramic tubular support and honeycomb cellular catalyst support. Extrusion is also utilized in the production of bricks and tiles, refractories, kiln furniture, heat exchanger tubes, porcelain electrical insulators, furnace tubes, magnets and electronic substrates. Extrusion schematic is shown in Figure 2-9(d).

A stiff paste is compacted in extrusion and forced through a nozzle for its shaping. The precursor should exhibit plastic behavior (*i.e.* at lower stresses, it behave like a rigid solid and deforms only when the stress reaches a certain value called the yield stress). The structure of extrusion-made precursor is homogeneous over the cross-section.

2.2.2.5. Sol-gel method

Leenaars *et al.* (1984) first developed the sol-gel technique for preparation of ceramic filters. Precise and desirable control of membrane pore size (particularly for small pores) is one of the main advantages of the sol-gel method [70-72]. Comprehensive

information on the sol-gel method can be found in literature [73, 74]. A membrane can be prepared by the sol-gel technique via two main routes, as shown in Figure 2-9(e).

- **Colloidal route:** A sol is formed by mixing metal salt with water. Membrane support is coated with that sol and it forms a colloidal gel on the support.
- **Polymer route:** A sol is formed by mixing metal–organic precursors with organic solvent. Then the sol is coated on a membrane support and it forms a polymer gel on that support.

The pore sizes of membranes prepared via the colloidal route are in ultrafiltration (UF) range. Such membranes are typically used for colloidal and large molecular weight solutes separation. They can also be used as a membrane support for further development of membranes with smaller pore size [75, 76]. Membranes fabricated through polymer route can be used for gas separation (as pore size of such membranes must be less than 1 nm). In such case, the support membrane (gamma-alumina) is fabricated through colloidal sol route. A smaller pore size is achieved for the selective layer of the membrane, made through polymer route, by low-branched cluster of inorganic polymer as compared to high-branched cluster [63].

2.2.2.6. Dip coating

The schematic for dip coating technique is shown in Figure 2-9(f). When the substrate is in the atmosphere with a relative humidity below 100 %, the drying process begins simultaneously with dip coating. The complete cycle of dipping, drying and calcination is repeated after calcination of the first layer in a multiple step process. The critical parameters in dip coating are:

- Coating speed or time.

- Viscosity of the particle suspension.

Water suspensions of commercially available sub-micron alumina powder (*i.e.* particle diameter of 500 nm) can be used to prepare an alumina coating with a pore size of approximately 100 nm [77].

2.2.2.7. Chemical vapor deposition

Chemical vapor deposition (CVD) uses chemical reactions that take place at high temperature in a gaseous medium (mixture of H_2, N_2, metal halides and HCs) which surrounds the membrane component. This technique deposits a layer of a compound (which can be same or different) on the membrane surface to modify its properties. Reactions as thermal decomposition, oxidation and hydrolysis take place for coating of layer by CVD. Figure 2-9(g) illustrates a typical CVD system.

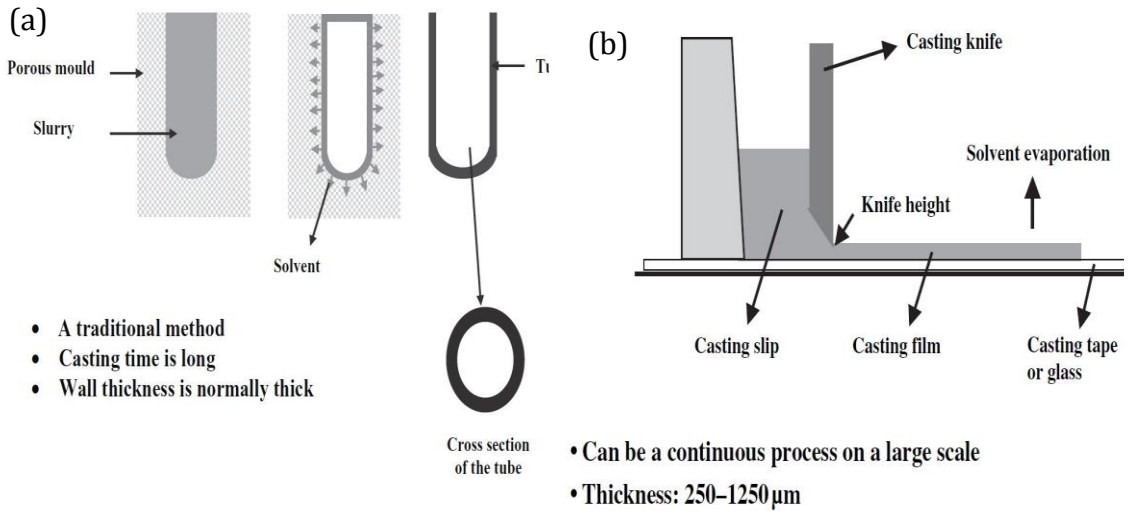

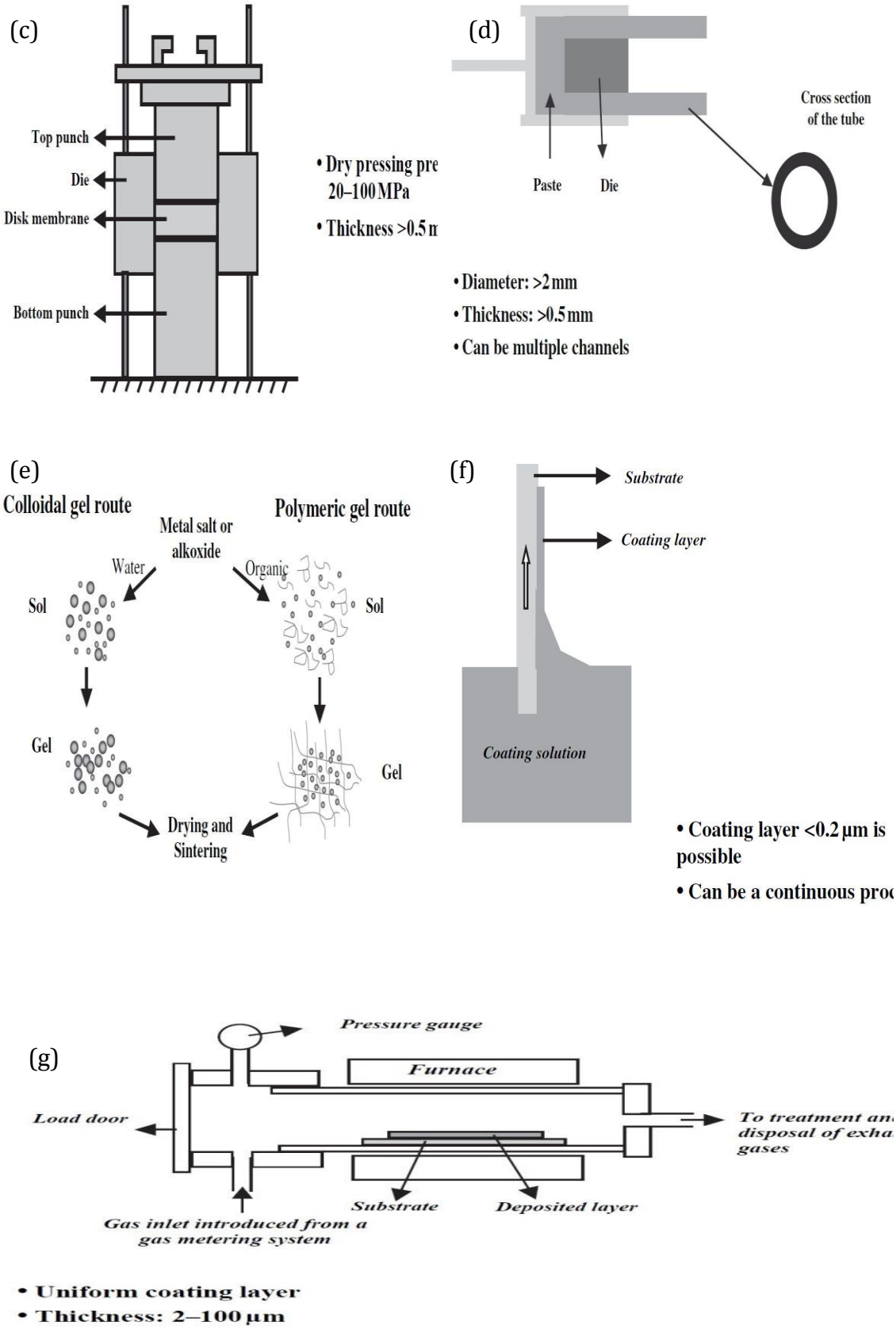

Figure 2-9: Schematics of ceramic membrane preparation methods (a) Slip casting (b) Tape casting (c) Pressing (d) Extrusion (e) Sol-gel method (f) Dip coating (g) Chemical vapor deposition (CVD) [63].

2.2.3. Performance of ceramic membranes

2.2.3.1. Comparison of filtration characteristics of ceramic and polymeric membranes in an anaerobic membrane bioreactor (AnMBR)

I.J. Kang *et. al* (2002) compared the filtration characteristics of organic (polymeric) and inorganic (ceramic) membranes in an AnMBR for the treatment of alcohol distillery wastewater on the basis of cake layer formation, back-flushing, physiochemical properties of the membrane materials and back-feeding effects [78]. Characteristic filtration results for both organic and inorganic membranes were plotted as time vs. reduced flux. The time curves of flux decline for both types of membranes were obtained and are given in Figure 2-10. Apparently, different filtration characteristics were observed for organic and inorganic membranes. For organic membranes, a steady state flux was developed at initial filtration stage right after when an abrupt flux decline was observed. While, on the other hand, the flux declined gradually over a long period of time in case of inorganic membranes.

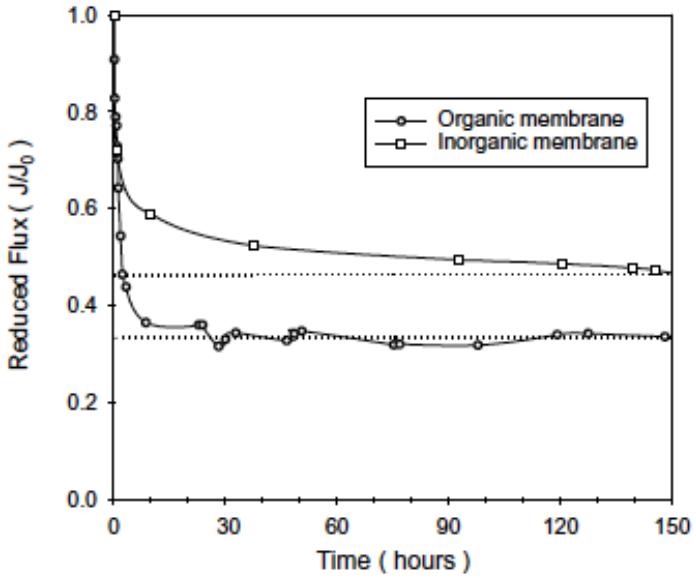

Figure 2-10: Comparison of flux decline curves of organic and inorganic membranes in the AnMBR system [78]

Their results revealed that in an AnMBR system, the filtration characteristics for both organic and inorganic membranes are quite different from each other. Examination of SEM images and struvite quantity in used membranes showed that presence of struvite in the pores of inorganic membranes is the main factor in flux decline of these membranes while, for organic membranes, the governing factor is the rough and fibrous nature of these membranes along with the thick cake layer of biomass and struvite formed on its surface. It was noted from differences between the back-feeding and back-flushing of both types of membranes that ligand exchange reaction and surface charge effect also plays an important role [78].

2.2.3.2. Comparison of ceramic and polymeric membranes in wastewater treatment: A study for oil and gas, rubber processing and palm oil industries [79]

Oil-gas produced water treatment, rubber processing and palm oil mill effluent treatment is commonly practiced around the globe. In such processes, membrane treatment is becoming an emerging choice due to their high-quality effluent and small foot print. However, high fat, oil and grease (FOG) contents in the effluent streams offer a serious challenge as it can cause severe organic fouling and reduce the filtration performance of polymeric membranes. For this reason, extensive pretreatment systems are installed in such processes to remove much of the FOGs before the membrane operation. The use of ceramic membranes can help reduce the number of pretreatment steps required due to their outstanding advantages as already mentioned in sub-section 2.2.1.1. In this study, conducted by Siemens, a comparison was made between the performance of ceramic and polymeric membranes for treatment of FOG wastewaters.

2.2.3.2.1 Operation performance comparison

Table 2-5 shows the results of ceramic membrane in comparison with an equivalent polymeric membrane for treating two different types of feeds. As it can be seen in Table 2-5, in presence of high FOG content the ceramic membranes foul less rapidly than the polymeric membranes, and the oil content in the permeate was less than 20 ppm for a feed FOG content of 30,000 ppm. Also ceramic membrane showed better performance parameters than the polymeric membrane for a feed FOG content of 9,700 ppm.

Table 2-5: Comparison of permeance and permeate quality of ceramic and polymeric membranes for two different types of feed [79]

	Ceramic membrane permeate	Polymeric membrane permeate
Permeance ($L.m^{-2}.h^{-1}bar^{-1}$)	400	< 1.4
O & G content (ppm)	< 10	around 50

Feed: *Untreated produced water*
Total O&G content: *30,000 (close to 3% wt. oil and grease)*
Total free oil content: *7,300 ppm*
Total dispersed oil content: *22,300 ppm*

	Ceramic membrane permeate	Polymeric membrane permeate
Permeance ($L.m^{-2}.h^{-1}bar^{-1}$)	200	around 20
O & G content (ppm)	< 150	around 5,000

Feed: *Simulated emulsion from biodiesel waste streams containing water, free fatty acids, fatty acid methyl esters, crude glycerol, surfactants*
Total O&G Content: *9,700 ppm*

The visual representation of the feed and permeate quality for produced water treatment is shown in Figure 2-11 and the results showed efficient performance by ceramic membrane. Figure 2-11(ii) b shows a visual representation of the feed and permeate of a hot liquid waste stream of 75 °C. Total TSS removal was obtained with ceramic membranes when wastewater feed contained 25% solids content latex suspension. At this high temperature, the polymeric membrane could not work

efficiently. Stable fatty acid methyl esters (FAME) were broken with surfactant emulsions in case of ceramic membranes, without addition of emulsion-breaking chemical dispersants (Figure 2-11(ii) c). The polymeric membrane showed a high rate of fouling and instability when subjected to filtration of FAME-water emulsions.

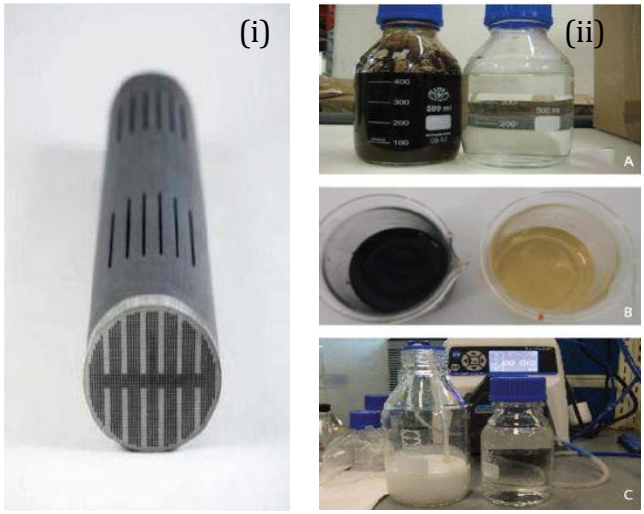

Figure 2-11: (i) Ceramic membranes (ii) Before and after ceramic filter (a) Oil-field produced water (b) Rubber plant wastewater (c) Simulated FAME-water emulsion [79]

2.2.3.2.2 Comparison of cleaning methods for ceramic and polymeric membranes

Table 2-6 shows a comparative study of some of the limitations of some cleaning techniques for ceramic and polymeric membranes. Generally there are more and varied cleaning options for ceramic membranes than those for polymeric membranes. For ceramic membrane systems, high-pressure back-pulse (up to 7 bar for one second or less / min) is a commonly used technique to enhance flux performance. Generally, the burst pressure for polymeric membranes is less than 7 bar, so high pressure back-pulse is not workable for polymeric membranes. Stronger or more concentrated oxidizing agents can be used during cleaning-in-place (CIP) procedures for light

fouling. Peroxide cleans are not usable for cleaning of polymeric membranes but these have no serious problem with ceramic membranes. Steam CIP cannot be used for polymeric membranes but can be used for ceramic membranes. If extensive organic fouling cannot be removed by steam sterilization then ceramic membranes can be regenerated by high heat treatment at 400 °C in the presence of air at atmospheric pressure for complete combustion of the accumulated organic foulants. Full flux recovery is possible with this method of membrane regeneration, if the foulants are entirely organic in nature. However, steam CIP would rather be a better option for performance recovery for feeds containing a substantial amount of non-organic foulants. Furthermore, heat treatment and steam CIP removes the need for liquid chemical disposal as the membrane modules are sterilized in a chemical-less manner.

Table 2-6: Limitations of different cleaning techniques for ceramic and polymeric membranes [79]

	1% NaOH followed by 1% Citric acid	60 °C 3 % NaOH	Steam treatment
Ceramic membrane	< 10 %	50 – 60 %	100 %
Polymeric membrane	< 5 %	Not possible	Not possible

2.2.3.2.3 Lifecycle cost evaluation

Capital expenditures (CAPEX) of commercial ceramic membrane modules is approximately five times higher than that for their polymeric counterparts. The operating life span for polymeric membranes typically falls between 3-5 years while the operating life for ceramic membranes is in excess of five times that for polymeric membranes. A ceramic membrane filtration plant has been operating since 1979 without a need for a change in membrane modules [80]. The reduction in operating

expenses (OPEX) can be up to 50% by switching polymeric membranes to ceramic membranes. This is because of;

- Rapid back-pulsing during operation (*i.e.* time between CIPs is prolonged).
- Heat and steam treatment to recover the performance of membrane (both are readily available in industrial facilities and the need for storage and disposal of cleaning reagents is removed).

2.2.4. Commercial market of ceramic membranes

Scarcity of high-quality water is becoming one of the major reasons behind growth in demand of ceramic membranes in filtration, purification and separation processes. Global ceramic membranes market is expecting to show highest growth in Asia-Pacific and North America among other regions. The market size of ceramic membranes is projected to reach $5.1 billion by 2020, registering a yearly growth of 11.7% between 2015 and 2020. Oil/Grease removal and water/wastewater treatment represents a strong market for ceramic membranes as they are easy to clean and are intrinsically resistant to fouling.

In aspect of technology, the market for nanofiltration ceramic membranes is the fastest-growing technology segment. Around 9% of the total ceramic membranes market is accounted by nanofiltration in 2014. Nanofiltration technology is applied for separation of natural organic and inorganic substances in liquid-phase membrane-based separation processes. The ability of sterilization, recycling and stability in extreme pH environments is making ceramic membranes a suitable technology for applications in various industries, such as food and beverages, water/wastewater treatment, pharmaceuticals etc. Such features make nanofiltration a promising option in comparison with other technologies using ceramic membranes (Figure 2-12) [81].

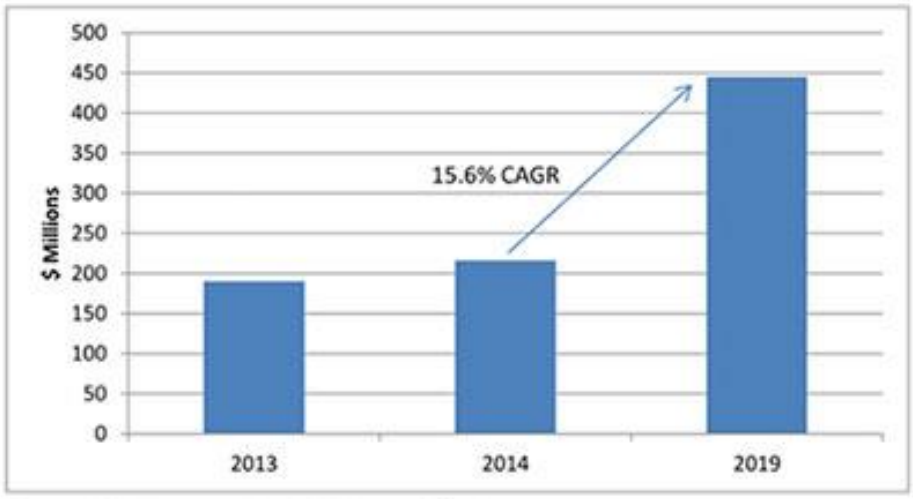

Figure 2-12: Increase in global market of ceramic nanofiltration membranes from the year 2013 to 2019 [81]

Rise in water related issues has increased the application of ceramic membranes in water and wastewater treatment industry and this is expected to continue in the near-future as well. According to an estimate in 2014, 55% of the total ceramic membrane market was consumed in this particular segment of industry [80]. Due to the increasing demand of recovery of materials, recycling, clarification of juices and beer, sterilization of milk, the food and beverage industry is projected to be the fastest-growing application segment, followed by biotechnology, between 2015 and 2020 [6].

Oil and gas industry also contribute in the market of ceramic membranes. Installations in the oil and gas industry to date have been few, with Veolia (CeraMem) currently the most active company in this area [82]. Young companies around the world are working to develop innovative methods of producing inorganic membranes, even as key established producers strive to bring down the manufacturing cost to compete with polymeric membranes on a whole-life cost basis (Figure 2-13) [83].

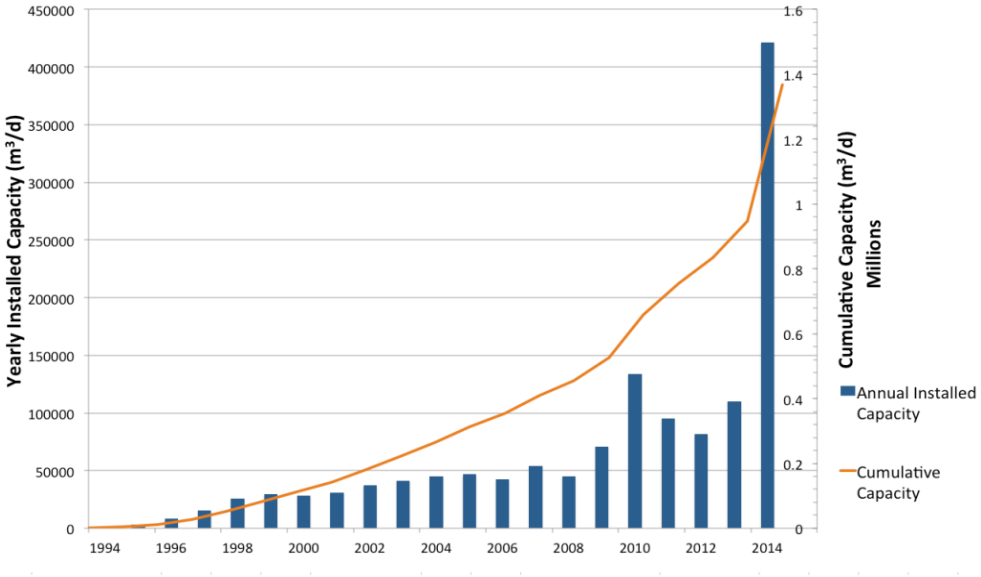

Figure 2-13: Increase in installation of ceramic membranes over 20 years (1994-2014) [83]

2.3. Membrane surface modification for fouling control

Membrane separation processes are essentially a surface phenomenon. In this process, the top surface layer or skin layer plays a vital role. Therefore, surface modification of membranes is a useful tool/method to counter membrane fouling issues and to enhance its performance.

Bacterial adhesion, micro-colony formation and biofilm maturation are the most important stages in biofilm formation, as illustrated in Figure 2-14. The primary purpose of modifying a membrane's surface is to retard one or more of these stages. For instance, increase in membrane's surface hydrophilicity, decrease in surface roughness and by providing negative charge to a membrane's surface can decrease the rate of bacterial adhesion. Similarly, incorporation of anti-microbial nanomaterials and self-assembling peptides that disrupt bacterial adhesion can help inactivating irreversibly adhered microorganisms.

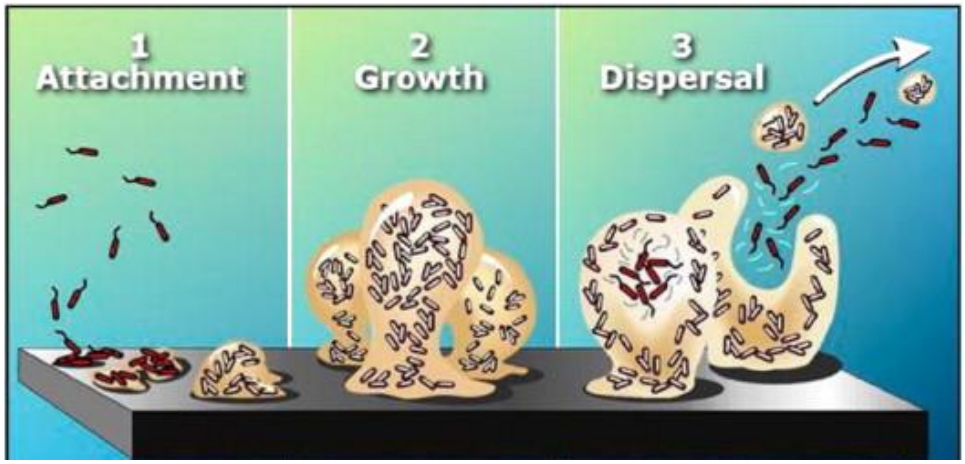

Figure 2-14: Illustration of biofilm formation on a solid's surface [84]

2.3.1. Membrane surface charge

Zeta potential measurement is done in order to quantify the charge on a membrane's surface. Negative charge is usually carried by the surface of reverse osmosis (RO), nanofiltration (NF) and ultrafiltration (UF) membranes. Sulfonic and/or carboxylic acid groups are the cause of such negative charge in a skin layer. Increase in pH of feed solution increases the negative charge of a membrane's surface due to an increase in dissociation of sulfonic/carboxylic functional groups.

When foulants carry a charge, it is quite important to consider the membrane surface charge to counter membrane fouling. Electrostatic repulsion forces between the foulants and the membrane prevent foulant deposition on the membrane when there is a similar charge on the surface and foulants [85]. However there is no definite correlation for membrane surface charge and fouling. In a previous study, surface modification of polyacrylonitrile (PAN) ultrafiltration (UF) membrane was carried out using heterogeneous photo-initiated graft polymerization of various acrylates or methacrylates having polyethyleneglycol (PEG), carboxyl, sulfopropyl, dimethylaminoethyl or trimethylammoniumethyl side groups which introduces carboxylic and sulfonic acid groups on membrane surface. This resulted in more

fouling reduction as compared to positively charged surfaces and showed better anti-fouling properties with permanently-attached anionic (sulfonic) and ionizable (carboxyl) group [86].

2.3.2. Surface hydrophilicity

It is generally assumed that an increase in hydrophilicity of a polymeric membrane can decrease fouling. However, there are only a few studies where surface hydrophilicity/-phobicity of the membrane is directly co-related to the membrane fouling.

Figure 2-15 illustrates that an increase in hydrophobicity (*i.e.* an increase in contact angle) results in a decrease in the flux ratio J_2/J_1, hence increase in fouling. However, only a limited range of contact angles (*i.e.* from 30° to 65°) is shown for the co-relation. Also this correlation has limited value, given the fact that changes in contact angle changes other membrane parameters. It is not safe to extrapolate the correlation in Figure 2-15 from very hydrophilic to very hydrophobic contact angle values, which is often exercised in the industry, particularly when ultra-low contact angle membranes are commercialized [87].

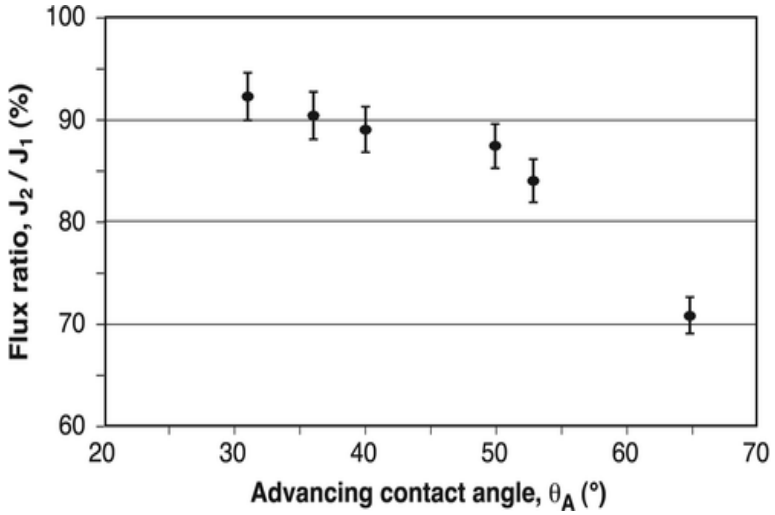

Figure 2-15: Correlation between flux and surface hydrophilicity (contact angle) [87]

Based on this assumption, many attempts have been made to modify the membranes' surface to increase its surface hydrophilicity.

Some of the techniques to increase the surface hydrophilicity are:

1. Adsorption
2. Coating
3. Surface chemical reaction
4. Surface grafting
5. Incorporation of hydrophilic polymer
6. Incorporation of nanoparticles

Table 2-7 gives an overview of the application of these techniques.

Table 2-7: Fouling reduction by increasing the surface hydrophilicity [87]

Base material	Treatment	Function of membrane
Adsorption		
PSf	Various polymers and surfactants	UF, β-lactoglobulin solution; fouling due to protein adsorption on the surface was reduced.
Coating		
PSf	PEI	UF, flux reduction in ovalbumin solution; flux reduction happened more because of hydrophilicity of the membrane than charge.
Surface Chemical Reaction		
PES	N_2, NH_3, Ar/NH_3 and O_2/NH_3 plasma	Decrease in protein fouling; water flux was increased, protein fouling was reduced and flux recovery was enhanced after gentle cleaning for modified membranes when compared to unmodified membrane.
Incorporation of hydrophilic polymer		
PES	Triblock copolymer in casting solution	UF, BSA filtration; modified membranes had an excellent recovery ratio and reduced irreversible fouling.
Incorporation of nanoparticles		
PVDF	Al_2O_3 nanoparticles	UF, oily wastewater filtration; excellent fouling resistance quality was showed by the modified membrane.

2.3.3. Incorporation of nanomaterials

Membranes become more reactive, instead of being a simple physical barrier, with the incorporation of anti-microbial nanomaterials. Hence multiple treatment goals can be achieved in one reactor while reducing the fouling.

2.3.3.1 Titania; Titanium dioxide (TiO_2)

Titania, because of its photocatalytic effect, is very effective for membrane surface modification as it can decompose organic chemicals and kill bacteria. Various active oxygen species such as hydroxyl radicals (-OH), hydrogen peroxide (H_2O_2) etc. are generated by titania photocatalysis due to reductive or oxidative reactions under light [88]. The outer membrane of the bacterial cells is further destroyed by such active oxygen species by decomposing the endotoxin. Kwak *et. al* (2001) fabricated a hybrid membrane by a self-assembly process composed of PA thin films underneath TiO_2 nano-sized particles. The antibacterial fouling potential was measured. It was found that under UV illumination, photocatalytic bactericidal efficiency was much higher for TiO_2-hybrid membranes compared to that of same membrane in darkness, as well as those for the unmodified membranes under either light condition [89].

A study has reported the use of TiO_2 nanoparticle self-assembled aromatic polyamide TFC membrane for bacterial anti-fouling. For this purpose, membrane surface was covered by a model suspension of *Escherichia coli. (E.coli.)* which was studied under UV light (500 $\mu W\ cm^{-2}$ intensity at 365 nm) and without UV light (dark condition). It is clear from Figure 2-16 that without UV light, TiO_2-hybrid TFC membrane slightly affected and decreased the survival ratio. This implies that even without UV light, TiO_2 itself may have minute photocatalysis on E. coli. The survival ratio of E. coli cells is reduced to 40% within 3 h and 37% within 4 h for the

unmodified TFC membrane under UV light. 10% of E. coli cells survived only after 3 h, reaching complete sterilization within 4 h with the TiO_2-hybrid membrane under UV light illumination. Remarkably higher photocatalytic bactericidal efficiency was observed for the TiO_2-hybrid membrane under UV light than that without illumination and unmodified TFC membranes. The photocatalytic bactericidal capability demonstrated by the TiO_2 self-assembled hybrid TFC membrane offers a strong potential for possible use as a new type of antifouling RO membrane. Kim *et al.* (2003) introduced the TiO_2 nanoparticles on a commercial RO membrane.

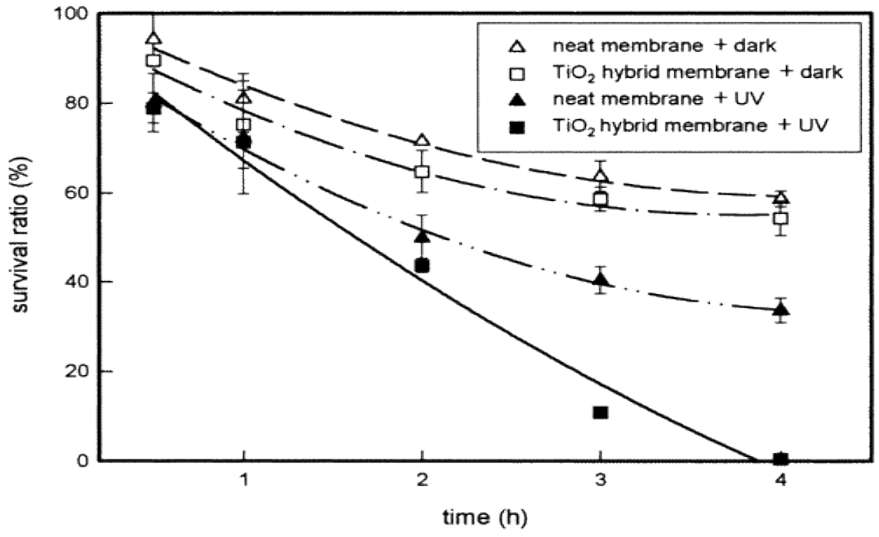

Figure 2-16: Photocatalytic bactericidal effects of the TiO_2-hybrid and unmodified aromatic polyamide TFC membranes with and without UV light illumination [89]

Figure 2-17 compares the survival ratios of *E. coli* in both unmodified and hybrid TFC membranes with and without light illumination. Under dark conditions, 60% of *E. coli* cells survived in the unmodified TFC membrane. In order to suppress the multiplication of cells, cell solution was used without nutrients in this experimental set-up. Thus, the natural diminution of cell population was unavoidable. Slightly less survival ratio was showed by TiO_2-hybrid membrane under the same conditions. 37%

of cells survived after 4 h UV illumination due to the inactivation effect caused by UV light, and this effect was accelerated by TiO_2 nanoparticles. The TiO_2-hybrid membrane (under UV light) reaches complete inactivation within 4 h. These results showed that the hybrid membranes under a given UV light wavelength can eliminate bacteria providing a photocatalytic bactericidal effects of TiO_2 [90].

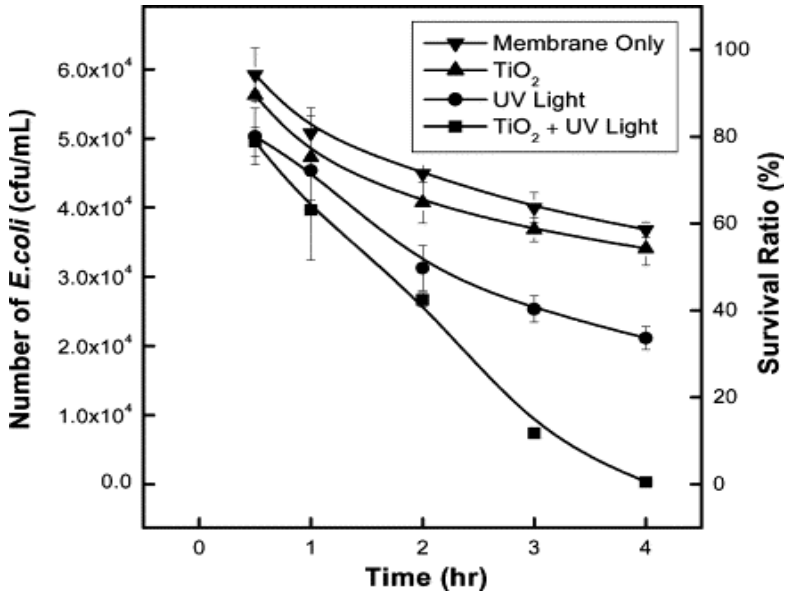

Figure 2-17: Cell number and survival ratio of *E. coli* in the hybrid and the unmodified TFC membranes with and without UV light illumination [90]

2.3.3.2 Carbon nanotubes (CNTs)

Carbon nanotubes have not received much attention as a potential material for inactivating bacteria, probably because it is hard to achieve its homogeneous and uniform dispersion in water and also the need for direct contact between the CNTs and targeted micro-organisms. Compared to conventional disinfectants, the rate of bacterial inactivation by CNTs is relatively low, however, it may be sufficient to control membrane biofouling by hindering the formation of a biofilm on the membrane surface [91].

A study provided the direct evidence that strong anti-microbial activity was exhibited by single-walled carbon nanotubes (SWCNTs). In their study, SEM images of cells exposed to SWCNTs and multi-walled carbon nanotubes (MWCNTs) revealed distinct morphological changes. After 1 h incubation with SWCNTs, most of the *E.coli* cells lost their cellular integrity with the majority of cells still intact, maintaining their outer membrane structures as cells in the control. The images in Figure 2-18 demonstrate that the extent of cell damage and the number of damaged cells are well-correlated to CNT size. SWCNTs are more toxic to *E. coli* than to MWCNTs because of its comparatively smaller diameter which allows greater physiochemical/mechanical interaction [92].

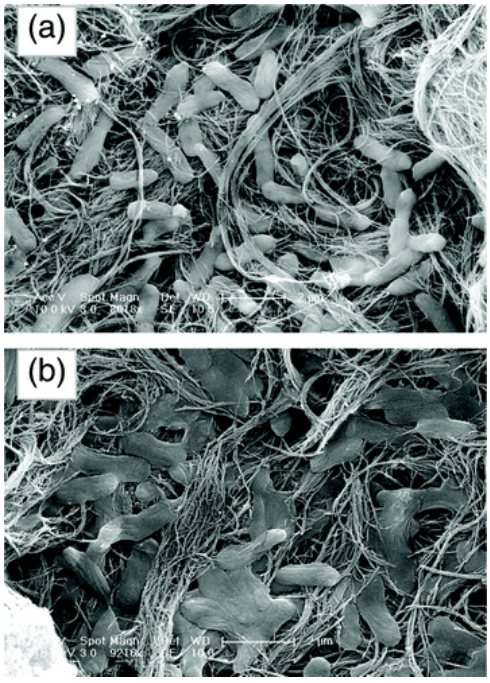

Figure 2-18: SEM images of E. coli cells exposed to CNTs. (a) Cells incubated with MWCNTs for 1 hr. (b) Cells incubated with SWCNTs for 1 hr. The bars in both images represent 2µm [92]

2.3.4. Development of low-biofouling composite membranes via interfacial polymerization

Thin-film composite membranes (TFC) for reverse osmosis (RO) and nanofiltration (NF) applications are mainly fabricated via interfacial polymerization (IP). In this process, a polysulfone microporous support is soaked in an aqueous solution of amine and is then immersed in a solution formed by mixing di-isocyanate in hexane. Afterwards, cross-linking takes place by heating the membranes to 110 °C. Results of membranes fabricated through IP show higher salt rejection and better water flux as compared to the resulting integrally-skinned asymmetric cellulose acetate membranes. But, it must be noted that IP is self-inhibiting as a limited amount of reactant is passed through the layer already formed [93].

A thin layer of polyamide (PA) is mostly present on the top surface of membranes formed via IP for NF and RO. *m*-phenylenediamine (MPD) and trimesoyl chloride (TMC) are the two active monomers involved in the formation of functional PA layers on RO/NF membranes. Recently, the IP technique has been used with the introduction of novel monomers to prepare TFC membranes. These monomers can result in better hydrophilicity and smoother surface due to the presence of more polar and functional groups, hence improving the membrane antifouling properties [94].

Adding inorganic modifiers in MPD or TMC solutions can make improvements in IP, which can in turn improve the biofouling properties of composite membranes. The fouling inhibition and surface properties of resultant membranes are enhanced by the introduction of modifiers in functional barrier layer. PES support based nanoparticle composite membranes were prepared via in situ IP procedure [95]. Nanoparticles of TiO_2 (30 nm) were dispersed in TMC. First step involves the immersion of PES support in aqueous m-phenyl diamine solution with 0.05 wt.% NaOH, while the

second step is subsequent immersion of TMC solution in 1,1-dichloro-1-fluoroethane as the excess reagent was removed in order to have a controlled reaction. As a result, PES support has a thin modified layer consisting of immobilized nanoparticles.

Jeong *et al.* (2007) also synthesized a thin-film nanocomposite (TFN) polyamide RO membrane via a dispersion of 0.004–0.4% (w/v) zeolite nanoparticles in TMC solution (Figure 2-19). The resultant membrane possesses high antifouling properties due to its lower roughness, increased hydrophilicity and more negative charge [96].

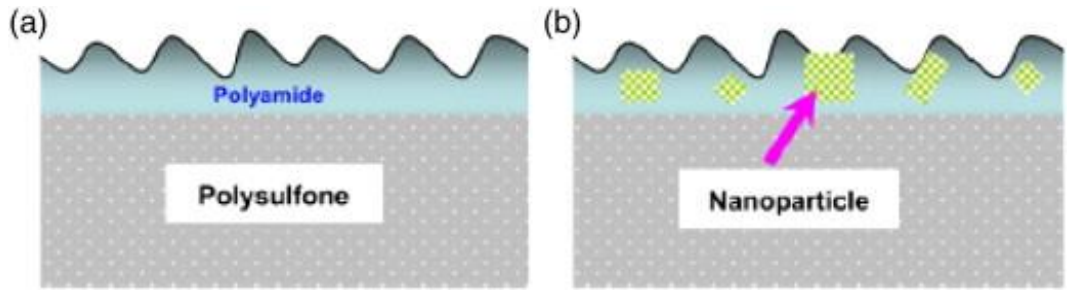

Figure 2-19: Schematic illustration of (a) TFC and (b) TFN membrane structures [96]

2.3.5. Layer-by-Layer assembly

Layer-by-Layer (LbL) assembly can be used for preparation of a low-fouling membrane surface, if polyelectrolytes are used for modification. In LbL membrane surface modification method, a polycation and a polyanion are alternately deposited on a porous substrate by means of electrostatic interaction and hydrogen bonding, as shown in Figure 2-20 (single-sided deposition is shown).

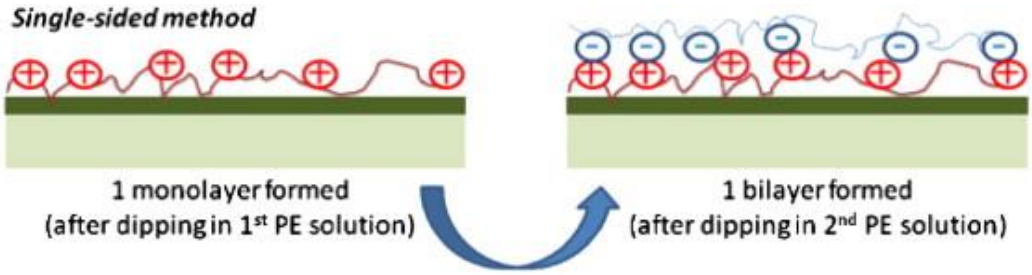

Figure 2-20: Schematic representation of membrane modification by the LbL method when only the membrane's active side is exposed and deposited with polyelectrolyte macromolecules [84]

Some advantages of the LbL method are given below:

- By varying the deposition conditions and types of polyelectrolytes, properties of the deposited layer can be optimized.
- High water flux can be attained by controlling the film thickness at the nanometer scale.
- The surface charge of the film can be either positive or negative (depending on whether the outer film is specified with a polycation or polyanion).
- Membrane surface with rough morphology can be significantly smoothed by LbL polyelectrolyte deposition. Membrane fouling is therefore expected to be reduced by LbL assembly.

Figure 2-21 shows the SEM images of an unmodified and original commercial RO membrane and the outer surfaces of the polyelectrolyte multilayered RO membranes. Figure 2-22 displayed the AFM images of these membranes. Figures 2-21A1, 2-22a clearly shows the surface morphology and rough surface topography of the original RO membrane. As the number of layers increases, the surface structure becomes smooth as shown in Figures 2-21B1, 2-21C1, 2-22b, 2-22c. The multilayered RO membrane surface is covered with a thin layer, in this case of modification with 6-

layers. As the number of layers increases to 12, the multilayered surface is further covered with polyelectrolytes and the valleys of the rough surface morphology are filled in with the deposition/coating of layers.

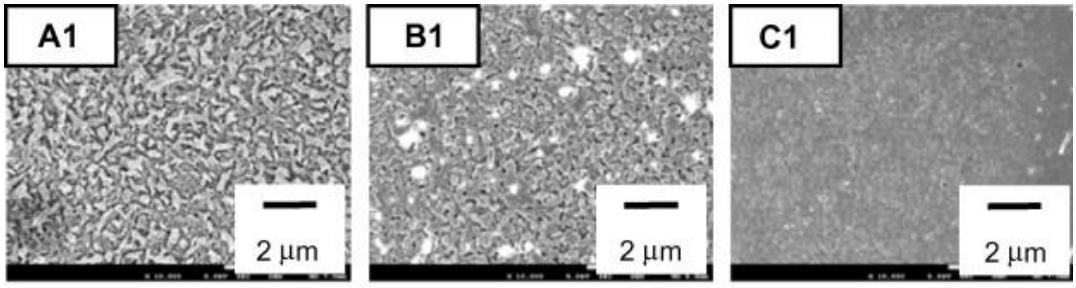

Figure 2-21: SEM images of polyelectrolyte multilayered RO membrane (a) 0-layered (b) 6-layered (c) 12-layered [97]

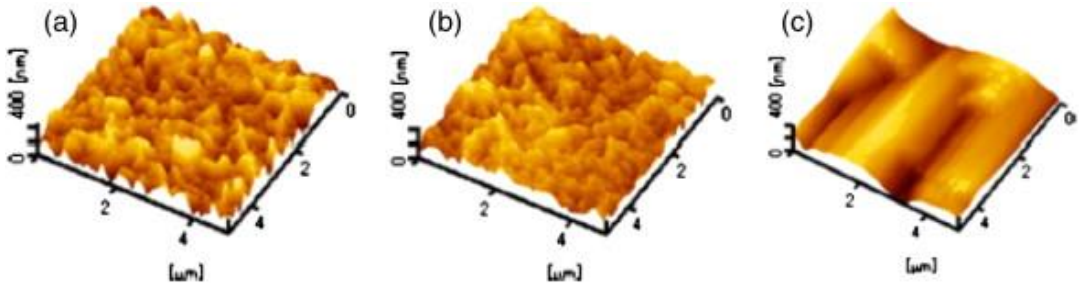

Figure 2-22: AFM images of outer surface of polyelectrolyte multilayered RO membrane (a) 0-layered (b) 6-layered (c) 12-layered [97]

Table 2-8 shows the relationship between the mean roughness (R_a) of multilayered RO membranes and the number of layers. This indicates that as the number of layers increased, the roughness decreased significantly. This result is in well-agreement with the SEM result. The antifouling capability of the polyelectrolyte multilayered RO membrane is expected to improve with such smoothed surface topography [97].

Table 2-8: Effect of number of layers on mean roughness of the outer surface of polyelectrolyte multilayered RO membranes [97]

Number of layers on RO Membrane	R_a (nm)
0 (Original)	54.9
6	44.0
12	34.8

2.3.6. Thin-film deposition methods for membrane surface modification

Thin-film deposition (TFD) is a process designed to create stratified layers of a very thin layer (ranging from few nanometers to micrometers) of material on a surface or previously deposited coating. The quality of film can be identified by its chemical and physical properties such as film density, adhesion and grain size.

There are different TFD methods which are used in lab and industrial scale, and are generally divided into two categories; physical or chemical vapor deposition. Physical vapor deposition (PVD) refers to a wide range of technologies where a material is released from a source and deposited on a substrate using mechanical, electromechanical or thermodynamic processes. It includes sputtering, electro hydrodynamic deposition, electron-beam evaporation, pulsed laser deposition (PLD), and others. While, on the other hand, chemical deposition takes place when a volatile fluid precursor produces a chemical change on a surface leaving a chemically deposited coating. Chemical vapor deposition (CVD), spin coating, and rarely-used, atomic layer deposition (ALD) are examples of chemical deposition process [98].

Comparison of these different TFD techniques is necessary to understand how each technique affects the surface features of a membrane substrate. A comparison of different TFD techniques is given in Table 2-9.

Table 2-9: Comparison of ALD with other surface deposition techniques (Taken/Reconstructed from presentation titled Atomic Layer Deposition: Introduction to the Theory and Cambridge Nanotech Savannah and Fiji, J Provine and Michelle Rincon, 2012, Stanford University, NNIN ALD Roadshow)

Method	ALD	Sputter	PLD	MBE	CVD
Thickness uniformity	G	G	F	F	G
Film density	G	G	G	G	G
Step coverage	G	P	P	V	V
Interface quality	G	P	V	G	V
Low temperature deposition	G	G	G	G	V
Deposition rate	F	G	G	F	G
Industrial applicability	V	G	P	V	G

G: Good
F: Fair
V: Varies
P: Poor

TFD has also its applications in surface modification to alter surface properties according to requirements. Many a times, ceramic materials are used for coating thin films to protect the substrate against corrosion, wear and oxidation. TFD manufacturing processes have major applications in semiconductor industry, compact discs, disc drives, solar panels and optical devices industries [99].

2.3.6.1. Atomic layer deposition (ALD)

In recent years, various substrates such as ceramics, polymers, porous materials and catalysts have been deposited via atomic layer deposition (ALD) as an effective technology for thin film deposition on substrates. ALD has shown potential advantages over alternative thin-film deposition (TFD) methods, such as various physical vapor deposition methods (PVD) (*i.e.* sputtering, electron-beam) and chemical vapor deposition (CVD) techniques, due to its control over material composition as well as thickness and conformality. The self-saturating and cyclic

nature of ALD processes is the reason behind such desirable characteristics of ALD processes [100, 101].

A typical ALD process consists of sequential reaction between alternating pulses of gaseous chemical precursors and the substrate, which is called half-reaction. During each half-reaction, a monolayer is formed through a self-limiting process in which the precursor is pulsed into a chamber under vacuum for a known amount of time to allow the complete reaction between substrate surface and precursor. Afterwards, the chamber is purged with an inert gas to remove the reaction by-products or unreacted precursor. This is then followed by the counter-reactant precursor pulse and purge, creating up to one layer of the desired material. This process is then cycled until the appropriate film thickness is achieved [102-104]. ALD schematic is shown in Figure 2-23(a).

One of the critical factors in using ALD over other competing techniques is the conformality of ALD-deposited films. The self-limiting characteristics of ALD restricts the reaction at the surface to only one layer of precursor which in turn provides conformality of high aspect-ratio and 3D-structured materials. Secondly, the precursor can disperse in deep pores and trenches allowing them to completely react with the surface due to sufficient precursor pulse times [105].

Moreover, high aspect-ratio structures and good control over thickness with high uniformity are expected due to subsequent ALD cycles, whereas PVD and CVD may result in non-uniformity due to shadowing effects and faster surface reactions respectively [106, 107]. Deposition rate controls and determines the thin-film layer thickness in the ALD method.

The ALD technique is gaining more focus and interest of researchers for different applications due to its good control over coating thickness and surface structures.

ALD is widely used in the semi-conductor industry for manufacturing of high-K dielectric materials. ALD has also attracted great interest in solar cell devices, modification of electrode surfaces and solid oxide fuel cells [108, 109]. Also, in a previous study, ALD-based surface modification of ceramic membranes for BSA retention has been investigated, however, to the best of our knowledge, the use of ALD for surface modification of ceramic membranes for water and wastewater treatment applications has not yet been reported [110].

2.3.6.2. Electron-beam physical vapor deposition

In electron-beam physical vapor deposition (e-beam deposition hereafter) method, a tungsten filament gives off an electron beam, which is used to bombard the target material under high vacuum. The atoms of the source material are evaporated to a gaseous phase due to the electron beam. Precipitation of these atoms in a vacuum chamber, having thin layer of anode, result in coating of everything. Advantage of this process is its ability to directly transfer energy in form of heat from the source material to the substrate resulting in efficient coating. Another advantage is the high deposition rate of this process, which can be as low as 1 nm per minute. Morphological and structural control on the films can be obtained by relatively high material utilization efficiency as compared to other processes. This process has industrial potential due to very high deposition rates, and can be used in aerospace industries for thermal barrier coatings, semiconductor industries for electronic and optical films, and cutting and tool industries for hard coatings. Moreover, precise layer monitoring and coating are also some of the advantages of this process. The rough and non-conformal coating quality is a major drawback of this method [111]. The major parameters that control the thickness and affect the quality of the thin-film

layer includes: voltage, current, time, deposition rate, target-to-substrate distance, deposition temperature and substrate holder rotation in rpm. The schematic of e-beam method is shown in Figure 2-23(b).

2.3.6.3 Sputter coating

Sputtering involves the coating of material from a source onto a substrate in a vacuum chamber. This is done by the bombardment of ionized gas on the target, which is usually an inert gas as argon. The semiconductor industry uses sputtering extensively to deposit thin films of different materials in integrated-circuit processing. Sputtering is also used for the coatings of anti-reflection glass for optical applications. The most-common application of sputtering is low-emissivity coatings on glass, used in double-pane window assemblies. Sputtering has an advantage over Knudsen cell or resistance evaporator as materials having high melting points can be coated easily [112]. The major parameters that control the thickness and affect the quality of the thin-film layer includes: voltage, time, target-to-substrate distance, deposition temperature and partial pressure of argon. The schematic diagram for sputter coating method is shown in Figure 2-23(c).

2.3.6.4. Pulsed laser deposition (PLD)

Pulses of laser energy are used in this extremely simple technique, to remove material from the target surface, as shown in Figure 2-23(d). A laser-produced plasma plume is created as the vaporized material containing ions, neutrals, electrons etc., rapidly expands away from the surface of the target. Re-condensation of the plume material results in film growth on the substrate. However, the actual situation may differ due to effects of different variables on thin film properties, such as substrate temperature,

gas pressure and laser fluence. However, considerable effort and time is required to optimize the process. Indeed, much of the early research into PLD focused on the empirical optimization of deposition conditions for different materials and applications, without the proper understanding of material transport processes [113].

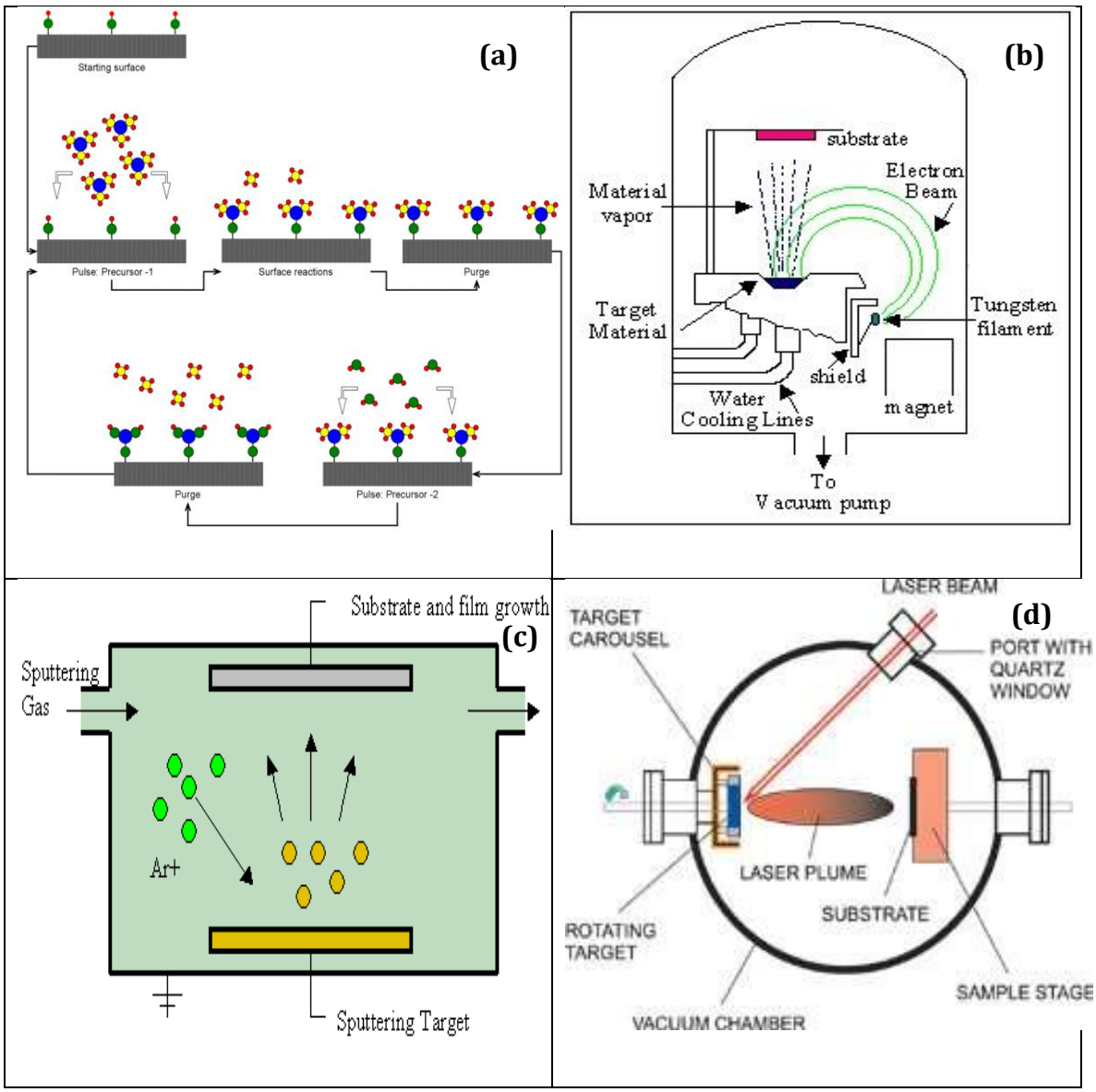

Figure 2-23: Schematics of thin-film deposition methods (a) Atomic layer deposition [114] (b) Electron-beam deposition [115] (c) Sputtering [116] (d) Pulsed laser deposition [117]

CHAPTER: 3
MATERIALS AND METHODS

Based on the scope and objectives of this study, a list of materials and methods to be used to carry out this PhD research has been identified. This chapter outlines the materials and methods applied in due detail, which can broadly be divided into the following two categories:

1. Membrane surface modification and characterization
2. Membrane filtration tests and analysis

The detail of each method employed is given below:

3.1. Membrane surface modification and characterization

3.1.1. Membrane surface modification by ALD, sputter and e-beam evaporation methods

A commercially available flat sheet alumina ultrafiltration (UF) membrane module (KeraNor, Norway) with a nominal surface pore size of 80 nm (as reported by the manufacturer) and effective filtration area of 60 cm^2 was used as the basis for modifying the surface. Ultrathin films of TiO_2 and SnO_2 were deposited on the porous alumina membranes at 150 °C using a Cambridge Nanotech Savannah ALD system. The sequence of TiO_2 ALD reaction applied consisted of; 1) a constant N_2 dose at 20 psi; 2) $TiCl_4$ dose for 0.2 sec; 3) $TiCl_4$ reaction time 15 sec; 4) H_2O dose for 0.015 sec; 5) H_2O reaction time 10 sec. This sequence constitutes one ALD cycle, which corresponds to a deposition growth rate of 0.05 nm per cycle. 600 ALD cycles were applied on the membrane surface, giving a film thickness of around 30 nm. The sequence of SnO_2 ALD reaction consisted of; 1) a constant N_2 dose at 20 psi, 2) Sn precursor (Tetrakis(diethylamido) tin(IV)) dose for 0.5 sec, 3) Sn precursor reaction time 15 sec, 4) O_3 oxidant dose for 0.2 sec, and 5) oxidant reaction time 10 sec.

Ultrathin films of TiO_2 having the same film thickness were also deposited on the alumina substrates using the sputter (NEXDEP 120) and e-beam (Denton Vacuum) systems. The deposition conditions were adjusted to obtain as comparable thickness of the TiO_2 film on the modified alumina membranes as possible. After the TiO_2-deposition, all the modified membranes were annealed at a high temperature of 500 °C to strengthen the interfacial adhesion between the TiO_2 film and the substrate membrane surface.

3.1.2. Membrane surface characterization

3.1.2.1. Scanning electron microscopy

The surface morphology of all TiO_2-modified alumina membranes was characterized by a field emission scanning electron microscope (FE-SEM) of model (NovaNanoSEM from FEI Company). Membrane samples were mounted on brass stubs and sputter coated with 1 nm thick gold layer to increase their conductivity. SEM images of the samples were taken at low and high magnifications.

3.1.2.2. Mean contact angle measurement

Mean water contact angle measurements were performed for alumina and all modified membranes using a Dropmeter A-100 contact angle goniometer. Deionized (DI) water was used as the probe liquid in all measurements. Membrane samples were dried at 40 °C in a vacuum oven prior to the measurement. For contact angle measurements, a dangling drop of DI water at the end of an ‘I’-shaped needle was carefully deposited onto the membrane surface to avoid the effect of falling force by gravity. Experimental error was minimized by taking average values of five measurements of water contact angle for each sample.

3.1.2.3. Atomic force microscopy

Surface roughness of the alumina and all modified membranes was determined by an atomic force microscope (AFM, Agilent Technologies) using the tapping mode. Membrane samples were fixed on a flat solid steel disc, which is magnetically attached to the support of instrument itself. The AFM tip makes gentle intermittent contact with the sample surface during scanning as the cantilever oscillates at its resonant frequency, providing the surface images. Analyses were repeated for at least five times for each sample to obtain an average value.

3.1.2.4. Transmission electron microscopy

Energy dispersive X-ray spectrum (EDS) of the ALD-modified membranes was taken by a transmission electron microscopy (TEM, Titan G2 80–300 ST, FEI). The TEM samples were prepared by scratching TiO_2 off alumina substrate and dispersing it in ethanol.

3.1.2.5. Thin-film thickness measurement

Thickness of the thin films deposited by each TFD method was measured by a mechanical surface profilometer (Veeco Dektak 150). The thin films of metal-oxide were deposited on a polished silicon substrate and a *'step'* was created with a tape or marker to measure the film thickness using the mechanical profilometer. Ten measurements were taken for each modified membrane to obtain an average thickness.

3.2. Membrane filtration tests and analysis

3.2.1. Clean water permeability (CWP) tests

Clean water permeability (CWP) was determined with MQ water for unmodified membranes and all modified membranes. Nominal pore size of the unmodified membrane was 80 nm, as reported by manufacturer, with effective filtration area of 30 cm^2. The CWP was determined by dead-end filtration experiments conducted at a pressure of 0.7 bar and 21 °C. The permeate flux was measured by collecting permeate over time on a balance connected to a computer. Average values were obtained by taking at least three measurements in order to minimize the experimental error.

3.2.2. Bovine serum albumin (BSA) adsorption tests

The fouling behavior was first assessed using a model compound. A membrane's propensity to fouling can be evaluated by the amount of BSA protein adsorbed onto the membrane surface [118]. A similar method has been applied for this test as used by previous researchers [119]. Adsorption tests were conducted by placing samples of the original alumina membrane and all modified membranes into separate glass vials filled with 5 mL of a phosphate buffer solution (pH=7.4) containing 1 g/L BSA. The glass vials were then incubated in a water bath at 28 °C for 12 h to reach equilibrium. The amount of adsorbed BSA was measured by calculating the difference between concentration of BSA in the bulk solution before and after adsorption. Concentration values were determined from the absorption intensity at 280 nm recorded on a UV-Vis spectrophotometer (UV-2550, Shimadzu). An average value was obtained by repeating the test for three times.

3.2.3. AnMBR filtration tests (side-stream, constant-flux)

Figure 3-1 shows the schematics of the lab-scale AnMBR used in this study. A continuous anaerobic completely stirred tank reactor (CSTR, Applikon Biotechnology, Netherlands) was operated in constant-flux mode with the membrane module operated in a side-stream mode, similar to that explained by other researchers [120]. The AnMBR system was well-stabilized and had been continuously operated for more than a year prior to the filtration runs made for this study. The effective volume of the CSTR tank was 2 liter. The AnMBR system was operated at a constant flux of 30 $L.m^{-2}.h^{-1}$. The hydraulic retention time (HRT) and organic loading rate (OLR) were fixed at 11 h and 0.87 $g.L^{-1}.d^{-1}$ respectively. Total organic carbon (TOC) concentration was 115 ± 5 mg/L. Influent chemical oxygen demand (COD) was 400 ± 10 mg/L, COD removal efficiency was around 90% ± 5% and mixed liquor suspended solids (MLSS) concentration was 5 ± 1 mg/L. COD and MLSS were determined according to standard methods [121]. The seed sludge was a pre-screened (0.5 mm mesh size) mixture of camel manure from Jeddah and anaerobic digester sludge from a wastewater treatment plant in Riyadh, Saudi Arabia. The sludge retention time (SRT) was approximated to be 1000 d, calculated by dividing the total sludge volume in the CSTR by daily sludge volume wastage. Using the built-in control systems of this commercial CSTR unit, the anaerobic bioreactor was kept completely mixed with a stirrer at speed of 200 ± 2 rpm, temperature of 35 ± 1 ^{o}C (mesophilic) and pH of 7 ± 0.1 during the whole operation. There was evidence of biogas generation in the AnMBR system, as it was stabilized and had been in operation a long time, however, the composition of the biogas was not measured during the filtration trials of this study. The AnMBR filtration runs were duplicated under the same operating conditions for each unmodified and modified membranes.

Change in the trans-membrane pressure (TMP) was recorded to assess the filtration performance of the membrane modules (*i.e.* fouling). The operating conditions of the AnMBR system are summarized in Table 3-1. The system was operated with a synthetic municipal wastewater feed, with composition as outlined in Table 3-2.

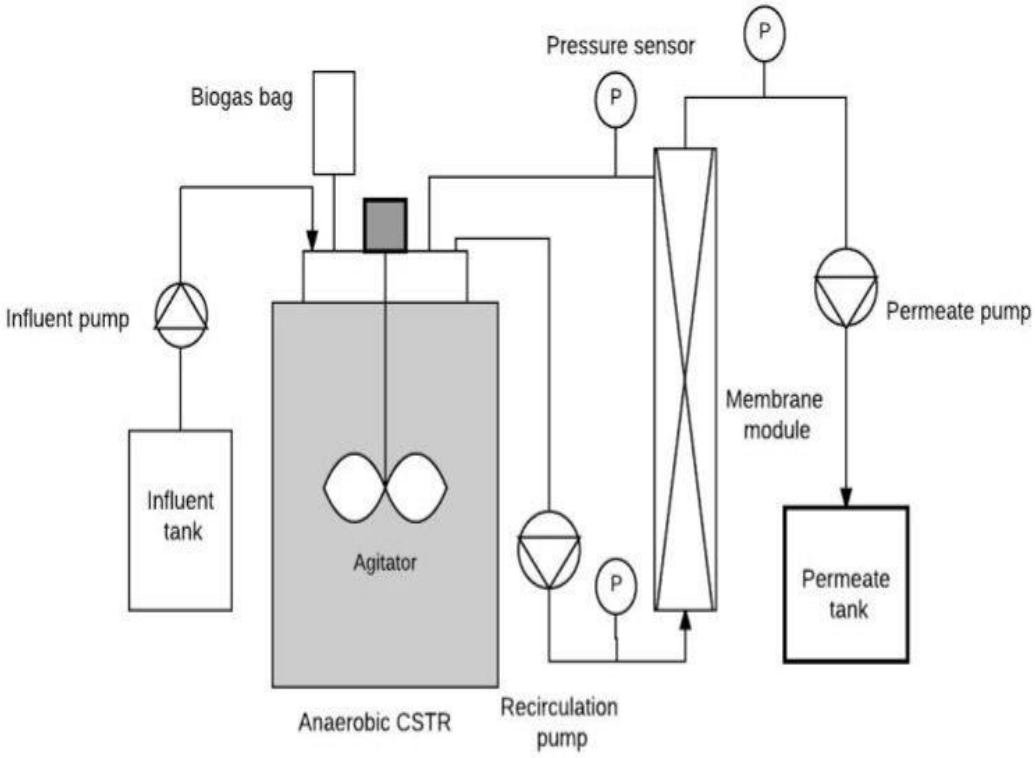

Figure 3-1: Schematic diagram of anaerobic MBR (AnMBR) setup

Table 3-1: Working conditions of AnMBR system

Working Volume	2 L
pH	7 ± 0.1
HRT	11 h
Membrane material	Alumina (KeraNor)
Membrane average surface pore size	80 nm
Membrane area	60 cm^2
Flux	30 $L/m^2.h$
Feed COD	400 ± 10 mg/L
COD removal efficiency	90 ± 5 %
MLSS	5 ± 1 g/L
OLR	0.87 g/L.d
Cross-flow velocity (CFV)	0.33 cm/s

Table 3-2: Composition of synthetic municipal wastewater

Components	Concentration (mg/L)
Urea	91.7
NH_4Cl	12.8
Na-acetate	79.4
Peptone	17.4
$MgHPO_4.3H_2O$	29.0
KH_2PO_4	23.4
$FeSO_4.7H_2O$	5.8
Starch	122
Milk powder	116
Yeast	52.2
$Cr(NO_3)_3.9H_2O$	0.77
$CuCl_2.2H_2O$	0.536
$MnSO_4.H2O$	0.108
$NiSO_46H_2O$	0.336
$PbCl_2$	0.100
$ZnCl_2$	0.208

3.2.4. Extracellular polymeric substances (EPS) extraction and analysis

The EPS components in the cake layer on the surface of the fouled membranes were extracted by ultra-sonication for 15 mins and filtered through a 0.45 µm filter paper. The Lowry method with bovine serum albumin as the standard reference [122] was used to measure the proteins. Carbohydrates were measured by the Dubois method using glucose as the standard reference [123]. EPS extraction and analysis tests were conducted after each filtration run.

3.2.5. Alginate filtration tests (dead-end, constant-pressure)

Alginate powder (Roche Company) was used to prepare alginate solutions by dissolving alginate powder in deionized (DI) water, and used shortly after preparation. The pH values were adjusted to 7.0 by addition of HCl or NaOH as needed in all solutions. All the experiments were carried out using the unmodified alumina membrane and the two ALD-TiO_2 and ALD-SnO_2 modified membranes, each with around 30 nm thick films. Temperature and pH of all the solutions were measured using a digital thermometer and a digital pH meter (Precisa series 900), respectively. All the experiments were conducted with a batch microfiltration cell. The membrane module was a rectangular cell which was connected to a solution reservoir at atmospheric pressure. A dead-end constant-pressure mode of operation was applied for the filtration tests using a vacuum pump on the permeate side. The trans-membrane pressure (TMP) was measured using two pressure meters before (atmospheric) and after (vacuum) the membrane cell. The volumetric flow rate was measured by continuously by measuring the filtrate volume. At the beginning of all the experiments, the solution reservoir was filled with DI water and the filtration was conducted with water until a steady condition was attained, then the solution reservoir and the membrane cell were evacuated and quickly refilled with the feed solution. All the experiments were conducted at room temperature (22°C ± 1) and feed concentrations of 1.5 g/L alginate at a constant TMP of 1.5 bar. The filtration runs were repeated three times for each membrane. The experimental set-up is shown in Figure 3-2.

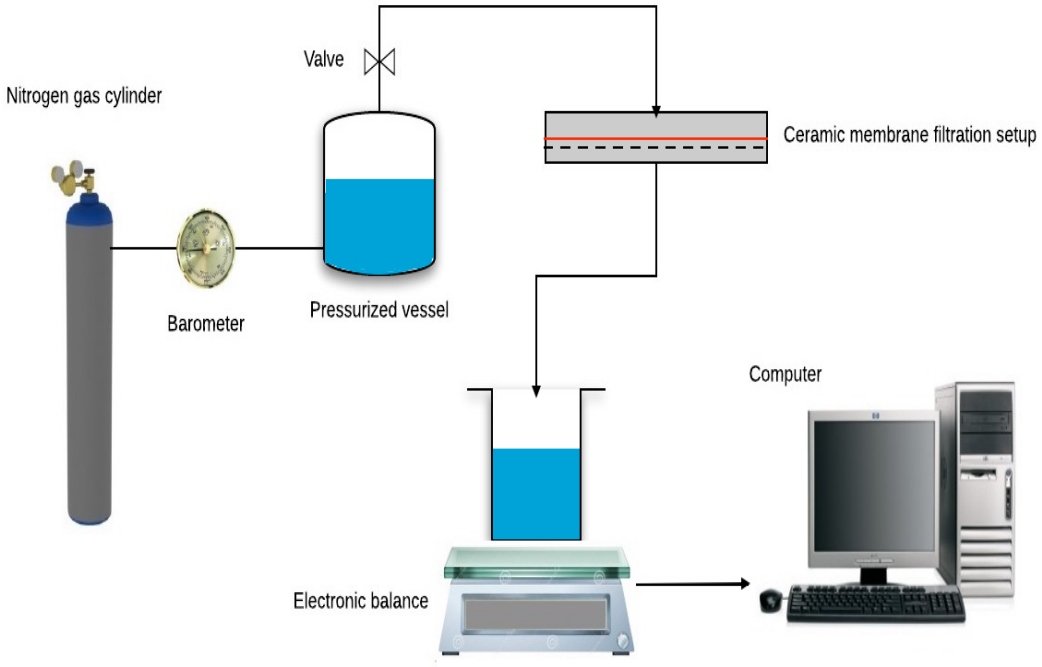

Figure 3-2: Constant-pressure alginate filtration setup

CHAPTER: 4

SURFACE MODIFICATION OF CERAMIC MEMBRANE WITH DIFFERENT THIN-FILM DEPOSITION METHODS AND APPLICATION IN ANAEROBIC MBR FOR WASTEWATER TREATMENT

Highlights

- Alumina membrane surface was modified with TiO_2 using atomic layer deposition (ALD), sputter and electron-beam evaporation methods.
- The TiO_2-modified alumina surfaces showed different characteristics for different thin-film deposition (TFD) methods.
- All TiO_2-modified membranes reduced membrane fouling in lab-scale AnMBR filtration tests.
- The ALD-modified membrane showed superior fouling inhibition performance in AnMBR filtration tests compared with other TFD methods.

Abstract

Membrane fouling is still a bottleneck that hampers the widespread application of MBR technology for wastewater treatment. Recently membrane surface modification has proved to be a useful method in water and wastewater treatment to improve surface hydrophilicity of membranes to obtain high water flux and to reduce fouling. Due to its anti-fouling properties, TiO_2 is well-known for surface modification in water treatment applications. In this study, thin film of same thickness of TiO_2 was deposited over ultrafiltration (UF) alumina membrane surfaces (average surface pore size = 80 nm) via different thin-film deposition (TFD) methods i.e. atomic layer deposition (ALD), sputter and electron-beam physical vapor deposition. The objective of this study was to compare the surface characteristics and the fouling inhibition performance of all these modified membranes in a lab-scale anaerobic membrane bioreactor (AnMBR) for wastewater treatment.

Clean water permeability (CWP) and bovine serum albumin (BSA) adsorption tests were conducted for unmodified and all modified membranes. Thorough surface characterization of unmodified and modified membranes was carried out including: contact angle measurement, atomic force microscopy (AFM) and scanning electron microscopy (SEM). When all the modified membranes were applied in a constant-flux AnMBR filtration system, they showed a lower fouling rate (*i.e.* slower rise in trans-membrane pressure) compared to the unmodified alumina membrane. However, the ALD-based modification showed a superior fouling inhibition performance in short-term AnMBR filtration tests compared to the other deposition methods. Extracellular polymeric substances (EPS) concentration measurement and analysis was also carried-out for fouled membranes. This study also revealed that same

thickness of TiO_2 thin film on alumina membrane surface showed different characteristics for different deposition methods.

4.1 Introduction

Deposition of retained particles, colloids, organic matter, etc. inside membrane pores or on the membrane surface causes fouling. Membrane flux can be significantly reduced by the fouling behavior and can seriously affect the operational performance of membrane-based water and wastewater treatment systems. Several previous studies revealed that an increase in membrane surface hydrophilicity results in better control of the fouling problem because organics and many other foulants are hydrophobic in nature. Recently atomic force microscopy (AFM) has been widely utilized to study the effect of surface roughness on membrane fouling at nanoscale. Studies showed that an increase in surface roughness of a membrane can increase the fouling problem. As fouling is essentially a surface phenomenon, researchers are very interested in surface modification of membranes to improve surface properties in order to counter the problem of membrane fouling in water and wastewater applications [87, 124, 125].

Thin-film deposition (TFD) has recently attracted attention for surface modification to alter the features of a specific surface according to requirements. The thin film is a layer of some material, deposited over a substrate, with a thickness ranging of few nanometers to several micrometers. Thin-film deposition has wide application in optical, battery and electronics industry. Thin films of ceramic materials are widely used in various industries where the substrate is highly protected from wear, corrosion and oxidation due to the intrinsic inertness and hardness of the thin ceramic film. Research is underway to develop thin film coating materials with superior properties [108, 109].

Various TFD methods, including physical and chemical deposition techniques, are being applied on laboratory and industrial scales for a wide range of applications. The

brief details of such TFD methods have been discussed in chapter 2 (sub-section 2.3.6) and a comparative study of different TFD techniques is given in Table 2-9.

Due to merits and demerits of different TFD techniques, a comparative study of these techniques was conducted to understand how each technique affects the features and significant properties of thin-film modified substrate surfaces. Therefore, the basic objective of this study was to modify the surface of a commercial alumina membrane (nominal surface pore size = 80 nm, as reported by the manufacturer) by a TiO_2 thin film using different deposition methods in order to compare the characteristics and fouling behavior of each modified membrane in a lab-scale anaerobic membrane bioreactor (AnMBR) treating synthetic wastewater. In this study, the atomic layer deposition (ALD), sputter and electron-beam (e-beam) deposition methods were used to deposit TiO_2 on an alumina membrane surface. The TiO_2-coated alumina membranes were further characterized in terms of surface hydrophilicity, surface roughness, clean water permeability (CWP) and bovine serum albumin (BSA) adsorption potential. Later, the unmodified alumina membrane and all modified membranes were applied in a lab-scale AnMBR filtration system to test their fouling behavior in a short-term operation. All modified membranes showed improved fouling inhibition performance compared to that of the unmodified alumina membrane. Concentration of extracellular polymeric substances (EPS) was also measured in the cake layer formed on the surface of the fouled membranes. This study revealed that membranes modified with different deposition methods exhibited different behavior in terms of surface characteristics and fouling behavior in the lab-scale AnMBR filtration system.

4.2 Materials and methods

4.2.1. Membrane surface modification by ALD, sputter and e-beam methods

A commercially available flat sheet alumina ultrafiltration (UF) membrane module (KeraNor, Norway) with a nominal surface pore size of 80 nm (as reported by the manufacturer) and effective filtration area of 60 cm^2 was used as the basis for modifying the surface. An ultrathin film of TiO_2 was deposited on the porous alumina membranes at 150 °C using a Cambridge Nanotech Savannah ALD system. An ALD cycle corresponds to a deposition growth rate of 0.05 nm. 600 ALD cycles were applied on the membrane surface, giving a film thickness of around 30 nm. Ultrathin films of TiO_2 having the same film thickness was also deposited on the alumina substrates using the sputter (NEXDEP 120) and e-beam evaporation (Denton Vacuum) systems. The deposition conditions were adjusted to obtain as comparable thickness of the TiO_2 film on the modified alumina membranes as possible. After the TiO_2-deposition, all the modified membranes were annealed at a high temperature of 500 °C to strengthen the interfacial adhesion between the TiO_2 film and the substrate membrane surface.

4.2.2. Membrane surface characterization

4.2.2.1. Scanning electron microscopy

The surface morphology of all TiO_2-modified alumina membranes was characterized by a field emission scanning electron microscope (FE-SEM) of model (NovaNanoSEM from FEI Company). SEM images of the samples were taken at low and high magnifications.

4.2.2.2. Mean contact angle measurement

Mean water contact angle measurements were performed for alumina and all modified membranes using a Dropmeter A-100 contact angle goniometer. Deionized (DI) water was used as the probe liquid in all measurements. Experimental error was minimized by taking average values of five measurements of water contact angle for each sample.

4.2.2.3. Atomic force microscopy

Surface roughness of alumina and modified membranes was determined by an atomic force microscope (AFM, Agilent Technologies) using tapping mode. Membrane samples were fixed on flat solid steel disc which is magnetically attached to the support of instrument itself. The experiment was repeated five times for each sample to obtain an average value.

4.2.2.4. TiO_2 thin-film thickness measurement

Thickness of TiO_2 film deposited by each TFD method is measured by mechanical surface profilometer (Veeco Dektak 150). Ten measurements were taken to obtain an average thickness.

4.2.3. Clean water permeability (CWP) tests

Clean water permeability (CWP) was determined with MQ water for unmodified membranes and all modified membranes. Nominal pore size of the unmodified membrane was 80 nm, as reported by manufacturer, with effective filtration area of 30 cm^2. The CWP was determined by dead-end filtration experiments conducted at a pressure of 0.7 bar and 21 °C. The permeate flux was measured by collecting permeate over time on a balance connected to a computer. Average values were obtained by taking three measurements in order to minimize the experimental error.

4.2.4. Bovine serum albumin (BSA) adsorption tests

The fouling behavior was first assessed using a model compound. A membrane's propensity to fouling can be evaluated by the amount of BSA protein adsorbed onto the membrane surface [118]. A similar method has been applied for this test as used by previous researchers [119]. Adsorption tests were done by placing samples of the original alumina membrane and all modified membranes into separate glass vials filled with 5 mL of a phosphate buffer solution (pH=7.4) containing 1 g/L BSA. The glass vials were then incubated in a water bath at 28 °C for 12 h to reach equilibrium. The amount of adsorbed BSA was measured by calculating the difference between concentration of BSA in the bulk solution before and after adsorption. Concentration values were determined from the absorption intensity at 280 nm recorded on a UV-Vis spectrophotometer (UV-2550, Shimadzu). An average value was obtained by repeating the test three times.

4.2.5. AnMBR filtration tests

A schematic of the lab-scale AnMBR system used in this study is shown in Figure 3-1 (Chapter 3). A continuous anaerobic completely stirred tank reactor (CSTR, Applikon Biotechnology, Netherlands) was operated in constant-flux mode with the membrane module operated in a side-stream mode, similar to that explained by other researchers [120]. The effective volume of the CSTR tank was 2 liter. The system was operated at a constant flux of 30 $L.m^{-2}.h^{-1}$. The hydraulic retention time (HRT) and organic loading rate (OLR) were fixed at 11 h and 0.87 $g.L^{-1}.d^{-1}$ respectively. Total organic carbon (TOC) concentration was 115 ± 5 mg/L. Influent chemical oxygen demand (COD) was 400 ± 10 mg/L, COD removal efficiency was around 90% ± 5% and mixed liquor suspended solids (MLSS) concentration was 5 ± 1 mg/L. COD and MLSS were determined according to standard methods [121]. There was evidence of biogas generation in the AnMBR system, however, the composition of biogas was not measured in this specific study. The AnMBR filtration runs were duplicated under the same operating conditions for each unmodified and modified membranes and trans-membrane pressure (TMP) recorded. The operating conditions of the AnMBR system and composition of synthetic municipal wastewater feed are given in Table 3-1 and Table 3-2 respectively.

4.2.6. Extracellular polymeric substances (EPS) extraction and analysis

The EPS in the cake layer on the fouled membrane surface was extracted by ultra-sonication for 15 mins and filtered by a 0.45 µm filter paper. The Lowry method, with bovine serum albumin as the standard reference [126], was used to measure the proteins concentration. Carbohydrates concentration were measured by the Dubois

method using glucose as the standard reference [127]. EPS extraction and analysis tests were conducted after each filtration run.

4.3 Results and discussion

4.3.1. Surface morphology of unmodified and TiO_2-modified alumina membranes

Thickness of each deposited TiO_2 film was measured by a mechanical surface profilometer (Veeco Dektak 150). The measured thickness values of TiO_2 films are found to be around 30 nm and are in reasonable agreement with the deposition conditions applied for the atomic layer deposition (ALD), sputter and electron-beam (e-beam) deposition methods. However, ALD was determined to have an excellent control over thickness and it can be finely tuned as compared to that for the sputter and e-beam methods.

The surface morphology of the unmodified and all modified alumina membranes (*i.e.* modified by ALD, sputter, e-beam) was investigated using a scanning electron microscope (SEM). Figure 4-1(a-d) presents the SEM images of the unmodified alumina membrane and all modified membranes (TiO_2 film thickness ~ 30 nm). Surface morphology of the unmodified alumina membrane, with an average surface pore size of 80 nm (as reported by manufacturer), can be observed in Figure 4-1(a). The conformal nature of the ALD-based TiO_2 film can be observed in Figure 4-1(d). The deposited TiO_2 takes the shape of alumina grains. This observation is in well-agreement with the basic operation principal of ALD. SEM images confirmed that TiO_2 film was uniformly deposited over the alumina substrate by the ALD method (Figure 4-1b). However, the images show that TiO_2 deposition was not as uniform for the sputter (Figure 4-1c) and e-beam (Figure 4-1b) based modification as it was for

the ALD-based modification. Hence, the ALD-based surface modification was concluded to be well-controlled and resulting in a uniform distribution of TiO_2 on the surface of the alumina membrane. The energy dispersive spectroscopy (EDS) spectrum of the TiO_2-modified alumina membrane is presented in Figure 4-1e, which confirms the presence of Ti and O and the surface of alumina membrane.

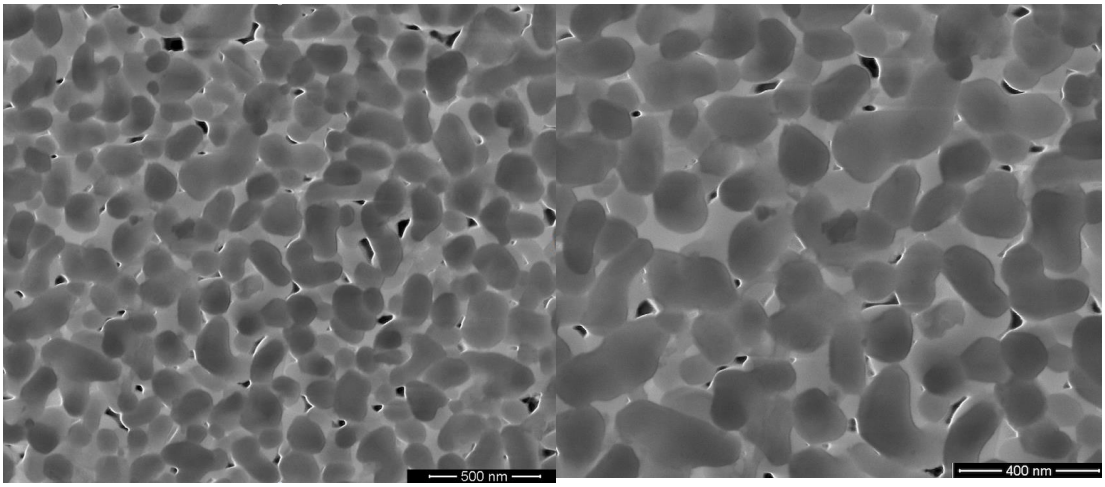

(a)

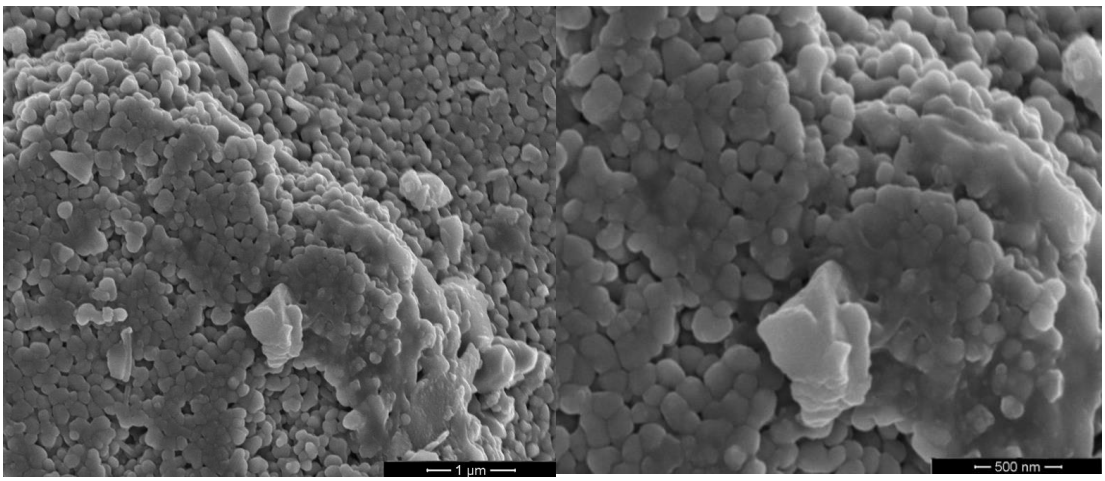

(b)

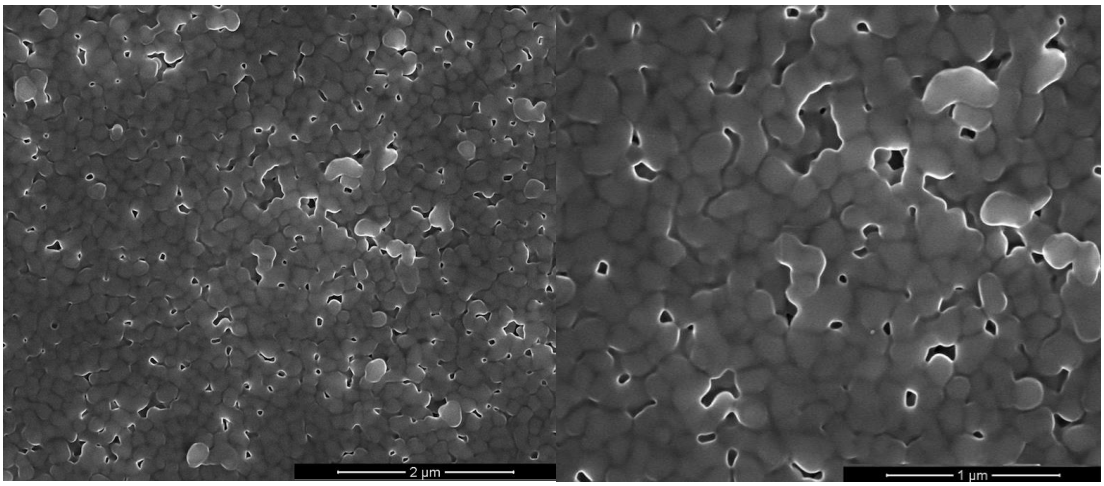

(c)

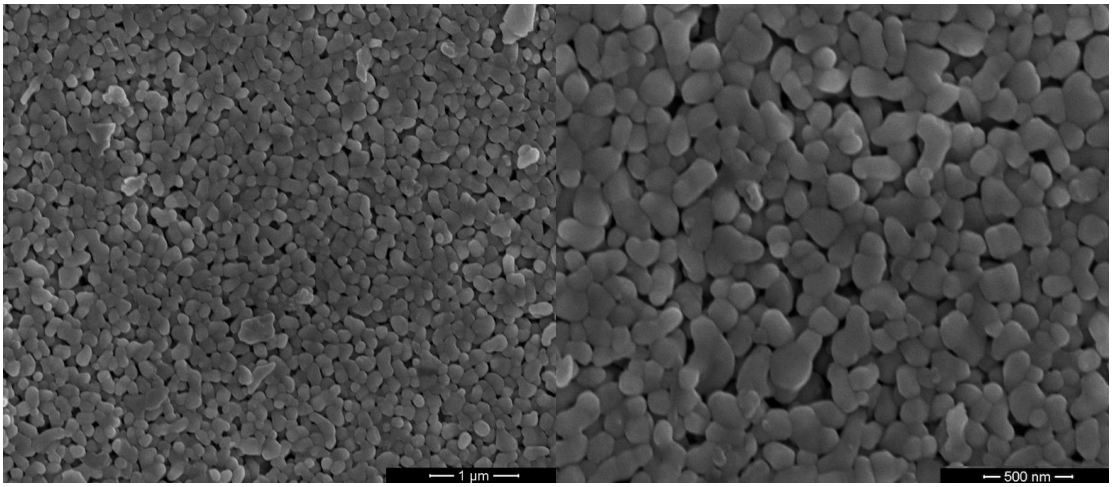

(d)

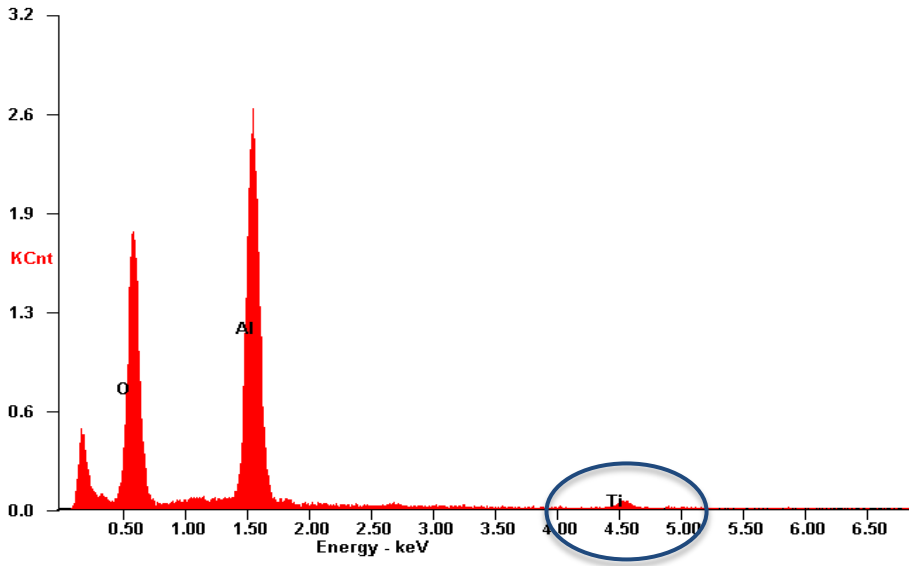

(e)

Figure 4-1: SEM surface images of (a) Unmodified alumina membrane at magnification 50,000 and 80,000 (b) e-beam TiO_2-modified alumina membrane at magnification 20,000 and 40,000 (c) Sputter TiO_2-modified alumina membrane at magnification 20,000 and 40,000 (d) ALD TiO_2-modified alumina membrane at magnification 20,000 and 40,000 (e) SEM-EDS spectrum showing presence of Al, O and Ti on the surface of a TiO_2-modified alumina membrane

4.3.2. Effect of TiO_2-modification with different TFD methods on surface hydrophilicity

Mean water contact angles of the unmodified alumina membrane and all modified membranes were measured. Figure 4-2 represents the contact angle plot for water droplets on unmodified and all modified membranes. It can be clearly seen that surface hydrophilicity of the unmodified alumina membrane (contact angle = 84.3°) significantly increased after deposition of the same thickness of TiO_2 film via different TFD methods. However, the ALD-based TiO_2 modification increased the surface hydrophilicity of the alumina membrane to a higher level compared to those based on sputter and e-beam modification. This is probably due to the fact that the ALD-TiO_2 coating was very conformal and uniform on the membrane surface, as observed in SEM images (Figure 4-1d). The conformal coating obtained resulted in a low contact angle of 26.2°, indicating high hydrophilicity and wettability for the ALD-TiO_2 modified surface. For sputter-TiO_2 modification, the coating was not as uniform and conformal as observed for ALD-modification, as can also be seen in SEM images (Figure 4-1c). The higher contact angle of 42.9° is assumed to be due to the more non-uniform distribution of TiO_2 onto the membrane surface giving lower wettability than that for the ALD-TiO_2 modification. In the case of e-beam deposition, a similar response was observed with a poorer quality, non-uniform and rougher surface obtained compared to that for ALD and sputter deposition (shown in SEM images Figure 4-1b). This resulted in a higher contact angle of. 53° compared with the membranes modified with ALD (26.2°) and sputter (42.9°) methods.

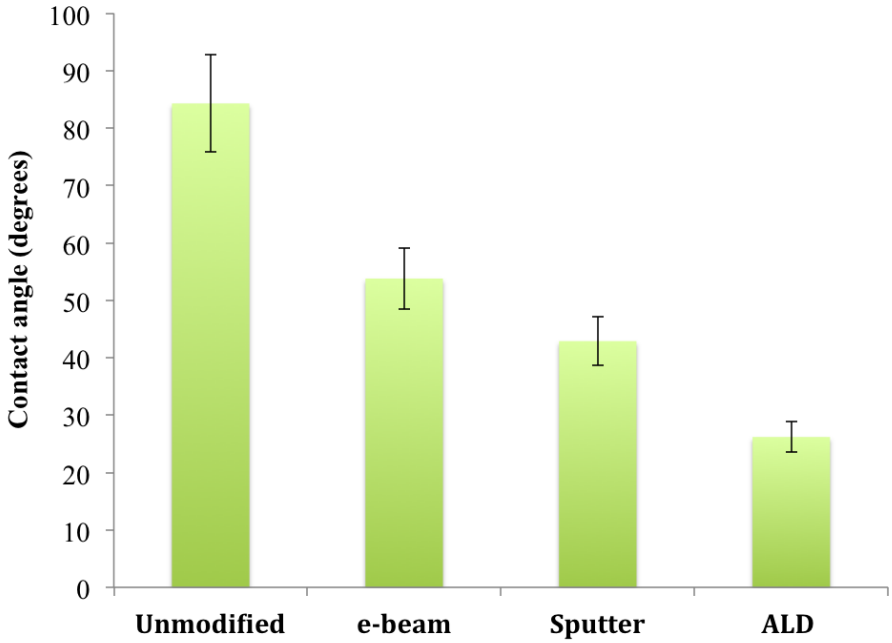

Figure 4-2: Contact angle of unmodified alumina membrane and membranes modified with TiO_2 deposition employing e-beam, sputter and ALD methods.

4.3.3. Clean water permeability of unmodified and TiO_2-modified alumina membranes

Clean water permeability (CWP) tests were conducted for unmodified alumina membrane and all modified membranes and results are plotted in Figure 4-3. CWP results are determined to be in well-accordance with SEM images and surface hydrophilicity results. Figure 4-3 shows that intrinsic CWP was determined to be 1200 $L.m^{-2}.h^{-1}.bar^{-1}$ for unmodified alumina membrane and 1155 $L.m^{-2}.h^{-1}.bar^{-1}$ for ALD-TiO_2 modified membrane. This finding implies that ALD-modified membranes nearly retained intrinsic CWP of bare alumina membrane. The CWP for sputter and e-beam modified membranes were determined to be 980 and 825 $L.m^{-2}.hr^{-1}.bar^{-1}$ respectively. Despite the fact that same thickness (30 nm) of TiO_2 thin film was deposited on alumina membrane surface by each deposition method, we have observed that CWP was decreased in a relatively higher fraction for sputter and

e-beam based surface modification as compared to that for ALD-based modification. The decrease in CWP by sputter and e-beam deposition coatings was attributed to a non-uniform and non-conformal coating which might block the surface pores and increased hydraulic resistance. Once again, the superior performance of ALD-based modification, in terms of retaining the CWP of original membrane, is attributed to the conformal coating of TiO_2 on the membrane surface which does not significantly blocked the surface pores of original alumina membrane compared to other TFD methods. This is also attributed to high surface hydrophilicity obtained as result of ALD-modification.

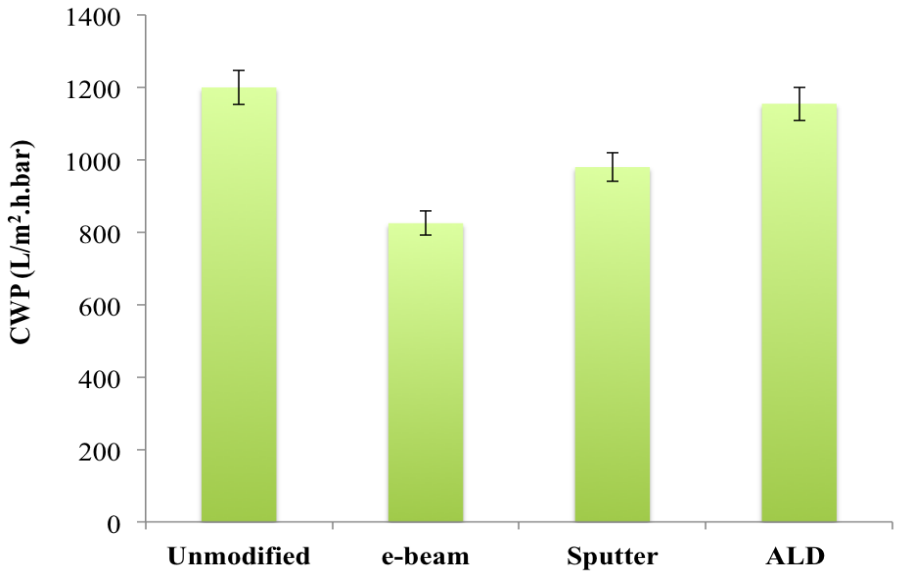

Figure 4-3: Clean water permeability (CWP) of unmodified alumina membrane and TiO_2-modified membranes using e-beam, sputter and ALD methods.

4.3.4. Effect of TiO_2-modification with different TFD methods on surface roughness

It has been reported previously that there is higher potential of fouling for higher surface roughness of a membrane, since more debris can be entrapped in a rougher surface [128-130]. For this reason, surface roughness of unmodified alumina and all modified membranes was measured analyzed by atomic force microscopy (AFM). The estimated root mean square roughness (R_{ms}) values for unmodified and all modified alumina membranes are plotted in Figure 4-4. Membrane surface roughness can be assessed by the R_{ms} value, with higher values represent a rougher surface [131]. Measurements indicate that the ALD-based surface modification results in the least rough surface comparison with the surface roughness obtained by the other deposition methods. Both the sputter and e-beam methods gave a relatively rougher surface than the ALD method, with the e-beam deposition resulting in an even higher surface roughness compared to the unmodified alumina membrane. These results are attributed to the working principles of ALD, sputter and e-beam deposition methods, where the ALD method has been reported to provide the most uniform and smooth thin-film deposition on a substrate surface. A rougher and less uniform TiO_2 coating was observed by the sputter and e-beam deposition methods. Based on these findings, we hypothesized that due to lowest surface roughness and highest surface hydrophilicity, the ALD-modified membranes are presumed to show a lower fouling potential for adsorption of a model protein foulant such as. bovine serum albumin (BSA).

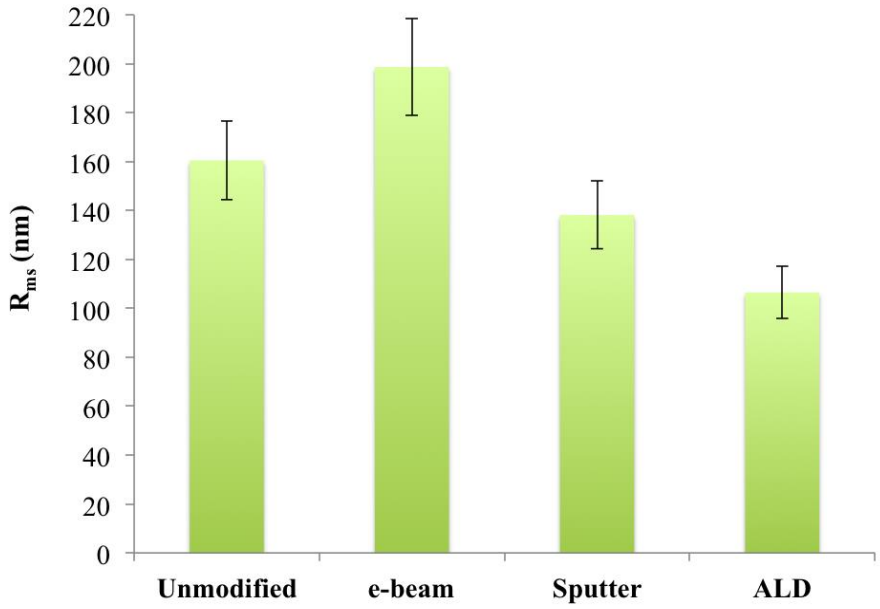

Figure 4-4: Root mean square roughness (R_{ms}) of unmodified alumina membrane and membranes modified with TiO_2 deposition using e-beam, sputter and ALD methods.

4.3.5. BSA adsorption potential of unmodified and TiO_2-modified alumina membranes

BSA is a model foulant and is widely used for its adhesion or adsorption testing on different surfaces [132]. A static BSA adsorption test was conducted for the unmodified alumina and all modified membranes. Results for BSA adsorption tests are shown in Figure 4-5. It is apparent that the ALD-modified membrane shows the least potential for BSA adsorption. This finding is attributed to the highest surface hydrophilicity and least surface roughness attained by ALD-TiO_2 modification of the alumina surface. The sputter-modified membrane showed slightly higher adsorption than ALD which is attributed to the rougher surface property. BSA adsorption results for the three modification methods appear to correlate with the surface hydrophilicity and roughness data obtained. It is interesting to note that the unmodified alumina membrane and e-beam modified membranes showed a similar and higher potential for

BSA adsorption. Although the e-beam modified has a lower contact angle than the unmodified membrane, surface roughness of the e-beam modified membrane is higher than the unmodified alumina membrane (Figure 4-4). It is postulated that as the surface roughness increases, chances of adhesion/attachment of particles also increases. Though the surface hydrophilicity of e-beam modified membrane was higher than that for the unmodified alumina membrane (Figure 4-2), but the effect of high hydrophilicity is compensated by the high roughness, and the resulting BSA adsorption potential was found nearly-similar to that for the unmodified alumina membrane due to a *'trade-off'* effect.

With this finding we hypothesized that ALD-modified membrane to show the least fouling potential in AnMBR filtration system in comparison with that for unmodified alumina membrane and membranes modified with other deposition methods.

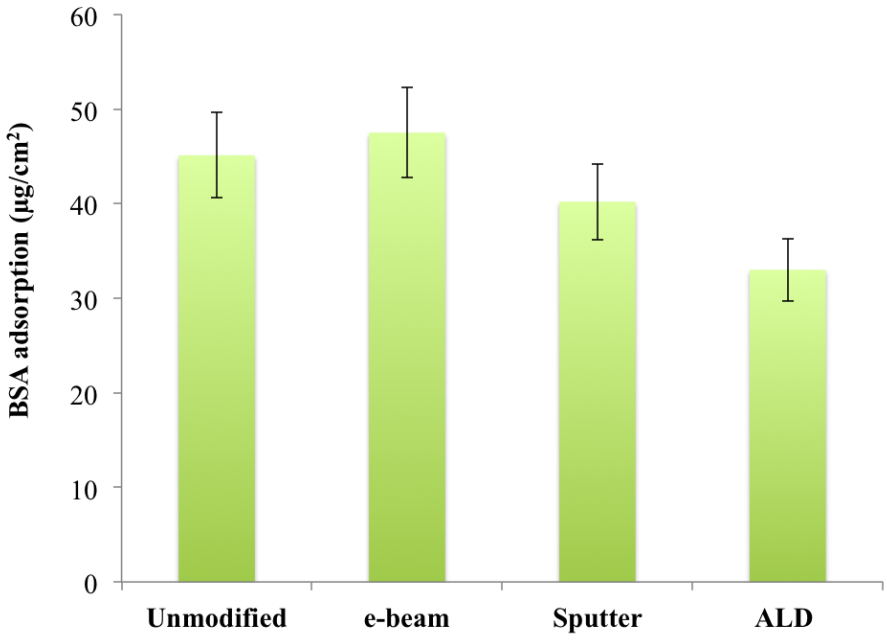

Figure 4-5: BSA adsorption potential for unmodified alumina membrane and TiO_2-modified membranes with e-beam, sputter and ALD methods.

4.3.6. Fouling control performance of TiO_2-modified membranes with different TFD methods in AnMBR filtration

The unmodified alumina membrane and all three membranes modified with TiO_2 thin film deposition, employing ALD, sputter and e-beam deposition techniques, were tested for fouling inhibition performance in a lab-scale AnMBR filtration system, fed with synthetic municipal wastewater. Schematic of AnMBR process system is shown in Figure 3-1. All membranes were tested under the same experimental conditions, as summarized in Table 3-1.

Trans-membrane pressure (TMP) profiles were recorded for all membranes at a constant-flux operation of 30 $L.m^{-2}.h^{-1}$ and are shown in Figure 4-6. We did not involve any cyclic operation here as this research was carried out as a comparative study only to measure lifetime of membrane, in contrary with case of real MBR operation where backwashing cycles and gas scouring are involved. Main reason for not including backwashing cycles was that this was a proto-type study which mainly focused on testing the initial potential/success of TiO_2-modified membranes by TFD methods in a lab-scale AnMBR filtration system, based on the surface features of each modified membrane. The aim was to use short-term operation so that the biological and other conditions of the reactor can be safely assumed to be the same for each run. The system was therefore operated at high flux and low CFV. However, in future studies should include successive filtration cycles with backwash and/or chemically enhanced backwash (CEB) to determine the presence of reversible and irreversible foulants in long-term operation at low / sustainable flux.

It can be seen in Figure 4-6 that there is a delay in TMP across membrane occurs, as the surface of unmodified alumina membrane is modified with TiO_2 via ALD, sputter and e-beam deposition methods. It took around 41, 52 and 74 hours for the

unmodified alumina membrane and membranes modified with e-beam and sputter methods respectively to reach a cut-off TMP level of 40 kPa. However ALD-modified membrane, with same thickness of TiO_2 layer, took around 103 hours to reach the same cut-off level of TMP. These results showed that all TiO_2-modified membranes showed better performance than unmodified alumina membrane in terms of fouling control in a short-term AnMBR filtration operation; however ALD-modification showed the superior performance than all other membranes. The delay in fouling is attributed to the significant increase in surface hydrophilicity and decrease in surface roughness caused by the TiO_2-modification of alumina surface. As ALD-TiO_2 surface modification resulted into highest hydrophilicity and least roughness, therefore fouling rate was determined to be the least for ALD-modified membranes in AnMBR filtration test.

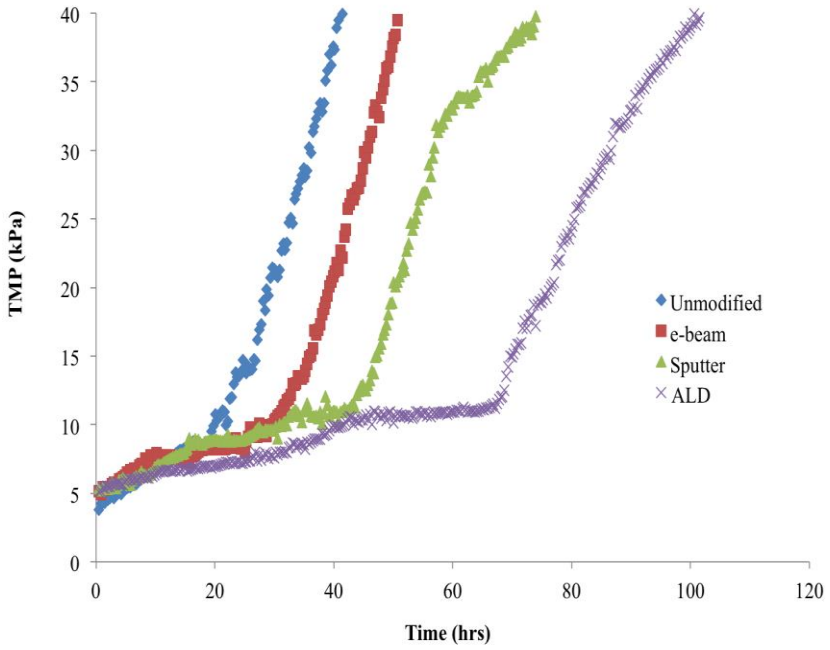

Figure 4-6: TMP vs. Time profiles in lab-scale AnMBR filtration for unmodified alumina membrane, and membranes modified with TiO_2 coating using e-beam, sputter and ALD methods

4.3.7. EPS components in cake layer

Membrane fouling in MBR has usually been attributed to occur as result of accumulation of extracellular polymeric substances (EPS) [133, 134]. After stopping the filtration operation, total concentrations of EPS (both proteins and carbohydrates) were measured and analyzed in the cake layer on the surface of all fouled membranes. Detailed characterization of these organic substances was not carried out in this investigation and the analysis results are presented in Figure 4-7.

It can be seen that EPS concentration (both proteins and carbohydrates) was determined to be least on the surface of ALD-modified membranes. Highest concentration of proteins and carbohydrates are found in the cake layer of fouled unmodified alumina membrane. Also it can be seen that total EPS concentration found on the surfaces of sputter and ALD-modified membranes are in well-agreement with their respective TMP profiles (Figure 4-6).

It was interesting to note that concentration of both proteins and carbohydrates were quite similar in the cake layer on the surface of fouled e-beam modified membrane and unmodified alumina membrane. Perhaps this is why there was not large difference of time delay for TMP to reach 40 kPa for both unmodified and e-beam modified membranes. This finding is attributed to the high surface roughness of e-beam modified membrane which compensated its high hydrophilicity and resulted into almost similar rate of fouling in AnMBR filtration test and a relatively higher concentration of organic matter was attached onto its surface when compared with the unmodified alumina membrane.

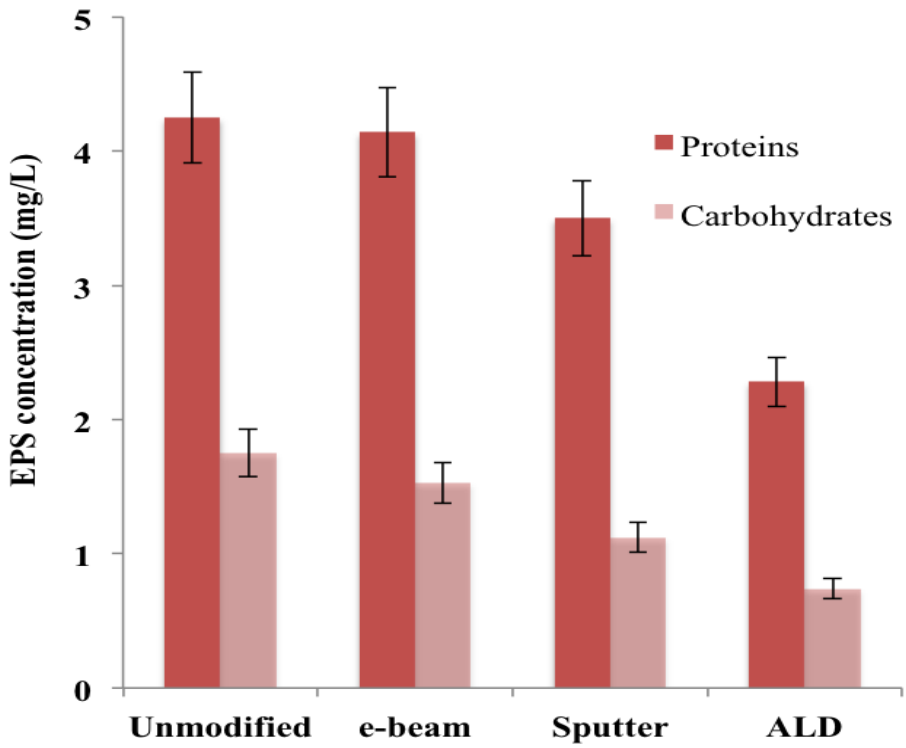

Figure 4-7: EPS concentration plot; concentration of proteins and carbohydrates on the surface of fouled unmodified alumina membrane and TiO_2-modified membranes using e-beam, sputter and ALD methods.

4.4 Conclusions

In this investigation, TiO_2 was deposited on the surface of alumina membrane by atomic layer deposition (ALD), sputter and electron-beam (e-beam) deposition methods. Basic objective of this research was to characterize the properties of TiO_2 film deposited by various deposition methods and to compare the fouling inhibition performance of all modified membranes in a lab-scale anaerobic membrane bioreactor (AnMBR) fed with synthetic wastewater. Following conclusions were drawn:

- TiO_2-modified membranes, for the same thickness of TiO_2 film, showed different surface characteristics for different thin-film deposition methods, in terms of hydrophilicity, roughness, clean water permeability and potential for BSA adsorption.

- All TiO_2-modified membranes exhibited lower rate of fouling in lab-scale AnMBR filtration test when compared with that for unmodified alumina membrane.
- ALD-TiO_2 modified membranes showed superior performance in terms of membrane's surface characteristics and fouling inhibition performance in AnMBR filtration test compared with those for modified with other deposition methods.

These findings have verified hypotheses no. 1-4 (Chapter: 1), with further studies to be conducted using only ALD as the chosen TFD method for surface modification of alumina membrane. Different ALD modification conditions were applied to test the membrane performance as function of the degree of surface modification.

CHAPTER: 5

SURFACE MODIFICATION OF CERAMIC MEMBRANES WITH DIFFERENT ALD-TiO_2 CYCLES FOR FOULING CONTROL IN AnMBR SYSTEM

Highlights

- Alumina membrane surface was modified with TiO_2 using atomic layer deposition (ALD).
- ALD-TiO_2 surface modification has significantly increased hydrophilicity and reduced roughness of original alumina membrane.
- Clean water permeability of original and modified membranes was comparable at lower number of ALD cycles applied.
- ALD-modified alumina membrane inhibited fouling in anaerobic membrane bioreactor (AnMBR) filtration.

Abstract

In this study, we used the chosen atomic layer deposition (ALD) method for modification of ultrafiltration alumina membrane surface with TiO_2 thin film. Major advantages of ALD include: uniform coating and 3D conformity, precise thickness control and good control over the surface structures created. In this study, different thicknesses of ALD-TiO_2 film were coated over alumina membrane and various surface properties of ALD-modified membranes were characterized including thin film thickness measurement, surface morphology, hydrophilicity and roughness. Basic objective of this research was to conduct a comparative study of fouling inhibition performance between ALD-modified and unmodified alumina membranes in a lab-scale anaerobic membrane bioreactor (AnMBR) for wastewater treatment.

ALD treatment enhanced hydrophilicity and reduced roughness of alumina membrane surface and modified membranes nearly retained intrinsic clean water permeability (CWP) of unmodified alumina membrane for lower number of ALD cycles applied. When the optimized ALD-modified membrane was applied in constant-flux anaerobic membrane bioreactor (AnMBR) filtration system, it showed better fouling inhibition performance, which results in slower trans-membrane pressure (TMP) rise-up, in comparison with that for unmodified alumina membrane. Relatively lesser amount of extracellular polymeric substances (EPS) components was found to be present in cake layer formed on the surface of fouled modified membrane when compared with that for unmodified membrane. Overall fouling inhibition performance of ALD-modified membrane in AnMBR filtration was attributed to increase in membrane surface hydrophilicity and decrease in surface roughness. This study shows the initial potential of ALD technology for membrane surface modification to provide a practical solution to counter fouling problem in MBR

systems and provides an opportunity for further exploration of its potential and its comparison with other surface deposition methods in wastewater treatment applications.

5.1 Introduction

The need for fresh water is expected to keep increasing with further development of human society. If water consumption remains the same as the current level, estimates predict that 60% of the world population will face water stress by the year 2025. Water scarcity is increasing in many regions and is a severe global problem. There is a need to seek non-conventional water sources to meet future demands, where wastewater reuse after suitable treatment is one strategy. Water reclamation and reuse is therefore inevitable in upcoming years. Due to its unique advantages, anaerobic membrane bioreactors (AnMBR), which combine anaerobic digestion and membrane filtration, is attracting remarkable interest in both research communities and industrial sectors for advanced wastewater treatment for reuse. Membrane fouling, which is caused by deposition or adsorption of foulants (e.g. microorganisms, organics, colloids etc.) on the surface or within membrane pores, however, still remains one of the key bottlenecks that hamper the widespread application of AnMBR technology for wastewater treatment [135]. Membrane fouling eventually leads to flux decline, higher energy consumption and potentially shorter life span of the membrane, ultimately resulting in reduced process efficiency and overall increase in operational cost.

Membrane surface modification has proved to be a useful method in (waste)water treatment applications where improving the hydrophilicity of a membrane can result in higher water fluxes and reduced fouling [136, 137]. Various techniques such as sputtering, chemical vapor deposition (CVD), pulsed laser deposition (PLD) can be used for applying surface coatings of different substrates to change the membrane properties [138]. However, these thin-film deposition (TFD) techniques have some limitations including lack of precise thickness control and producing weak interfacial

adhesion between the film and the membrane surface. In recent years, atomic layer deposition (ALD) has emerged as an effective technology for thin film deposition on surface where various substrates can be used, e.g. polymers, ceramics, catalysts and porous materials [100, 101]. Principally, in terms of surface coating, ALD technology exhibit superior characteristics over other TFD methods, as summarized in Table 2-9 (Chapter 2) and investigated through the findings in Chapter 4 of this PhD thesis.

ALD is a CVD technique that has been used for well-controlled deposition of inorganic layers capable of depositing a thickness in range of a few nanometers. In principle, ALD works by repeating a series of self-limited / controlled gas-phase surface reactions that occur in a wide range of temperature. In a typical ALD process, a monolayer is formed in each ALD cycle when desired precursors are alternatively pulsed and, by a purge step, separated from each other in the gas phase. This procedure is repeated for precise tuning of thickness of deposited film [102-104].

In an ALD process, vaporization of both precursors occurs enabling them to reach tiny pores and adsorb on walls of pores, or make reactions with already adsorbed precursors [105]. Secondly, reactions of ALD process take place on the surface of substrate, resulting in production of continuous thin films, that create highly uniform and conformal coating layers [107]. Thirdly, the thickness of ALD-coated layers can be controlled and tuned precisely simply by varying the ALD cycles with a thickness tuning step usually less than 1 Å [106].

As the ALD technique offers good control of surface structures created, it is gaining more interest and focus by researchers for various applications. ALD can produce outstanding dielectric layers and is already widely applied in the semiconductor industry for making high-K dielectric materials. ALD has also attracted great interest as a novel approach in modifying electrode properties via

surface coating in lithium and sodium-ion batteries [108, 109]. Additionally, in some previous studies, ALD-based surface modification of ceramic membranes for BSA retention and precise pore size tuning for polymeric membranes has been investigated [110, 139], however, despite the numerous advantages, to our knowledge, the use of ALD for surface modification of ceramic membranes for water/wastewater treatment applications has not yet been reported. Therefore, the key objective of this study was to compare the surface characteristics of ALD-modified alumina membranes, with those for unmodified ceramic membrane for application in a lab-scale anaerobic MBR (AnMBR) filtration test.

In this study, TiO_2 thin film was deposited over alumina substrate, as reports in the literature have shown it to display anti-fouling properties in wastewater treatment [140]. The alumina membranes were modified by depositing ALD-TiO_2 films with varying thicknesses. Following an assessment of the deposition layer thickness, an optimized modified membrane was selected for anti-fouling comparison with an unmodified membrane in a lab-scale AnMBR filtration test, fed with synthetic wastewater.

5.2 Materials and methods

5.2.1 Membrane surface modification and characterization

Commercially available flat sheet alumina ultrafiltration (UF) membranes (KeraNor, Norway) with a nominal surface pore size of 80 nm (as reported by manufacturer) and effective filtration area of 60 cm^2 were used as the unmodified membranes. Ultrathin films of TiO_2 were deposited on porous alumina membranes at 150 °C by using a Cambridge Nanotech Savannah ALD system. One ALD cycle corresponds to a growth rate of 0.05 nm per cycle. By varying the number of ALD cycles, different

thicknesses of TiO_2 were generated. Later, ALD-modified membranes were annealed at high temperature of 500 °C.

The resulting surface morphology of unmodified and TiO_2-modified alumina membranes were characterized by a field emission scanning electron microscope (FE-SEM, NovaNanoSEM, FEI). EDS spectrum of ALD-modified membranes was taken by a transmission electron microscopy (TEM, Titan G^2 80–300 ST, FEI). The TEM samples were prepared by scratching TiO_2 off alumina substrate and dispersing it in ethanol. TiO_2 thin-film thicknesses were measured by mechanical surface profilometer (Veeco Dektak 150). Ten measurements were taken to obtain an average thickness. Water contact angle measurements were performed for unmodified membranes and all ALD-modified membranes using a Dropmeter A-100 contact angle goniometer. Experimental error was minimized by taking average values of five measurements of contact angle for each sample. The surface roughness of unmodified and ALD-modified membranes was determined by an atomic force microscope (AFM, Agilent Technologies) using tapping mode. This experiment was repeated five times for each sample to obtain an average value.

5.2.2 Clean water permeability (CWP) tests

Clean water permeability (CWP) was determined with MQ water for unmodified and all ALD-modified alumina membranes. Nominal surface pore size of unmodified membrane was 80 nm, as reported by manufacturer, with effective filtration area of 30 cm^2. The CWP was determined by dead-end filtration experiments conducted at 0.7 bar and 21 °C. The permeate flux was measured by collecting permeate over time on a balance connected to a computer. Average values were obtained by taking three measurements in order to minimize the experimental error.

5.2.3 Bovine serum albumin (BSA) adsorption tests

The fouling behavior was first assessed using a model compound. A membrane's propensity to fouling can be evaluated by the amount of BSA protein adsorbed onto the membrane surface [118]. A similar method has been applied for this test as used by previous researchers [119]. The ALD-modified and unmodified membranes were separately placed into glass vials filled with 5 mL of 1 g/L BSA phosphate buffer solution (pH=7.4). The glass vials were then incubated in a water bath at 28 °C for 12 h to reach equilibrium. The amount of the adsorbed BSA was measured by calculating the difference between concentration of BSA in the solution before and after adsorption. Concentration values were determined from the absorption intensity at 280 nm recorded on a UV-Vis spectrophotometer (UV-2550, Shimadzu). An average value was obtained by repeating the test three times.

5.2.4 AnMBR filtration tests

The schematic of the lab-scale AnMBR system used in this study is shown in Figure 3-1 (Chapter 3). A continuous anaerobic completely stirred tank reactor (CSTR, Applikon Biotechnology, Netherlands) was operated in a side-stream mode at constant-flux of 30 $L.m^{-2}.h^{-1}$, as explained by other researchers [120]. The effective volume of the CSTR tank was 2 L. The hydraulic retention time (HRT) and organic loading rate (OLR) were fixed at 11 h and 0.87 $g.L^{-1}.d^{-1}$ respectively. Total organic carbon (TOC) concentration was 115 ± 5 mg/L. Influent chemical oxygen demand (COD) was 400 ± 10 mg/L, COD removal efficiency was around 90% ± 5% and mixed liquor suspended solids (MLSS) concentration was 5 ± 1 mg/L. COD and MLSS were determined according to standard methods [121]. The AnMBR filtration runs were duplicated under the same operating conditions for each membrane, and

trans-membrane pressure (TMP) recorded. The operating conditions of the AnMBR system and composition of synthetic wastewater feed are given in Table 3-1 and Table 3-2 respectively.

5.2.5 Extracellular polymeric substances (EPS) extraction and analysis

The EPS components in the cake layer on the surface of fouled membranes were extracted by ultra-sonication for 15 mins and filtered by a 0.45 µm filter paper. The Lowry method with bovine serum albumin as the standard reference [122] was used to measure the proteins. While, carbohydrates were measured by the Dubois method using glucose as the standard reference [123]. EPS extraction and analysis tests were conducted after each filtration run.

5.3 Results and discussion

5.3.1. Surface morphology and TiO_2-film thickness measurement of ALD-modified alumina membranes

The surface morphology of unmodified and ALD-modified alumina membranes was observed by scanning electron microscope (SEM). Figure 5-1(a-b) presents SEM images of the unmodified alumina membrane (0 ALD cycles) and the TiO_2-modified membrane employing 600 ALD cycles. The SEM images of other TiO_2-modified membranes (200 ALD cycles, 400 ALD cycles, 1000 ALD cycles and 1600 ALD cycles) are presented in Figure 5-1(c-f). Figure 5-1(a) presents the surface image of unmodified alumina membrane (0 ALD cycles) with an average pore size of 80 nm, as reported by manufacturer. When the TiO_2 layer was deposited by ALD, the conformal and uniform nature of ALD-deposited TiO_2 film can be seen in Figure 5-1 (b-f). The deposited TiO_2 takes the shape of the original alumina grains, however, as

thickness increases the surface porosity decrease proportionally, and the TiO_2 film becomes denser and eventually blocks a significant portion of surface pores of the unmodified alumina membrane. This observation is in agreement with the basic operation principals of ALD. The energy dispersive spectroscopy (EDS) spectrum of TiO_2-coated alumina membrane was checked by TEM and is presented in Figure 5-1 (g), which confirms the presence of Ti and O on the surface of the alumina membrane.

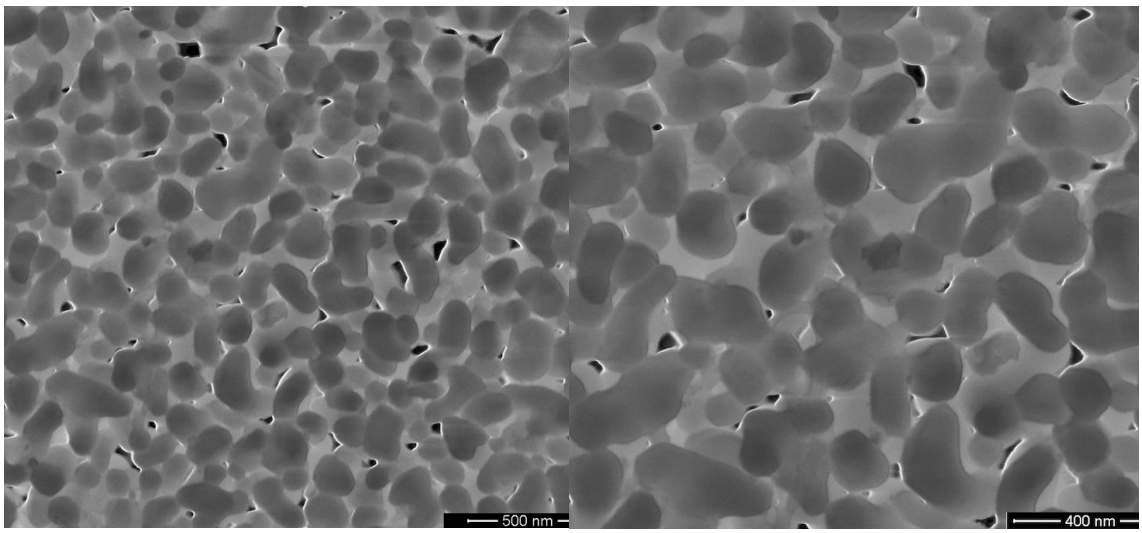

(a)

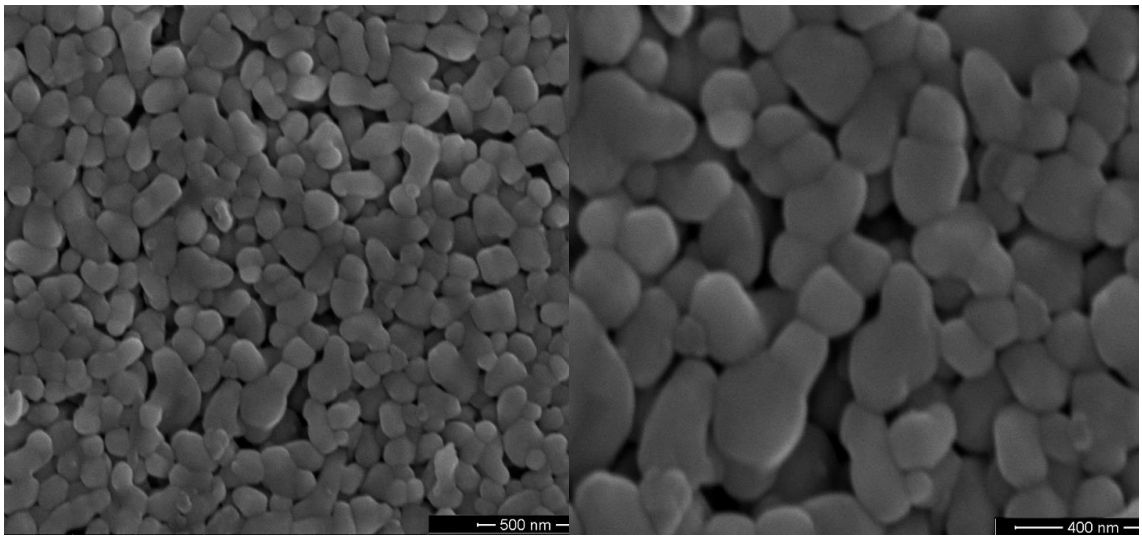

(b)

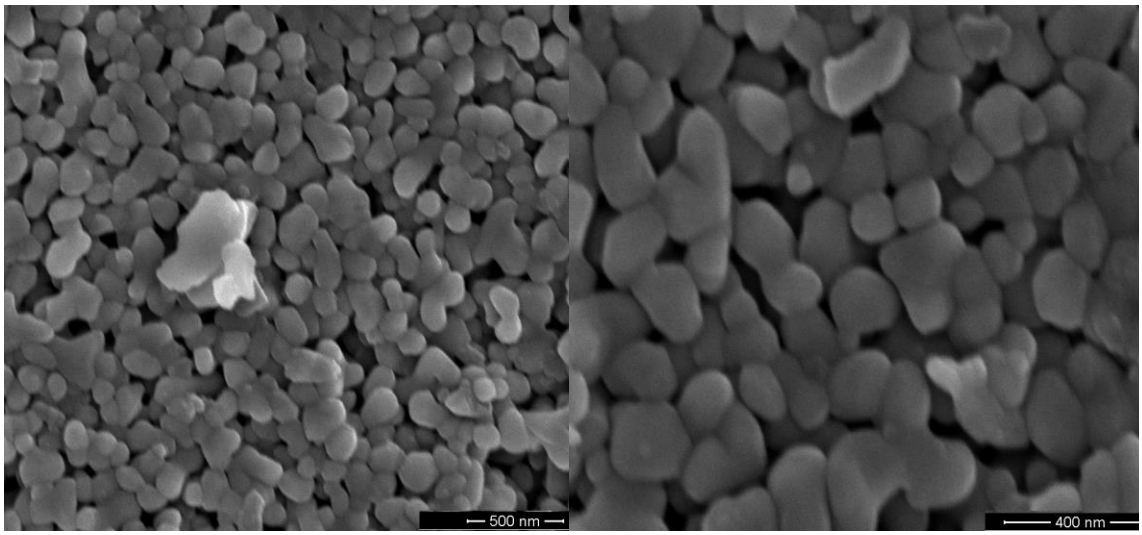

(c)

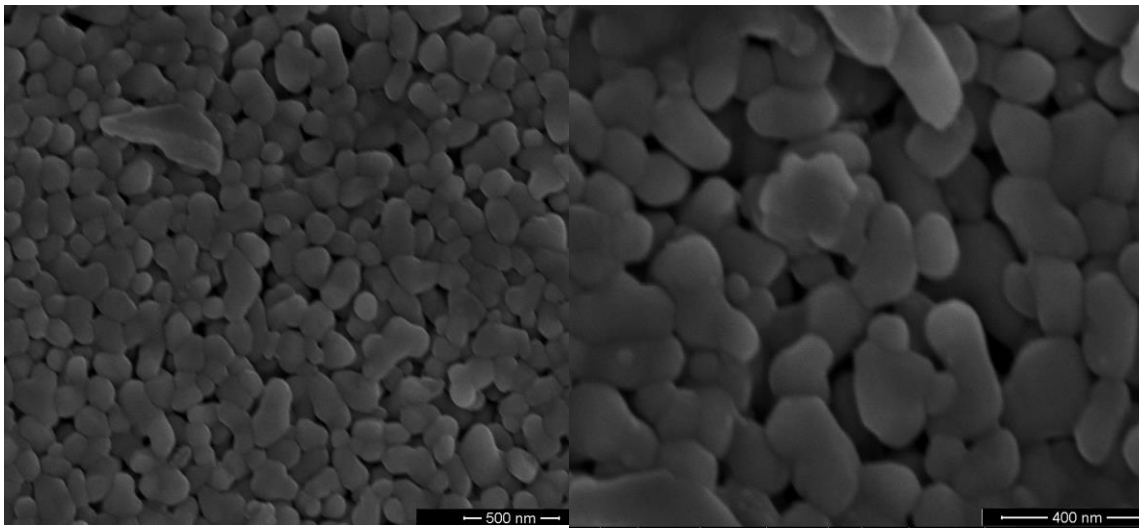

(d)

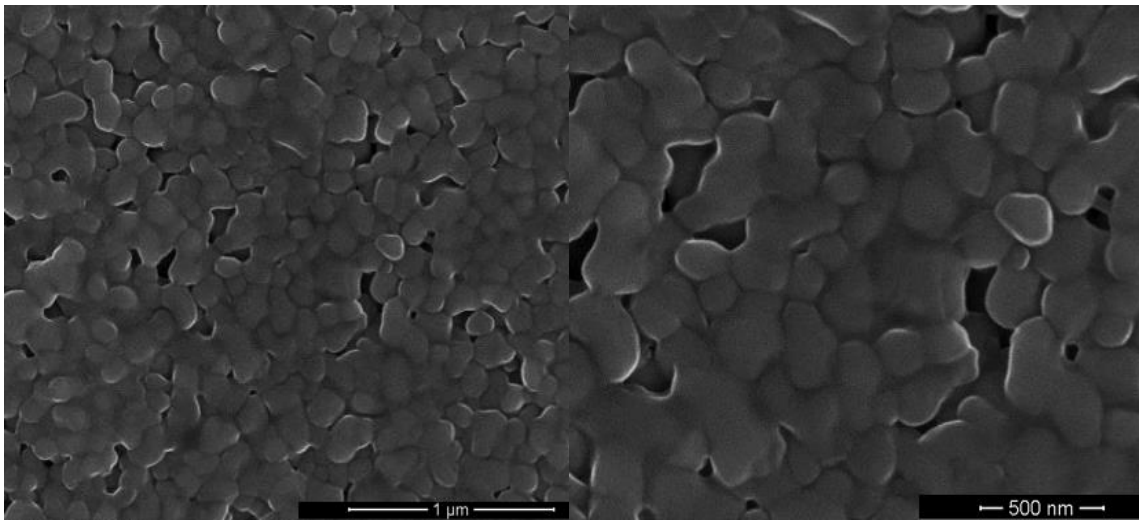

(e)

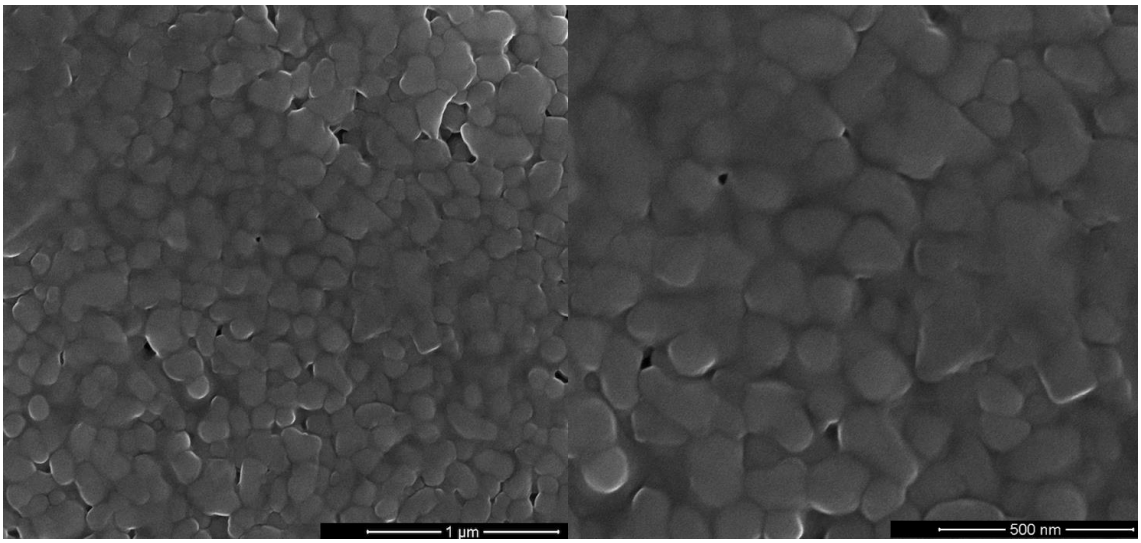

(f)

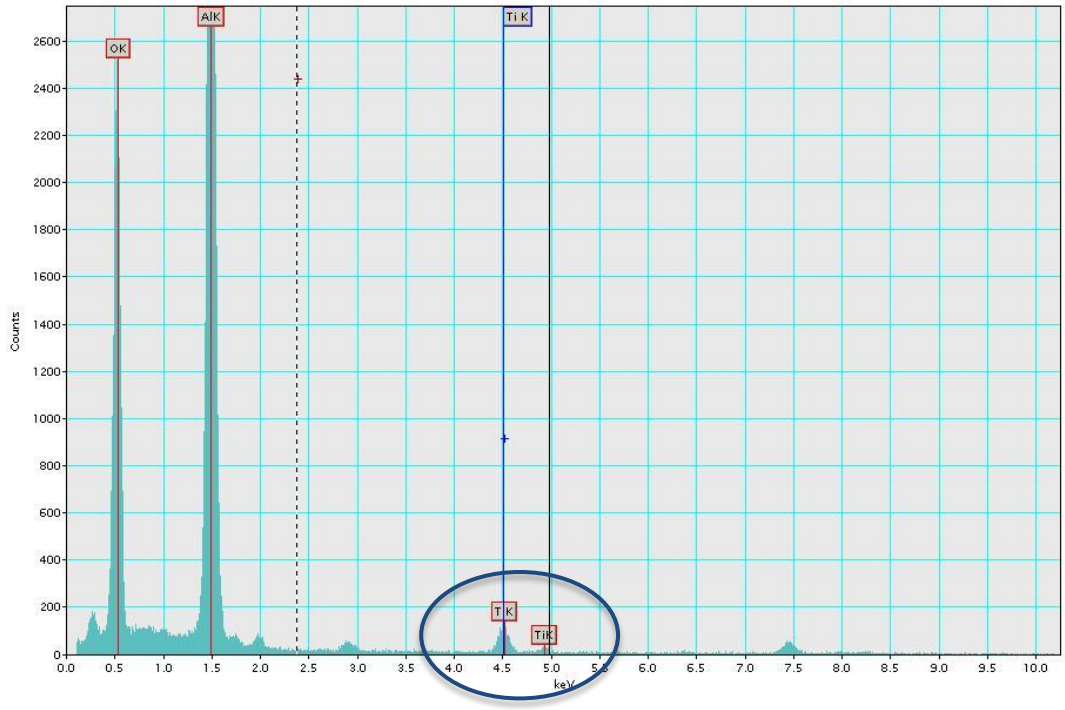

(g)

Figure 5-1: SEM surface images at magnification; 50,000 and 80,000 of (a) unmodified alumina membrane (0 ALD cycles) and ALD-TiO_2 modified alumina membranes with (b) 600 ALD cycles (c) 200 ALD cycles (d) 400 ALD cycles (e) 1000 ALD cycles (f) 1600 ALD cycles (g) TEM-EDS spectrum showing presence of Ti and O on the surface of ALD-TiO_2 modified alumina membrane

A set of modified membranes was made with different thicknesses of TiO_2 coatings. By varying the number of ALD cycles at a constant deposition rate (0.05 nm/ALD cycle) a desired thickness could be made. The thickness of each ALD-TiO_2 deposited film was measured by a mechanical profilometer. The measured thickness

values of TiO_2 films are in good-agreement with anticipated values based on the ALD process conditions as presented in Figure 5-2. This indicates that the ALD method has an excellent control over thickness and it can be finely tuned to meet the desired or optimal coating thickness.

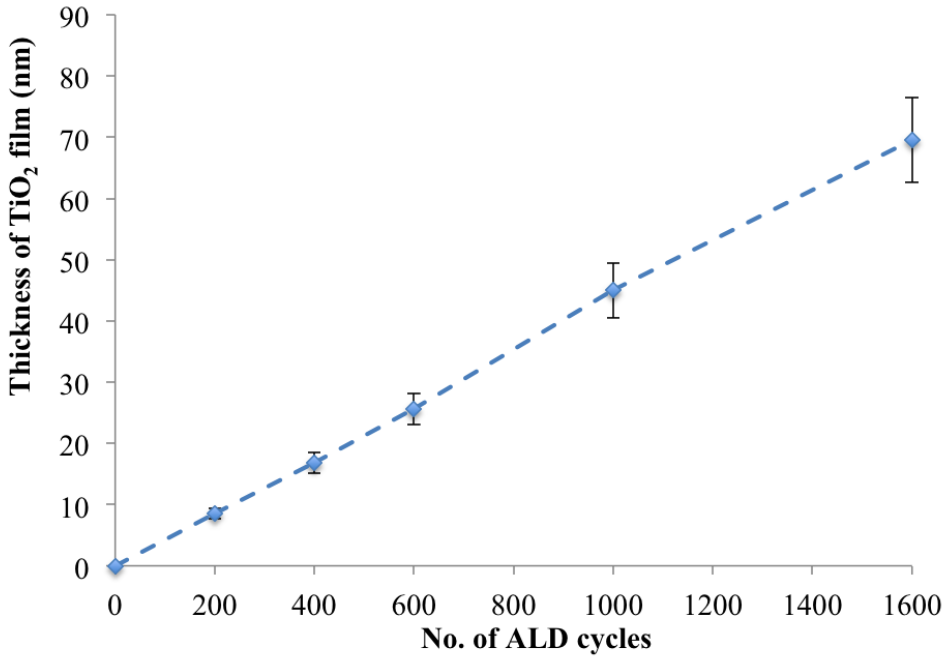

Figure 5-2: Thickness of TiO_2 film on the surface of modified alumina membranes as function of number of ALD cycles.

5.3.2. Effect of ALD-TiO_2 cycles on surface hydrophilicity of modified alumina membranes

The hydrophobicity / hydrophilicity of a surface are commonly determined by measuring water contact angles. Measurements were made for the unmodified alumina membrane and ALD-modified membranes with varying deposition layer thickness. Figure 5-3 presents the contact angle measurements of water droplets on the unmodified and all ALD-modified membranes. It can be clearly seen that surface hydrophilicity of the unmodified alumina membrane significantly increases after TiO_2

deposition on its surface via the ALD method. Even the presence of a very thin film of TiO_2 (thickness 10 nm ≈ 200 ALD cycles) reduced the contact angle from 84.3° to 30.9°. The hydrophilicity expressed by contact angle remains more or less the same for all ALD-modified membranes as the thickness of TiO_2 film is increased, corresponding to the increase in number of ALD cycles from 200 to 1600. This result is attributed to the conformity and uniformity of ALD-TiO_2 thin film over the surface of the alumina membrane. It depicts that approximately same amount of TiO_2 is deposited uniformly in each monolayer over the membrane surface independent of the numbers of ALD cycles applied.

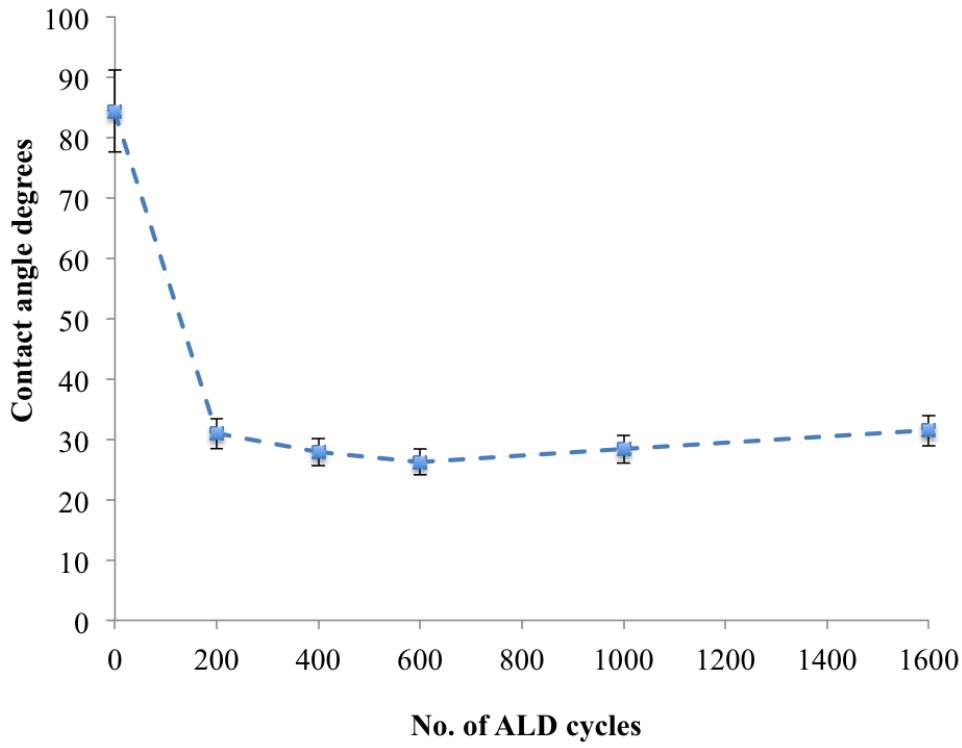

Figure 5-3: Contact angle of unmodified and TiO_2-modified alumina membranes as function of number of ALD cycles.

5.3.3. Clean water permeability of alumina membranes modified with different number of ALD-TiO_2 cycles

Clean water permeability (CWP) tests were conducted for the unmodified alumina membrane and each of the TiO_2-modified membrane with varying number of ALD cycles. Results presented in Figure 5-4 show that the intrinsic CWP for the unmodified alumina membrane was determined to be 1200 $L.m^{-2}.h^{-1}.bar^{-1}$ and does not decrease significantly for the lower number of ALD cycles (*i.e.* 200, 400 and 600 ALD cycles). The CWP was measured to be 1185 $L.m^{-2}.hr^{-1}.bar^{-1}$, 1167 $L.m^{-2}.hr^{-1}.bar^{-1}$ and 1155 $L.m^{-2}.hr^{-1}.bar^{-1}$ for the 200, 400 and 600 ALD cycles respectively. This finding implies that for the lower number of ALD cycles, the ALD-modified membranes have a slight reduction in CWP but essentially retain a similar value irrespective of TiO_2 film thickness. SEM images of the membranes show that as the number of ALD cycles increase, the TiO_2 film starts to become denser/thicker, hence, at higher numbers of ALD cycles the deposited film can block the surface pores of the original alumina membrane, representing an increase in hydraulic resistance. Although, in principle, the ALD-TiO_2 layer can block the surface pores with increasing number of ALD cycles, no significant decrease in CWP was observed up to 600 ALD cycles. This is attributed to the increased hydrophilicity of ALD-modified membrane that compensates the added resistance by an additional thin film layer on the membrane surface. A similar observation has been reported by McCloskey *et. al.* (2012) [124]. However, results show that at higher numbers of ALD cycles (e.g. 1000 and 1600) a noticeable decrease in CWP is observed (*i.e.* 1050 and 940 $L.m^{-2}.h^{-1}.bar^{-1}$ respectively). This indicates that at higher numbers of ALD cycles, the TiO_2 layer appears to become denser and significantly blocks the surface pores of the unmodified membrane thereby increasing the resistance for CWP. This

observation is consistent with the SEM images presented in Figure 5-1. Miller *et. al.* (2014) also reported that CWP of modified membranes was reduced due to reduction in effective pore size [141].

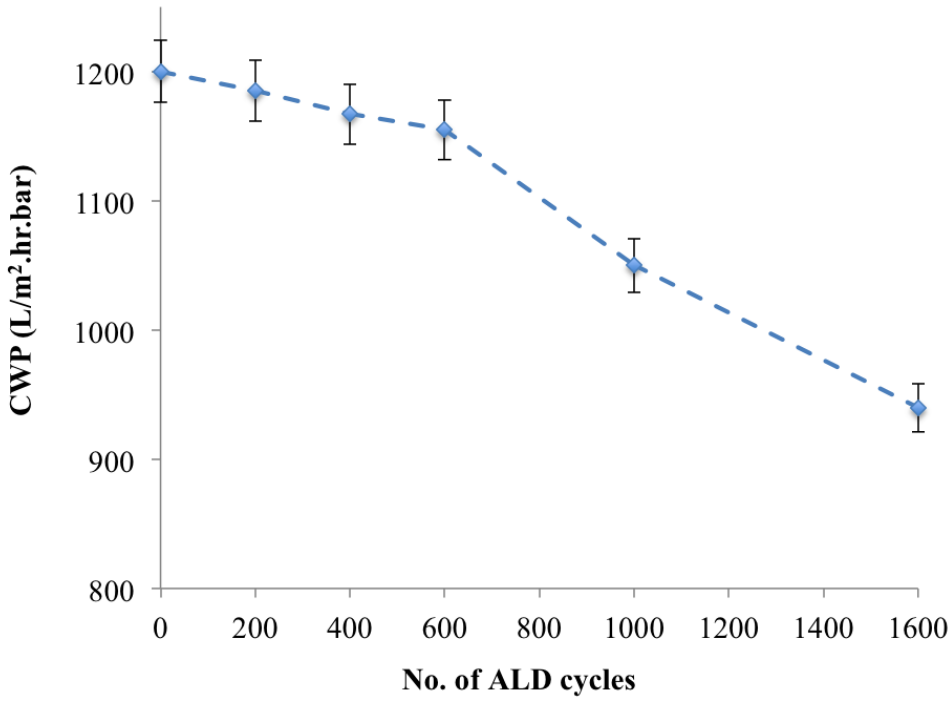

Figure 5-4: Clean water permeability (CWP) of unmodified and TiO_2-modified alumina membranes as function of number of ALD cycles.

5.3.4. Effect of ALD-TiO_2 cycles on surface roughness of modified alumina membrane

Membrane surface roughness has been reported in literature to be an important parameter that affects membrane fouling in that rough surfaces have a higher potential for debris and colloidal material to be entrapped [128-130]. Therefore, in this study the surface roughness of the unmodified alumina membrane and ALD-modified membranes was analyzed by atomic force microscopy (AFM). Resulting AFM images are shown in Figure 5-5(a-f), with estimated root mean square of roughness (R_{ms}) and mean roughness (R_a) values given in Table 5-1. Surface roughness can also be

indicated by other parameters such as maximum height and Z-range, however, R_{ms} and R_a values are typically used [131]. In this study we have therefore also chosen to use R_{ms} and R_a values to indicate surface roughness.

The unmodified alumina membrane was found to have the roughest surface. With surface modification via ALD-TiO_2 deposition, the surface roughness is seen to decrease with mean roughness values decreasing proportionally with increasing number of ALD cycles. The trend of decrease in surface roughness with increasing number of ALD cycles is plotted in Figure 5-5 (g).

These results clearly indicate that the ALD-TiO_2 modification reduced surface roughness resulting in a smoother membrane surface. The lower surface roughness is assumed to have a positive effect in enhancing anti-fouling potential of the ALD-modified membranes compared to the unmodified membrane when applied in an AnMBR filtration system.

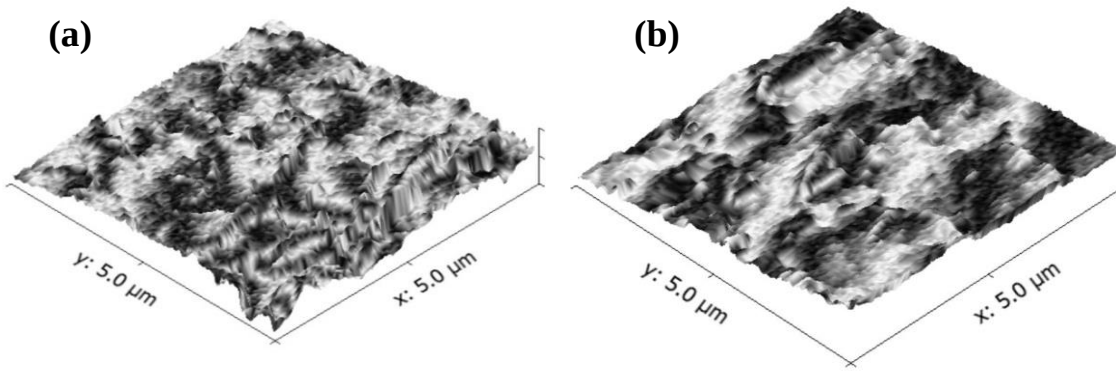

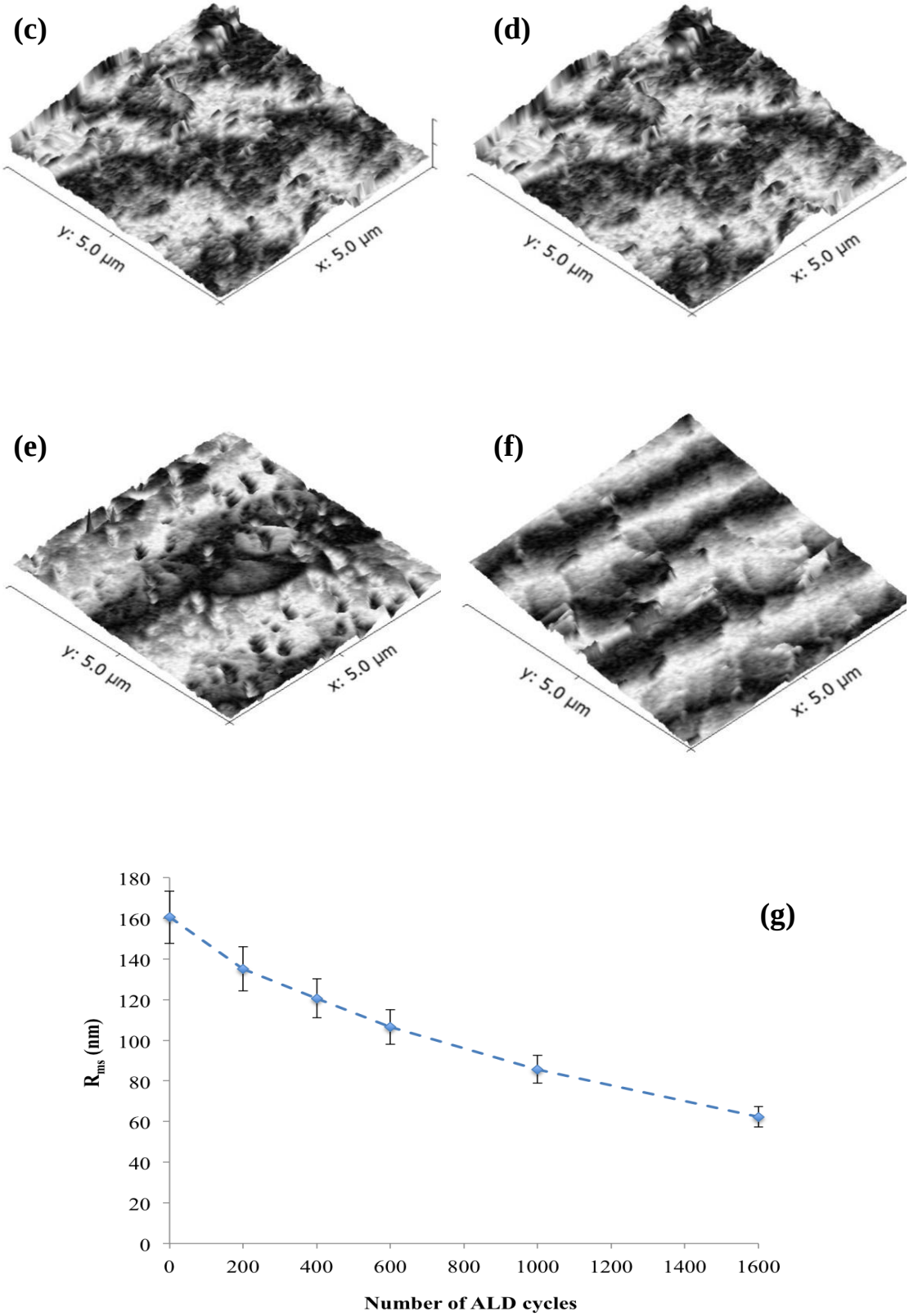

Figure 5-5: AFM images of alumina membranes after TiO_2-modification with (a) 0 ALD cycles (b) 200 ALD cycles (c) 400 ALD cycles (d) 600 ALD cycles (e) 1000 ALD cycles (f) 1600 ALD cycles along with (g) root mean square roughness (R_{ms}) plot as function of number of ALD cycles.

Table 5-1: Analyzed results of mean roughness (R_a) and root mean square roughness (R_{ms}) values of unmodified and ALD-modified alumina membranes

No. of ALD cycles	R_a (nm)	R_{ms} (nm)
0	137.6	160.5
200	112.3	135.1
400	100.5	120.6
600	87.9	106.5
1000	70.3	85.7
1600	50.8	62.3

5.3.5. BSA adsorption potential of ALD-TiO_2 modified alumina membranes

Static BSA adsorption tests were conducted for the unmodified and ALD-modified membranes to investigate their respective adsorption potential for BSA as a first indication on fouling potential by organic matter. Results for BSA adsorption tests are shown in Figure 5-6. Results show that the unmodified alumina membrane has a greater potential for BSA adsorption. The potential for BSA adsorption is less for the ALD-modified membranes, and is seen to decrease with increasing number of ALD cycles. This finding is attributed to the increased hydrophilicity of the membrane surface that reduces the potential for BSA adsorption. This finding can also be attributed to the reduced surface roughness of the modified membranes as a function of increased ALD cycles, as a smooth surface is less prone to adhesion of solids compared to that for a rough surface. Hence, BSA adsorption test results correlate with contact angle and surface roughness results for all ALD-modified membranes. Based on this test, it is presumed that ALD-modified membranes will show a lower fouling potential in AnMBR filtration systems compared to that for an unmodified alumina membrane.

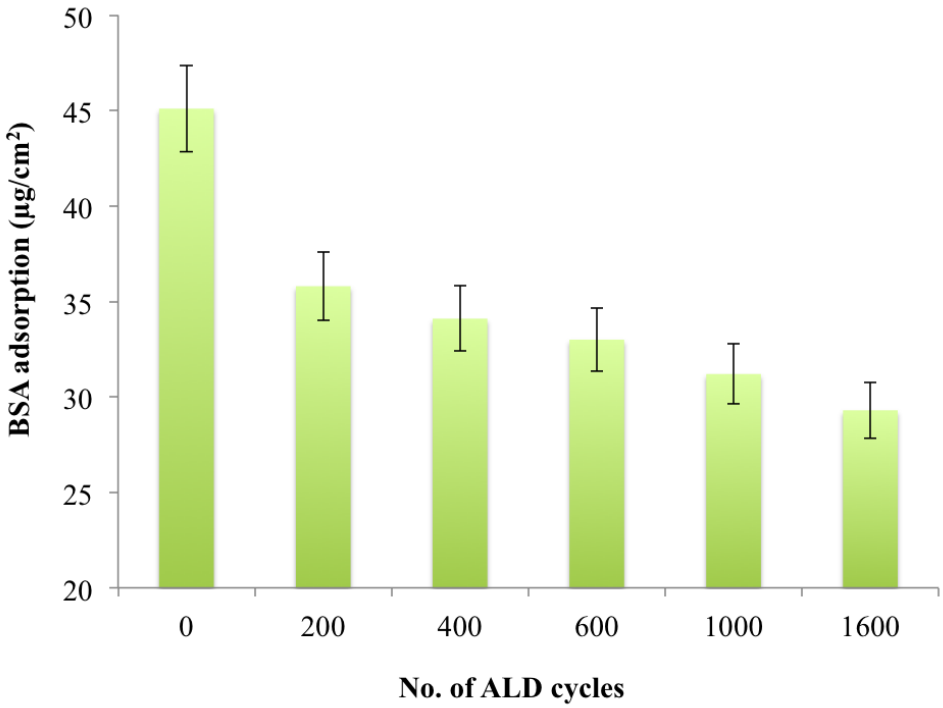

Figure 5-6: BSA adsorption potential of unmodified and TiO_2-modified alumina membranes as function of number of ALD cycles.

5.3.6. Fouling inhibition performance of ALD-TiO_2 modified alumina membrane in AnMBR filtration operation

The TiO_2-modified alumina membrane with 600 ALD cycles was selected for comparison with the unmodified alumina membrane to assess their fouling behavior in a lab-scale AnMBR system, fed with synthetic wastewater (Figure 3-1). The selection of the ALD-TiO_2 modified membrane with 600 cycles was made based on the following: (i) the minimum water contact angle (26.2°) was measured for the membrane modified employing 600 ALD cycles (Figure 5-3); (ii) intrinsic CWP of the unmodified alumina membrane was nearly retained by the TiO_2-modified membrane with 600 ALD cycles, while the CWP was significantly reduced for modifications with higher number of ALD cycles (Figure 5-4); (iii) the measured adsorption potential of BSA was found not largely different for all the TiO_2-modified membranes (Figure 5-6); (iv) also the mechanical strength of the TiO_2 film deposited

by 600 ALD cycles was presumed to be superior to that of 200 and 400 ALD cycles. It should be noted that the TiO_2-modified membranes with ALD cycles exceeding 600 formed a dense film on the membrane surface, which ultimately could impact the rejection performance of certain substances such as micro-pollutants etc. However, the target of this study was focused on assessing the fouling behavior of the modified membranes and the membranes with higher number of cycles were not selected.

An increase in trans-membrane pressure (TMP) under constant-flux operation can be related to the increase in membrane fouling rate. The AnMBR filtration system was operated with a constant-flux of 30 $L.m^{-2}.h^{-1}$, with both membranes (unmodified and modified) tested under the same experimental conditions, as summarized in Table 3-1. This experiment was conducted as a comparative study and therefore operated continuously, without backwash or gas bubbling as is commonly applied in full-scale MBR operations. The system was continuously operated until each membrane reached a TMP of 40 kPa, as it is considered a cut-off TMP value for commercial MBR systems. TMP profiles measured for both membranes are shown in Figure 5-7.

It is quite apparent in Figure 5-7 that the ALD-modified membrane exhibits a less propensity for fouling compared to the unmodified alumina membrane under the conditions tested. Whereas the unmodified membrane reached a TMP of 40 kPa in around 40 hours, the ALD-modified membrane took around 100 hours to reach the same level of TMP under the same experimental conditions. These results showed a performance improvement of around 2.5 times for the ALD-modified membrane (600 cycles) as compared to that for the unmodified alumina membrane. This initial study suggests that the ALD-modified membrane showed a significantly lower overall fouling rate than the unmodified alumina membrane when tested in a lab-scale AnMBR filtration system. This difference in fouling rate between the two membranes

is attributed to the significant increase in surface hydrophilicity and decrease in surface roughness due to surface modification of the alumina membrane by ALD-TiO_2 treatment.

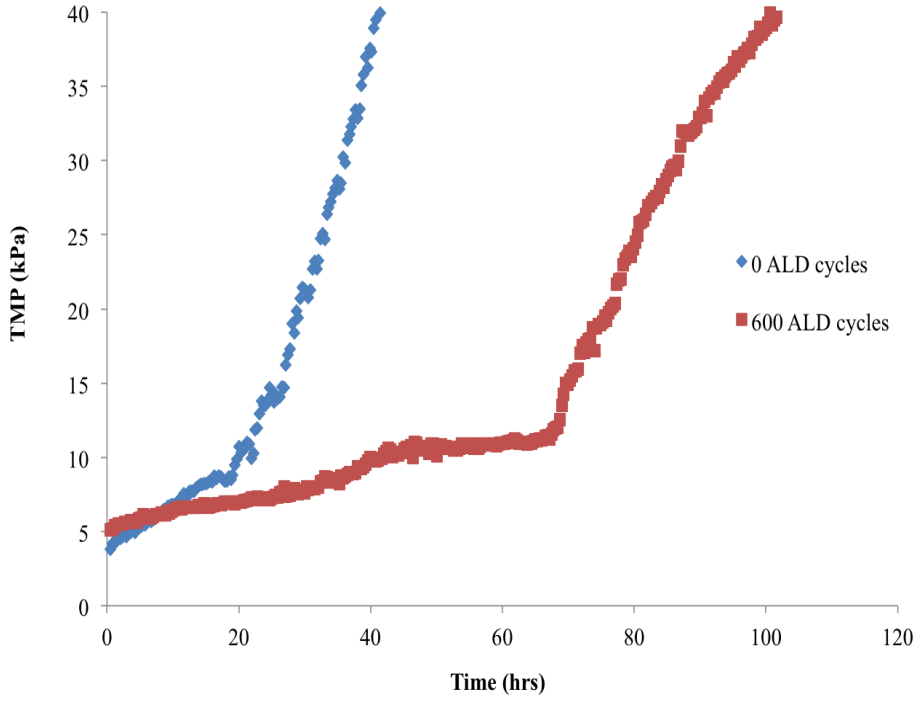

Figure 5-7: Trans-membrane pressure (TMP) vs. Time profile of unmodified (0 ALD cycles) and ALD-TiO_2 modified (600 ALD cycles) alumina membranes in AnMBR filtration test

5.3.7. EPS components in cake layer

Membrane fouling in MBR systems has been generally attributed to the accumulation and adsorption of extracellular polymeric substances (EPS) [133, 134]. An analysis of the cake layer formed on the surface of both fouled membranes was therefore conducted. Total concentrations of EPS (both proteins and carbohydrates) were measured and analyzed at the end of the filtration run, with results shown in Figure 5-8. These results indicate that almost 1.8 times more proteins and 2.3 times more carbohydrates were found in the cake layer on the surface of the unmodified alumina membrane compared to that deposited on the surface of the ALD-modified

membrane. Once again, this finding was attributed to increase in surface hydrophilicity and improved surface topography of the modified membrane, which help in reducing the adhesion and adsorption of organic matter onto it. Also, this data is in good agreement with the BSA adsorption results (Figure 5-6). EPS production is the result of microbial activity and a smoother surface has less potential for bacterial adhesion, which might result in relatively less microbial activity on the surface of the ALD-modified membrane than the unmodified membrane, hence less concentration of EPS was produced and attached on the surface of the modified membrane. Consequently, the lower concentration of EPS on the ALD-modified membrane surface results in a slower TMP rise and slower fouling rate than that for the unmodified membrane. Detailed characterization of these organic substances was not carried out in this investigation.

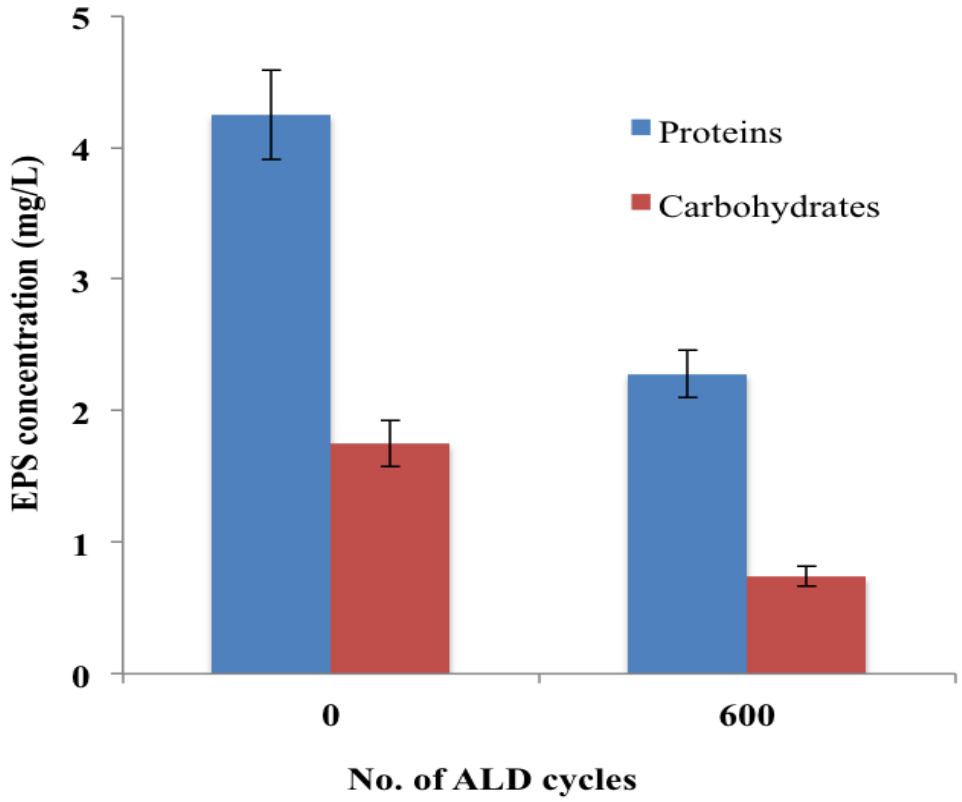

Figure 5-8: EPS Concentration of proteins and carbohydrates on the surface of fouled unmodified (0 ALD cycles) and TiO_2-modified (600 ALD cycles) alumina membranes.

5.4. Conclusions

In this study a commercial alumina ceramic membrane surface was modified by thin-film deposition of TiO_2 using the ALD method. The objective of this research was to assess the fouling behavior of ALD-modified membrane compared to that of the unmodified alumina membrane. An initial comparative test was conducted by operating both membranes in a lab-scale AnMBR system fed with synthetic wastewater. Characterization of the ALD-modified membranes showed precise thickness control of a TiO_2 thin film, high hydrophilicity and less surface roughness. The ALD-modified membranes also showed a lower adsorption potential for model foulant BSA and showed a lower rate of fouling in a lab-scale AnMBR operation in comparison with those for an unmodified alumina membrane. Summary of the findings is given below:

- The ALD method deposited a linearly controlled thickness of TiO_2 film on the surface of an alumina membrane, with different number of ALD cycles employed in this study.
- Even a very thin film of TiO_2 (thickness around 10 nm @ 200 ALD cycles) reduced the water contact angle of the original alumina membrane from 84.3° to 30.9°, hence the ALD-based modification enhanced surface hydrophilicity of the membrane. However, membrane hydrophilicity does not improve significantly for higher numbers of ALD cycles employed in this study. This shows that approximately same amount of TiO_2 is deposited uniformly in each monolayer over the membrane surface, independent of the numbers of ALD cycles applied.
- For lower number of ALD cycles (*i.e.* 200, 400, 600), the modified membranes nearly retained the intrinsic CWP of the alumina membrane (*i.e.*

1200 $L.m^{-2}.h^{-1}.bar^{-1}$). This finding was attributed to an increase in surface hydrophilicity of the alumina membrane with ALD-TiO_2 modification, which compensated the added hydraulic resistance that a deposited TiO_2 film might add. However, CWP declines sharply when the ALD cycles exceed 600, where the TiO_2 film becomes denser at higher ALD cycles (*i.e.* 1000 and 1600) and the thickness of the deposition layer significantly blocks the surface pores of the unmodified membrane.

- ALD-treatment also significantly reduced the surface roughness of the unmodified alumina membrane. A lower surface roughness was observed on the modified membranes with increasing number of ALD cycles, (Figure 5-5g).
- All ALD-modified membranes showed less potential for BSA adsorption in comparison with that for the unmodified alumina membrane.
- The optimized TiO_2-modified membrane with 600 ALD cycles showed a significant anti-fouling performance in a lab-scale constant-flux AnMBR filtration system in comparison with that for the unmodified membrane. Under the same operating conditions, the ALD-modified membrane took around 2.5 times of time-delay to reach a cut-off TMP of 40 kPa than that for unmodified membrane.
- Lower concentrations of proteins and carbohydrates were found in the cake layer formed on the surface of the fouled ALD-modified membrane as compared with those on the unmodified membrane (Figure 5-8). This finding was attributed to the increased hydrophilicity and reduced surface roughness of ALD-modified membranes, which helped in reducing the attachment of organic matter onto the membrane surface.

This investigation demonstrates the potential of the ALD method to be used as a possible practical solution for membrane surface modification to counter fouling problems in AnMBR filtration for wastewater treatment. However, further investigation is needed to work on improving the characteristics of the thin-film by varying the ALD process conditions and thin-film deposition by alternative metal-oxides for further testing and enhancing the anti-fouling potential of ALD-modified membranes for application in a larger scale.

CHAPTER: 6

COMPARATIVE STUDY OF ALGINATE FOULING INHIBITION POTENTIAL OF CERAMIC MEMBRANE MODIFIED WITH ALD-TiO_2 and ALD-SnO_2

Highlights

- Unmodified, ALD-SnO_2 and ALD-TiO_2 modified alumina membranes were tested for alginate fouling potential in a dead-end filtration system.
- This is the first report on ALD-SnO_2 modified alumina membranes for testing alginate fouling potential.
- Irrespective of the metal-oxide used, both ALD-modified membranes showed lower fouling potential than the unmodified membrane.
- Alginate fouling control potential was very similar for both the ALD-modified membranes.

Abstract

Membrane fouling is an inherent phenomenon in all membrane filtration processes. The membrane properties and characteristics as well as the type of feed water are important factors determining the different types of fouling response and behavior. Membrane properties related to hydrophilicity have been shown in various studies to be changed by different methods of surface modification. Such modified membranes can be efficiently utilized in water treatment applications to reduce fouling and increase water flux. Recently, we have shown that ALD can be used for surface modification of ceramic membranes and it results into: precise thin film thickness control, uniform coating and a precise control over the surface structures created. In this study, an ultrafiltration (UF) alumina membrane surface was modified with different oxide layers (*i.e.* TiO_2 and SnO_2) using the ALD method and a comparative study was conducted to assess their respective fouling inhibition potential during alginate filtration. TiO_2 is well-known for its fouling inhibition performance in water and wastewater treatment applications; however, to our knowledge this is the first investigation on application of SnO_2-modified membranes in this area.

Clean water permeability (CWP) tests were conducted for the unmodified alumina membrane and the ALD-TiO_2 and ALD-SnO_2 modified membranes. Thorough surface characterization, *i.e.* thin film thickness measurements, mean water contact angle measurements, roughness measurements, surface morphology, was carried out for all membranes. When all membranes were tested in a constant-pressure dead-end alginate filtration system, both the ALD-modified membranes showed slower flux decline in comparison with that of the unmodified alumina membrane, irrespective of the type of metal-oxide deposited on the surface. Alginate fouling potential was found to be very similar for both modified membranes, with a negligible difference

observed. The outcomes of this study show that SnO_2 coating of alumina membranes is a potential anti-fouling strategy that warrants further investigation for future membrane modification (or fabrication) which can be applied in water and wastewater treatment systems.

6.1 Introduction

In the previous phases of this PhD research, ALD is determined to be the best thin-film deposition (TFD) method for surface modification of a ceramic membrane and ALD-TiO_2 modified alumina membranes were proven to show superior results, as compared to pristine alumina membranes, in terms of surface characteristics and membrane fouling control in a lab-scale AnMBR system for wastewater treatment. Therefore, it becomes an issue of interest on how can a different and novel metal-oxide deposited by ALD might modify or alter the surface features of the alumina membrane to improve the anti-fouling performance in a membrane filtration system.

Having the same research question in mind, in this study a comparative study between an alumina membrane modified with ALD-TiO_2 and a similar modification with SnO_2 via the ALD method was conducted. SnO_2 has been widely used in several electrochemical applications and is known to have good hydrophilic properties [142, 143]. Based on previous experiments with fouling control in AnMBR filtration by applying highly hydrophilic surfaces through ALD-TiO_2 modification of alumina membrane, making a hydrophilic surface by SnO_2-modification was assumed to give a similar anti-fouling potential in a water-based membrane filtration system based hydrophilicity and surface roughness. SnO_2 was therefore chosen as an alternative metal-oxide for comparison with TiO_2 coating using the ALD method. The main objective of the study was to compare the surface characteristics (*i.e*. hydrophilicity, roughness, morphology etc.) of both ALD-TiO_2 and ALD-SnO_2 modified alumina membranes and to assess the fouling inhibition potential in lab-scale dead-end constant-pressure filtration tests using alginate as a model compound. It is also to be noted that, as of yet, there are no reports of application of SnO_2-modified ceramic membranes in water/wastewater treatment applications. Therefore, to our knowledge,

this is the first investigation on alginate fouling inhibition performance of an alumina membrane modified with SnO_2 thin films using the ALD method. Previously, alginate has been identified and used as a model foulant to study the filtration behavior and fouling mechanisms in various studies [144-149]. Therefore, in this study, alginate was chosen as a model foulant to test the fouling inhibition potential of each modified membrane. It is important to note that this investigation was conducted as a pre-screening test to study the interaction of ALD-SnO_2 modified membrane with alginate foulant. The study therefore used a simple dead-end constant-pressure filtration system for this part of study instead of using a more complex AnMBR filtration system, as used for the previous phases of this study. Based on the outcomes of the ALD-SnO_2 modified membrane performance in these pre-screening alginate filtration tests, application in an AnMBR system could be considered. The results showed that the ALD-SnO_2 modified membrane exhibited good surface characteristics and alginate fouling inhibition performance; hence SnO_2 coating is an option that should be further investigated as a potential anti-foulant strategy in water and wastewater treatment applications.

6.2 Materials and methods

6.2.1. Membrane surface modification

Commercially available flat sheet alumina UF membrane modules (KeraNor, Norway) with a nominal surface pore size of 80 nm (manufacturer specifications) and effective filtration area of 60 cm^2 were used in this study. Ultrathin films of TiO_2 and SnO_2 were deposited on the porous alumina membranes at 150 °C using a Cambridge Nanotech Savannah ALD system. One ALD cycle corresponds to a growth rate of 0.05 nm per cycle. 600 ALD cycles were applied on the membrane modification for

depositions of both TiO_2 and SnO_2 films. The membranes were annealed at a high temperature of 500 °C after the ALD-modification to further strengthen the interfacial adhesion between the deposited films and substrate.

6.2.2. Membrane surface characterization

The thicknesses of the ALD-TiO_2 and ALD-SnO_2 thin films were measured by mechanical surface profilometer (Veeco Dektak 150). Ten measurements were taken to obtain an average thickness. The surface morphology of unmodified alumina, TiO_2-modified and SnO_2-modified membranes was characterized by a field emission scanning electron microscope (FE-SEM), model NovaNano SEM (from FEI Company). Mean water contact angle measurements were performed for unmodified and both modified membranes using a Dropmeter A-100 contact angle goniometer. Experimental error was minimized by taking average values of five measurements of contact angle for each sample. Surface roughness of the alumina and modified membranes was determined by an atomic force microscope (AFM, Agilent Technologies, USA) using the tapping mode. This experiment was repeated for at least five times for each sample to obtain an average value.

6.2.3. Clean water permeability (CWP) tests

Clean water permeability (CWP) was determined with MQ water for the unmodified and modified membranes. The CWP was determined by dead-end filtration experiments conducted at 0.7 bar and 21 °C. The permeate flux was measured by collecting permeate over time on a balance connected to a computer. Average values were obtained by taking three measurements in order to minimize the experimental error.

6.2.4. Alginate filtration tests

Alginate powder (Roche Company) was used to prepare alginate solutions by dissolving alginate powder in deionized (DI) water, and used shortly after preparation. The pH values were adjusted to 7.0 by addition of HCl or NaOH as needed in all solutions. All the experiments were carried out using the unmodified alumina membrane and the two ALD-TiO_2 and ALD-SnO_2 modified membranes, each with around 30 nm thick layer. Temperature and pH of all the solutions were measured using a digital thermometer and a digital pH meter (Precisa series 900), respectively. All the experiments were conducted with a batch microfiltration cell. The membrane module was a rectangular cell which was connected to a solution reservoir at atmospheric pressure. A dead-end constant-pressure mode of operation was applied for the filtration tests using a vacuum pump on the permeate side. The trans-membrane pressure (TMP) was measured using two pressure meters before (atmospheric) and after (vacuum) the membrane cell. The volumetric flow rate was measured by continuous measuring of the filtrate volume. At the beginning of all the experiments, the solution reservoir was filled with DI water and the filtration was conducted with water until a steady condition was attained, then the solution reservoir and the membrane cell were evacuated and quickly refilled with the feed solution. All the experiments were conducted at room temperature (22 °C ± 1) and feed concentrations of 1.5 g/L alginate at a constant TMP of 1.5 bar. The filtration runs were repeated at least three times for each unmodified and ALD-modified membranes. The experimental set-up is shown in Figure 3-2.

6.3 Results and discussion

6.3.1 Surface morphology of unmodified, ALD-TiO_2 and ALD-SnO_2 modified alumina membranes

The surface morphology of the unmodified and both ALD-modified membranes was determined by scanning electron microscope (SEM) analysis. Figure 6-1(a-c) presents SEM images of the unmodified alumina membrane, ALD-TiO_2 and ALD-SnO_2 modified membranes respectively. ALD-films with TiO_2 and SnO_2 were grown at a constant deposition rate (0.05 nm/ALD cycle) for 600 ALD cycles and the thickness was measured by a mechanical profilometer. The measured thickness values of the TiO_2 and SnO_2 films were found to be slightly different from each other, however, both were in good agreement with anticipated values (i.e. 30 nm) based on the ALD process conditions. This slight difference in thickness of both deposited thin-films was attributed to the growth of different metal-oxides by ALD method.

Figure 6-1(a) presents an example of the surface images of the unmodified alumina membrane with an average pore size of 80 nm. When TiO_2 and SnO_2 films were deposited by ALD, the conformal nature of the ALD-deposited layers can be seen from Figures 6-1(b) and 6-1(c) respectively. The deposited films nearly take the shape of the original alumina grains. However, due to the thickness of the ALD-deposited layer, the surface porosity of the original membrane decreased proportionally. The ALD-film also appears to block a portion of the surface pores of the unmodified alumina membrane. This observation is in agreement with the basic operation principle of the ALD method. The energy dispersive spectroscopy (EDS) spectrum of TiO_2 and SnO_2 modified alumina membranes is presented in Figure 6-1(d-i and d-ii) respectively, which confirms the presence of Ti and Sn on the surface of the original membrane.

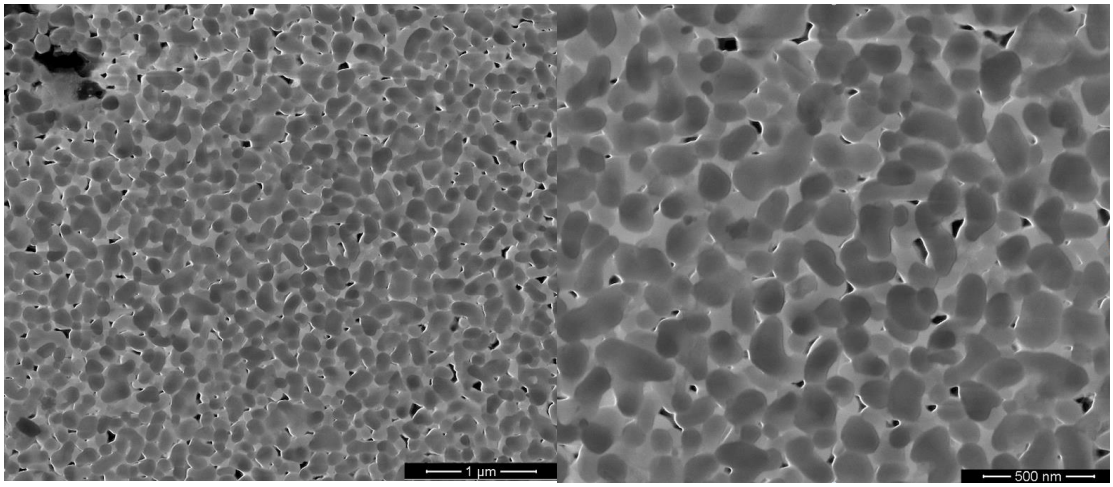

(a)

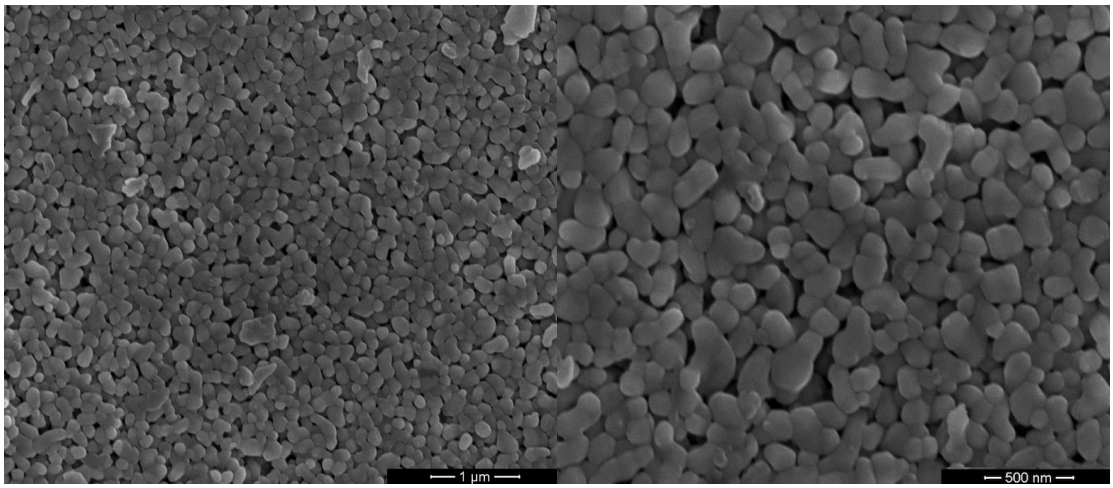

(b)

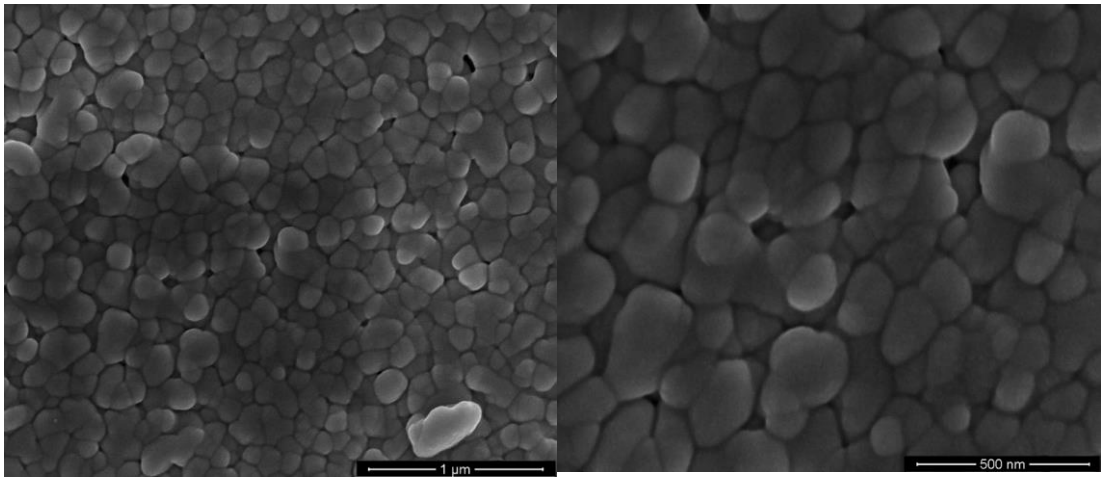

(c)

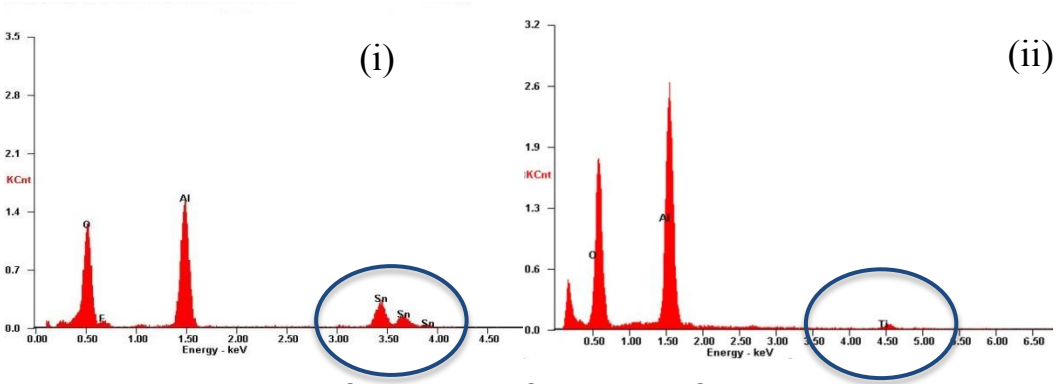

Figure 6-1: SEM surface images of (a) unmodified alumina membrane at magnification 25,000 and 50,000 (b) ALD-TiO_2 modified membrane at magnification 25,000 and 50,000 (c) ALD-SnO_2 modified membrane at magnification 40,000 and 80,000 and SEM-EDS spectrum of (d-i) ALD-TiO_2 membrane (d-ii) ALD-SnO_2 membrane

6.3.2 Effect of ALD-TiO_2 and ALD-SnO_2 modification on surface hydrophilicity

The hydrophobicity / hydrophilicity of a surface are commonly determined by measuring water contact angles. Measurements were made for the unmodified alumina membrane and the two ALD-modified membranes. Figure 6-2 presents the contact angle plot of water droplets on the surface, where it can be clearly seen that the surface hydrophilicity of the original alumina membrane is significantly increased by the deposition of both TiO_2 and SnO_2 thin films. The observed contact angle of the original substrate was 84.3°, and reduced to 26.2° for the ALD-TiO_2 modified membranes and to 38.2° for the ALD-SnO_2 modification. The difference observed between surface hydrophilicity of ALD-TiO_2 and ALD-SnO_2 modified membranes is not large though the contact angles measured indicate a slightly less hydrophilic property for SnO_2. The previous study reported that ALD-TiO_2 modified membrane improved the surface hydrophilicity of an alumina membrane and also helped reduce membrane fouling in a lab-scale AnMBR operation. Considering the similar hydrophilic characteristics of the ALD-SnO_2 modified membranes it is reasonable to

assume that the ALD-SnO_2 modification will have a similar effect on fouling control in wastewater treatment systems.

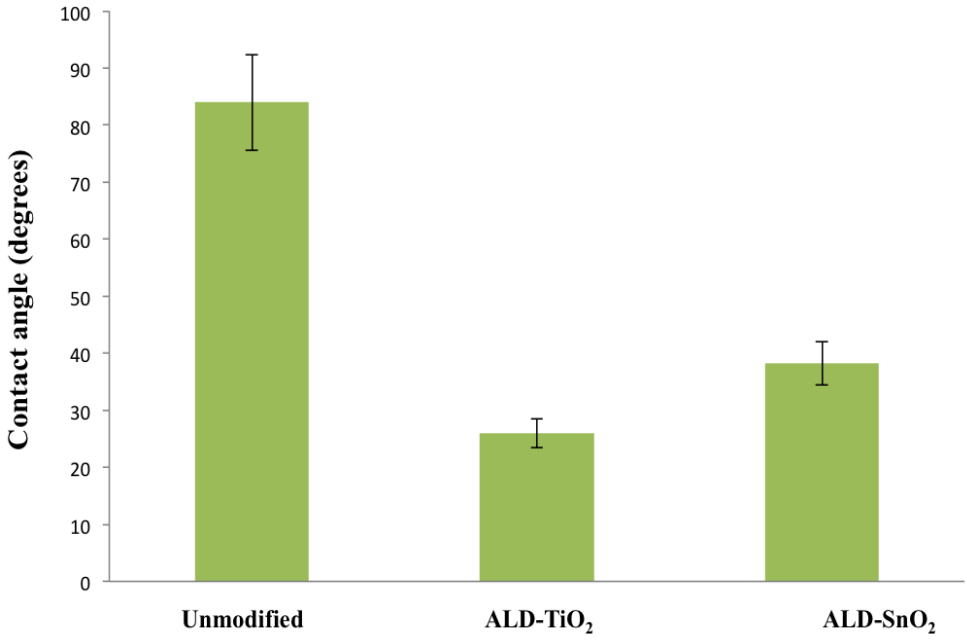

Figure 6-2: Contact angle of unmodified, ALD-TiO_2 and ALD-SnO_2 modified alumina membranes.

6.3.3 Clean water permeability of unmodified, ALD-TiO_2 and ALD-SnO_2 modified alumina membranes

Clean water permeability (CWP) tests were conducted for the unmodified alumina membrane and both ALD-modified membranes. Results presented in Figure 6-3 show the CWP for the three membranes tested. The CWP of the unmodified alumina membrane was 1200 $L.m^{-2}.h^{-1}.bar^{-1}$ and 1155 $L.m^{-2}.h^{-1}.bar^{-1}$ and 1126 $L.m^{-2}.h^{-1}.bar^{-1}$ for ALD-TiO_2 and ALD-SnO_2 modified membranes respectively. The CWP of the ALD-TiO_2 and ALD-SnO_2 membranes are similar and the deposition of the thin film layer does not significantly decrease the CWP compared to the original membrane. The results imply that with the same thickness of the ALD-coated film applied to both membranes (*i.e.* 30 nm), the modification did not significantly block the surface pores

of the original membrane and essentially retain the intrinsic CWP of the original membrane, but is sufficient to change the membrane surface hydrophilicity.

The SEM images of the membranes (Figure 6-1) also show that the ALD-based modification does not appear to significantly block the surface pores of the original alumina membrane. This is of course a function of the deposited film thickness where an increase in ALD cycles will deposit a thicker layer which starts to become dense and block the surface pores, hence reducing the intrinsic CWP of the original membrane, as reported earlier. Miller *et.al.* (2014) also reported that the clean water permeability of modified membranes was reduced due to reduction in effective pore size [141].

A smaller fraction of reduction in CWP for both ALD-modified membranes can also be attributed to their increased hydrophilicity, which compensates the added resistance by additional thin film layer on membrane surface. A similar observation has been reported by McCloskey *et.al.* (2012) where the effect of a decrease in pore size has been effectively offset due to an increase in hydrophilicity of the pores [124].

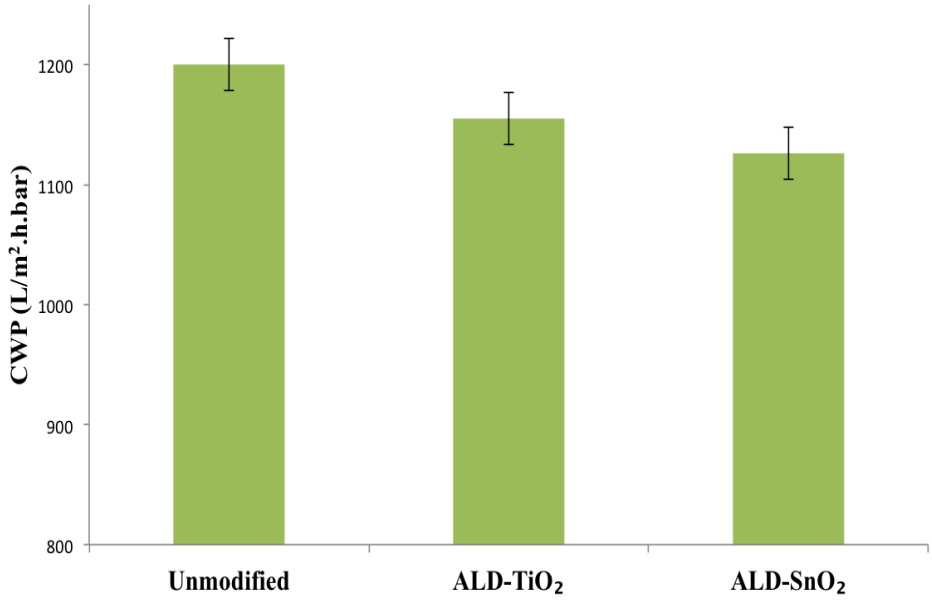

Figure 6-3: Clean water permeability (CWP) of unmodified, ALD-TiO_2 and ALD-SnO_2 modified alumina membranes.

6.3.4 Effect of ALD-TiO_2 and ALD-SnO_2 modification on surface roughness

Membrane surface roughness has been reported in literature to be an important parameter that affects membrane fouling in that rough surfaces have a higher potential for debris and colloidal material to be entrapped [25, 128, 150]. Therefore, in this study the surface roughness of the unmodified alumina membrane and both ALD-modified membranes was analyzed by atomic force microscopy (AFM). The respective images are shown in Figure 6-4(a). Surface roughness can be defined by various parameters, maximum height, Z-range and root mean square roughness (R_{ms}). Z-range and maximum height values usually do not give very accurate and precise measure of surface roughness and the R_{ms} value is typically used [131]. Therefore, in this study R_{ms} values to indicate surface roughness has been used. The higher the value of R_{ms}, the rougher the membrane surface would be. Measured R_{ms} values are plotted in Figure 6-4(b). The unmodified alumina membrane was found to have the roughest surface. The surface roughness was considerably decreased with the ALD-

deposition of both TiO_2 and SnO_2. Interestingly, the ALD-SnO_2 modification was observed to reduce the roughness to a relatively larger degree than the ALD-TiO_2 coating.

Compared to the ALD-TiO_2 modification, the ALD-SnO_2 modified membrane has a slightly higher contact angle and lower CWP values, however, the smoother surface obtained may compensate the anti-fouling potential. As such, both modified membranes are presumed to have a similar performance when applied in a water/ wastewater filtration system.

(a)

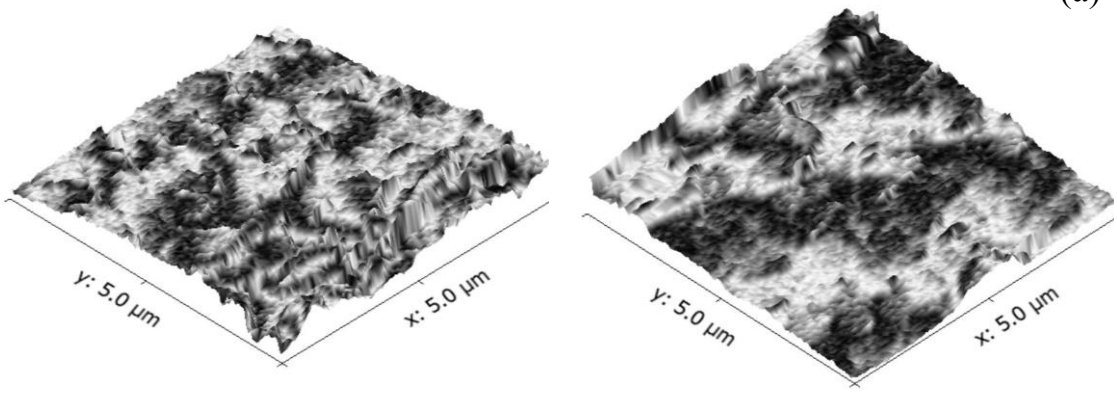

(i) Unmodified alumina membrane (ii) ALD-TiO_2 modified membrane

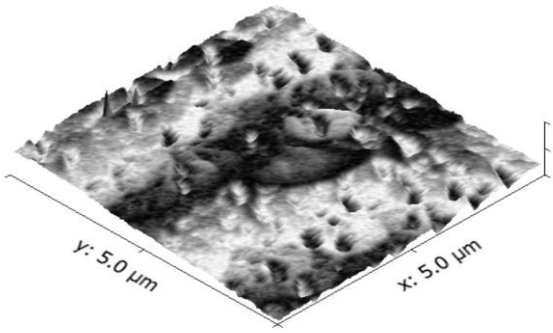

(iii) ALD-SnO_2 modified membrane

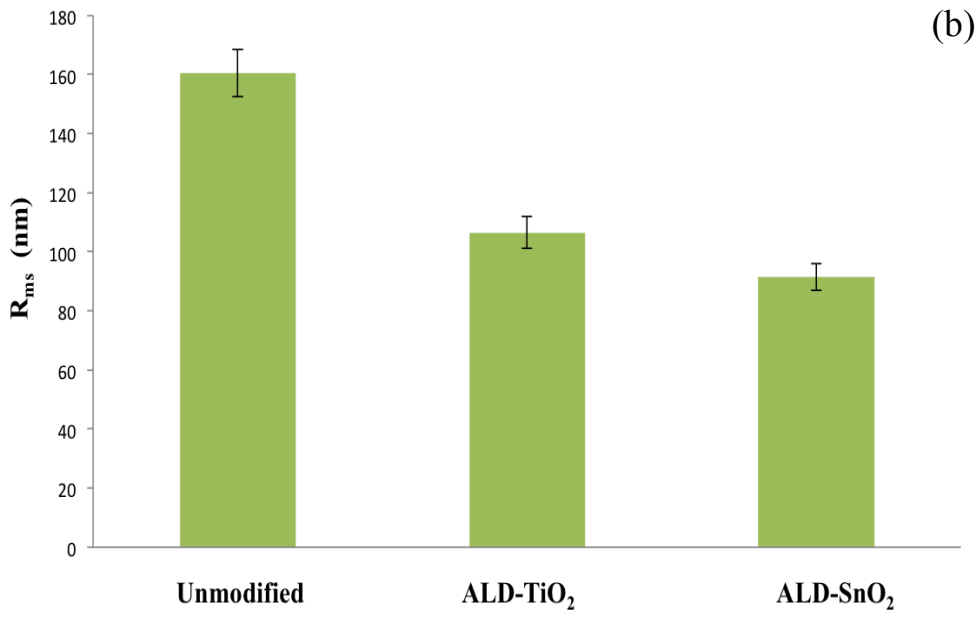

Figure 6-4: (a) AFM images of (i) unmodified alumina membrane (ii) ALD-TiO_2 modified membrane (iii) ALD-SnO_2 modified membrane and (b) Root mean square roughness (R_{ms}) of unmodified, ALD-TiO_2 modified and ALD-SnO_2 modified alumina membranes.

6.3.5 Fouling inhibition performance of ALD-TiO_2 and ALD-SnO_2 modified membranes in dead-end alginate filtration

Dead-end alginate filtration tests were conducted for the unmodified and both ALD-modified membranes to investigate the filtration performance with respect to fouling potential by organic matter. Results for normalized flux of alginate filtration tests for all membranes are shown in Figure 6-5. The unmodified alumina membrane was observed to have a greater potential for alginate fouling with a rapid flux decline in the first hour of filtration before stabilizing at about 55% of the initial flux. After 4 hours of operation a 65% of flux decline was observed for the original alumina membrane. The potential for alginate fouling was found to be relatively lesser for both modified membranes. As compared to alumina membrane, ALD-TiO_2 and ALD-SnO_2 membranes exhibited reduced flux decline of 34% and 40% after 1.5 hours of filtration respectively. This flux decline was then finally increased to about 46% and

50% for ALD-TiO_2 and ALD-SnO_2 membranes respectively, after the filtration operation of 4 hours. This finding is attributed to the increased hydrophilicity and reduced roughness of modified membranes' surface which helped reduce the potential for attachment / adhesion of the specific organic matter on the surface. It was also observed that there was a negligible amount of difference between the flux decline of ALD-TiO_2 modified membrane (i.e. 46%) and ALD-SnO_2 modified membrane (i.e. 50%). This can be explained by the fact that though the surface hydrophilicity of original alumina membrane was enhanced by ALD-TiO_2 modification in a relatively larger fraction than that for ALD-SnO_2 modification; however, surface roughness of the original membrane was reduced more by ALD-SnO_2 as compared with that for ALD-TiO_2. Therefore, due to a *'trade-off effect'* between the surface hydrophilicity and roughness of both modified membranes, we have observed a minute amount of difference in total percentage flux decline (hence fouling potential) between ALD-TiO_2 and ALD-SnO_2 modified membranes. Finally, based on this test, it was presumed that ALD-SnO_2 based surface modification of alumina membrane can be further tested as an anti-fouling strategy in water/wastewater treatment applications.

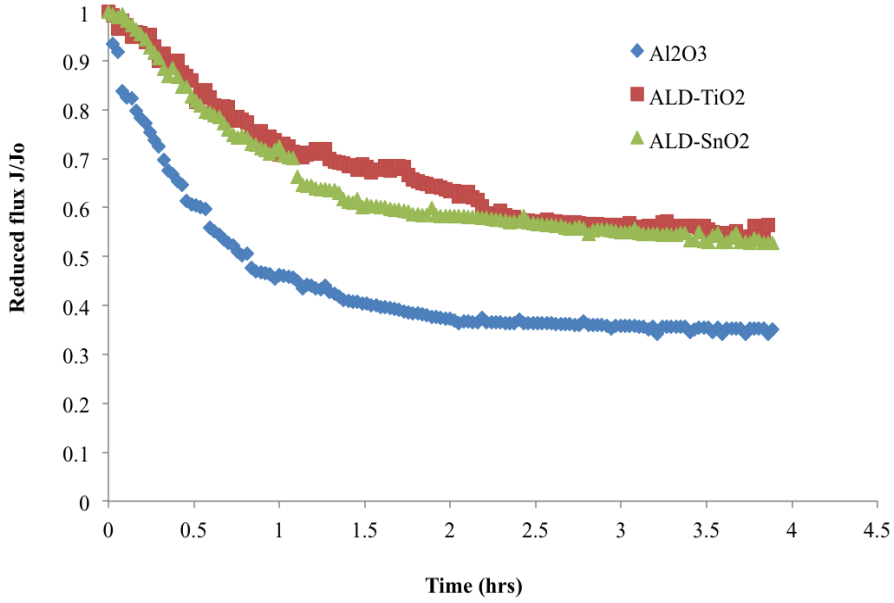

Figure 6-5: Normalized flux in UF of alginate dilute aqueous solutions with unmodified, ALD-TiO_2 and ALD-SnO_2 modified alumina membranes

6.4 Conclusions

To our knowledge, this is the first study of ALD-SnO_2 based surface modification of an alumina membrane for application in dead-end alginate filtration system for testing the fouling potential of the modified membrane. The ALD-SnO_2 modified membrane is compared with an unmodified alumina and ALD-TiO_2 modified membranes in terms of surface characteristics and fouling inhibition performance in alginate filtration system. Following conclusions were drawn:

- Different metal-oxides (TiO_2 and SnO_2), deposited by ALD, on a porous alumina membrane showed slightly different characteristics in terms of CWP, surface hydrophilicity and surface roughness.
- Irrespective of the oxide used for surface modification, both ALD-SnO_2 and ALD-TiO_2 modified membranes exhibited a lower rate of fouling (*i.e.* slower flux

decline) in a lab-scale dead-end alginate filtration test when compared with that for the unmodified alumina membrane.

- Alginate fouling potential of alumina membranes modified with TiO_2 and SnO_2 was determined to be very similar with negligible differences measured, in a lab-scale filtration test. This finding demonstrates the future potential of SnO_2 to be used as an anti-fouling strategy for membrane modification or fabrication for water/wastewater treatment applications.

This experiment could not verify hypothesis no. 5 (Chapter 1), suggesting that different surface features of the membranes would impact their different anti-fouling potential rather than the choice of metal-oxide used for membrane surface modification as long as similar properties are achieved.

CHAPTER: 7

CONCLUSIONS AND FUTURE WORK

7.1. Conclusions

This PhD research was carried out in the following three phases:

1. Investigate different surface modification techniques of a commercial alumina ceramic membrane with different thin-film deposition (TFD) methods, with the aim to provide a less fouling membrane to be applied in an anaerobic membrane bioreactor (AnMBR) process for advanced wastewater treatment.
2. Assess properties and characteristics of chosen surface modification method. Atomic layer deposition (ALD) was chosen using TiO_2 to deposit a thin film on an alumina membrane. The effect of different ALD-TiO_2 cycles for fouling control in AnMBR system was investigated.
3. A comparative study of alginate fouling inhibition potential of the optimal modified alumina membrane was conducted. Modification with an alternative metal-oxide was also conducted, with the comparative tests including ALD-SnO_2 and ALD-TiO_2 membranes.

In the first phase of this PhD research, a commercial alumina membrane was modified by deposition of comparable thickness of TiO_2 through different TFD methods, *i.e.* ALD, sputter and electron-beam (e-beam) deposition. Thorough surface characterization of the unmodified and TiO_2-modified membranes was carried out including; thin-film thickness measurement, contact angle measurement, scanning electron microscopy (SEM), electron dispersive spectroscopy (EDS), atomic force microscopy (AFM). The unmodified alumina membrane and all modified membranes were tested for clean water permeability (CWP) and bovine serum albumin (BSA) adsorption potential, with the aim of testing the most suitable membrane in a lab-scale

AnMBR filtration system. Following conclusions were drawn from this phase of the research activity:

- For the same thickness of TiO_2 thin-film, all modified membranes showed different surface characteristics for different TFD methods, in terms of hydrophilicity, roughness, CWP and BSA adsorption potential.
- In the AnMBR filtration test, all membranes modified with TiO_2 deposition with different TFD methods showed better fouling inhibition performance as compared to that for the unmodified alumina membrane.
- ALD was determined to be the best TFD method for TiO_2-modification of alumina surface, as it showed superior performance in terms of surface characteristics and fouling inhibition performance in AnMBR filtration, as compared to sputter and e-beam deposition. Also, less composition of extracellular polymeric substances (EPS) components was determined to be attached on the surface of ALD-modified membrane, as compared with all other membranes.

In the 2nd phase of this PhD research, ALD was chosen as the preferred method for surface modification of the alumina membrane. TiO_2 was deposited on the surface of the alumina membranes by applying 200, 400, 600, 1000 and 1600 ALD cycles. Thorough surface characterization of all ALD-modified membranes was carried-out. Optimum thickness of the TiO_2 thin-film was determined through surface characterization of all ALD-modified membranes and was compared with the unmodified alumina membrane for fouling inhibition performance in lab-scale AnMBR filtration test. Following conclusions were drawn from the experiments:

- Nearly linearly-controlled thicknesses of TiO_2-film were deposited by the ALD method, on the surface of the alumina membrane, for different number of ALD cycles.
- ALD-TiO_2 modification enhanced the surface hydrophilicity of the unmodified alumina membranes. Even 200 ALD cycles of TiO_2 coating (film thickness of around 10 nm) enhanced the surface hydrophilicity of the original alumina membrane by reducing the water contact angle from 84.3° to 30.9°. However, the higher number of ALD-TiO_2 cycles did not significantly increase the membrane's surface hydrophilicity, indicating that approximately same amount of TiO_2 is deposited conformly in each monolayer over the membrane surface, independent of the number of ALD cycles applied.
- ALD-modified membranes nearly retained the intrinsic CWP of the alumina membrane (*i.e.* 1200 $L.m^{-2}.h^{-1}.bar^{-1}$) for the lower number of ALD cycles (*i.e.* 200, 400, 600). This finding was attributed to an increase in surface hydrophilicity of the alumina membrane with TiO_2 modification, which compensated the increased hydraulic resistance caused by the additional film thickness. However, higher numbers of ALD cycles (*i.e.* 1000, 1600) decreased the CWP to a larger degree as the TiO_2 film become denser at higher ALD cycles and thus starts blocking surface pores of the unmodified alumina membrane. This effect was apparent based on the respective SEM image analysis of the various modified membranes.
- Surface roughness of the unmodified alumina membrane was significantly reduced with the TiO_2-modification, varying with different number of ALD cycles. With increasing number of ALD cycles the surface roughness was reduced, shown in Figure 5-5(g).

- The TiO_2-modified membrane modified with 600 ALD cycles was determined to have the optimum thin-film thickness and showed a significantly better anti-fouling performance, in terms of trans-membrane pressure (TMP) delay, than the unmodified alumina membrane in a lab-scale constant-flux AnMBR filtration test.
- Lower concentrations of proteins and carbohydrates were found in the cake layer formed on the surface of the fouled ALD-modified membrane compared to that on the surface of the fouled unmodified membrane (Figure 5-8). This finding was attributed to the increased hydrophilicity and reduced surface roughness of the ALD-modified membrane, which helped in reducing the attachment of organic matter onto the membrane surface.

In the 3rd phase of this PhD research, the potential of an alternative metal-oxide to modify the membrane surface properties was investigated. The ALD-TiO_2 modified alumina membrane was compared with an ALD-SnO_2 modified alumina membrane. Both modified membranes were compared in terms of surface characteristics and alginate fouling inhibition potential in a dead-end filtration system. To our knowledge this is the first study of an ALD-SnO_2 based surface modification of an alumina membrane for application in alginate filtration system for testing the fouling potential of modified membrane. Following conclusions were drawn:

- ALD-modification of the alumina membrane with different metal-oxides (TiO_2 and SnO_2) showed slightly different surface properties in terms of CWP, hydrophilicity and roughness.
- Both ALD-SnO_2 and ALD-TiO_2 modified membranes showed a lower rate of fouling (*i.e.* slower flux decline) than the unmodified alumina membrane in a

dead-end constant-pressure alginate filtration test, irrespective of the oxide used for surface modification.

- Alginate fouling potential was determined to be very similar for both ALD-modified membranes, with a negligible difference measured (Figure 6-5). This finding demonstrates the future potential of SnO_2 to be used as an anti-fouling strategy for membrane modification and/or fabrication when applied in water/wastewater treatment applications.

7.2 Prospects of future research work

Following directions can be further explored in continuation / extension of this PhD research:

1. **Surface modification of ceramic/polymeric membranes with different ALD metal-oxides:** Surface properties and filtration performance of different membrane substrates modified with ALD of different available metal-oxides (Al_2O_3, ZrO_2, ZnO, SiO_2, HfO_2, MoO_3 or a combination etc.) can be further tested. Also ALD technique can be further compared with other TFD methods (pulsed laser deposition, molecular vapor deposition etc.) for surface modification of membranes for application in membrane filtration systems.
2. **MBR filtration process conditions:** To study the effect of variation in MBR filtration process conditions (Flux, strength of wastewater, hydraulic retention time (HRT), organic loading rate (OLR), cross-flow velocity (CFV), backwashing, cleaning methods etc.) on the anti-fouling performance of ALD-modified membranes for wastewater treatment.
3. **Other membrane filtration systems:** Anti-fouling performance of ALD-modified membranes can also be tested in other membrane filtration systems (e.g.

RO, aerobic MBR, algal MBR etc.), based on a similar strategy as applied in this PhD research.

4. **MBR configuration:** Performance of ALD-modified ceramic membranes can be investigated as function of MBR configuration (suspended vs. attached growth)
5. **ALD process conditions:** Effect of variation in ALD process conditions (deposition rate, deposition temperature etc.) on the surface characteristics and ALD-modified membranes can be studied.

REFERENCES

[1] M. Kummu, P.J. Ward, H. de Moel, O. Varis, Is physical water scarcity a new phenomenon? Global assessment of water shortage over the last two millennia, Environmental Research Letters, 5 (2010) 034006.

[2] P. Le-Clech, Membrane bioreactors and their uses in wastewater treatments, Applied microbiology and biotechnology, 88 (2010) 1253-1260.

[3] B.-Q. Liao, J.T. Kraemer, D.M. Bagley, Anaerobic membrane bioreactors: applications and research directions, Critical Reviews in Environmental Science and Technology, 36 (2006) 489-530.

[4] R.K. Dereli, M.E. Ersahin, H. Ozgun, I. Ozturk, D. Jeison, F. van der Zee, J.B. van Lier, Potentials of anaerobic membrane bioreactors to overcome treatment limitations induced by industrial wastewaters, Bioresource Technology, 122 (2012) 160-170.

[5] C.B. Ersu, S.K. Ong, Treatment of wastewater containing phenol using a tubular ceramic membrane bioreactor, Environmental technology, 29 (2008) 225-234.

[6] M.a. Markets, Ceramic Membrane Market by Material (Titania, Alumina, Zirconium Oxide), by Application (Water and Wastewater Technology, Pharmaceuticals, Food and Beverage, Chemical Processing, Biotechnology), by Technology (Ultrafiltration, Microfiltration, Nanofiltration), by Region - Global Trends & Forecasts to 2020", Market reports, (2014).

[7] V. Vatanpour, S.S. Madaeni, R. Moradian, S. Zinadini, B. Astinchap, Novel antibifouling nanofiltration polyethersulfone membrane fabricated from embedding TiO 2 coated multiwalled carbon nanotubes, Separation and purification technology, 90 (2012) 69-82.

[8] Y. Ye, P. Le Clech, V. Chen, A.G. Fane, B. Jefferson, Fouling mechanisms of alginate solutions as model extracellular polymeric substances, Desalination, 175 (2005) 7-20.

[9] D. Bixio, C. Thoeye, J. De Koning, D. Joksimovic, D. Savic, T. Wintgens, T. Melin, Wastewater reuse in Europe, Desalination, 187 (2006) 89-101.

[10] H.E. Muga, J.R. Mihelcic, Sustainability of wastewater treatment technologies, Journal of environmental management, 88 (2008) 437-447.

[11] P. Côté, H. Buisson, C. Pound, G. Arakaki, Immersed membrane activated sludge for the reuse of municipal wastewater, Desalination, 113 (1997) 189-196.

[12] T. Melin, B. Jefferson, D. Bixio, C. Thoeye, W. De Wilde, J. De Koning, J. Van der Graaf, T. Wintgens, Membrane bioreactor technology for wastewater treatment and reuse, Desalination, 187 (2006) 271-282.

[13] J.R.M. Willetts, N.J. Ashbolt, R.E. Moosbrugger, M.R. Aslam, The use of a thermophilic anaerobic system for pretreatment of textile dye wastewater, Water science and technology, 42 (2000) 309-316.

[14] M. Sattler, Anaerobic processes for waste treatment and energy generation, Citeseer, 2011.

[15] H. Lin, W. Peng, M. Zhang, J. Chen, H. Hong, Y. Zhang, A review on anaerobic membrane bioreactors: applications, membrane fouling and future perspectives, Desalination, 314 (2013) 169-188.

[16] A. Santos, S. Judd, The commercial status of membrane bioreactors for municipal wastewater, Separation Science and Technology, 45 (2010) 850-857.

[17] S. Zhang, Y. Qu, Y. Liu, F. Yang, X. Zhang, K. Furukawa, Y. Yamada, Experimental study of domestic sewage treatment with a metal membrane bioreactor, Desalination, 177 (2005) 83-93.

[18] J.-O. Kim, J.-T. Jung, Performance of membrane-coupled organic acid fermentor for the resources recovery form municipal sewage sludge, Water science and technology, 55 (2007) 245-252.

[19] R.W. Baker, Membrane technology and applications, John Wiley & Sons, Ltd, (2004) 96-103.

[20] B. Rezania, J.A. Oleszkiewicz, N. Cicek, Hydrogen-driven denitrification of wastewater in an anaerobic submerged membrane bioreactor: potential for water reuse, Water science and technology, 54 (2006) 207-214.

[21] S. Zeigler, Treatment of Low Strength Wastewater Using Bench-Scale Anaerobic Membrane Bioreactor, Proceedings of the Water Environment Federation, 2007 (2007) 9207-9218.

[22] H. Lin, J. Chen, F. Wang, L. Ding, H. Hong, Feasibility evaluation of submerged anaerobic membrane bioreactor for municipal secondary wastewater treatment, Desalination, 280 (2011) 120-126.

[23] K. Wong, I. Xagoraraki, J. Wallace, W. Bickert, S. Srinivasan, J.B. Rose, Removal of viruses and indicators by anaerobic membrane bioreactor treating animal waste, Journal of environmental quality, 38 (2009) 1694-1699.

[24] S.H. Baek, K.R. Pagilla, Aerobic and anaerobic membrane bioreactors for municipal wastewater treatment, Water environment research, 78 (2006) 133-140.

[25] Y. He, P. Xu, C. Li, B. Zhang, High-concentration food wastewater treatment by an anaerobic membrane bioreactor, Water Research, 39 (2005) 4110-4118.

[26] S.I. Padmasiri, J. Zhang, M. Fitch, B. Norddahl, E. Morgenroth, L. Raskin, Methanogenic population dynamics and performance of an anaerobic membrane bioreactor (AnMBR) treating swine manure under high shear conditions, Water research, 41 (2007) 134-144.

[27] A.P. Trzcinski, D.C. Stuckey, Continuous treatment of the organic fraction of municipal solid waste in an anaerobic two-stage membrane process with liquid recycle, Water research, 43 (2009) 2449-2462.

[28] M. Xu, X. Wen, X. Huang, Y. Li, Membrane fouling control in an anaerobic membrane bioreactor coupled with online ultrasound equipment for digestion of waste activated sludge, Separation Science and Technology, 45 (2010) 941-947.

[29] E. Jeong, H.-W. Kim, J.-Y. Nam, Y.-T. Ahn, H.-S. Shin, Effects of the hydraulic retention time on the fouling characteristics of an anaerobic membrane bioreactor for treating acidifi ed wastewater, Desalination and Water Treatment, 18 (2010) 251-256.

[30] D. Jeison, W. Van Betuw, J.B. Van Lier, Feasibility of anaerobic membrane bioreactors for the treatment of wastewaters with particulate organic matter, Separation Science and Technology, 43 (2008) 3417-3431.

[31] M. Herrera-Robledo, J.M. Morgan-Sagastume, A. Noyola, Biofouling and pollutant removal during long-term operation of an anaerobic membrane bioreactor treating municipal wastewater, Biofouling, 26 (2010) 23-30.

[32] D. Jeison, P. Telkamp, J.B. Van Lier, Thermophilic sidestream anaerobic membrane bioreactors: the shear rate dilemma, Water environment research, 81 (2009) 2372-2380.

[33] S.-H. Roh, Y.N. Chun, J.-W. Nah, H.-J. Shin, S.-I. Kim, WastewaterTreatment by Anaerobic Digestion Coupled with Membrane Processing, Journal of Industrial and Engineering Chemistry, 12 (2006) 489-493.

[34] S.F. Aquino, A.Y. Hu, A. Akram, D.C. Stuckey, Characterization of dissolved compounds in submerged anaerobic membrane bioreactors (SAMBRs), Journal of Chemical Technology and Biotechnology, 81 (2006) 1894-1904.

[35] A. Spagni, S. Casu, N.A. Crispino, R. Farina, D. Mattioli, Filterability in a submerged anaerobic membrane bioreactor, Desalination, 250 (2010) 787-792.

[36] J. Kim, C.-H. Lee, K.-H. Choo, Control of struvite precipitation by selective removal of {\ text {NH}}^{{\ text {+}}} _ {{\ text {4}}} with dialyzer/zeolite in an anaerobic membrane bioreactor, Applied microbiology and biotechnology, 75 (2007) 187-193.

[37] P. Sui, X. Wen, X. Huang, Membrane fouling control by ultrasound in an anaerobic membrane bioreactor, Frontiers of Environmental Science & Engineering in China, 1 (2007) 362-367.

[38] A. Saddoud, I. Hassaïri, S. Sayadi, Anaerobic membrane reactor with phase separation for the treatment of cheese whey, Bioresource technology, 98 (2007) 2102-2108.

[39] M.-S. Kim, D.-Y. Lee, D.-H. Kim, Continuous hydrogen production from tofu processing waste using anaerobic mixed microflora under thermophilic conditions, International journal of Hydrogen energy, 36 (2011) 8712-8718.

[40] A. Pierkiel, J. Lanting, Membrane-coupled anaerobic digestion of municipal sewage sludge, Water Science and Technology, 52 (2005) 253-258.

[41] P.R. Berube, E.R. Hall, Removal of methanol from evaporator condensate using a high temperature membrane bioreactor: determination of optimal operating temperature and system costs: A promising alternative to conventional methods, Pulp & paper Canada, 101 (2000) 54-58.

[42] B.E.L. Baêta, R.L. Ramos, D.R.S. Lima, S.F. Aquino, Use of submerged anaerobic membrane bioreactor (SAMBR) containing powdered activated carbon (PAC) for the treatment of textile effluents, Water Science and Technology, 65 (2012) 1540-1547.

[43] X. Zhang, Z. Wang, Z. Wu, F. Lu, J. Tong, L. Zang, Formation of dynamic membrane in an anaerobic membrane bioreactor for municipal wastewater treatment, Chemical Engineering Journal, 165 (2010) 175-183.

[44] S.H. Baek, K.R. Pagilla, H.-J. Kim, Lab-scale study of an anaerobic membrane bioreactor (AnMBR) for dilute municipal wastewater treatment, Biotechnology and Bioprocess Engineering, 15 (2010) 704-708.

[45] B. Lew, S. Tarre, M. Beliavski, C. Dosoretz, M. Green, Anaerobic membrane bioreactor (AnMBR) for domestic wastewater treatment, Desalination, 243 (2009) 251-257.

[46] F. Meng, B. Liao, S. Liang, F. Yang, H. Zhang, L. Song, Morphological visualization, componential characterization and microbiological identification of membrane fouling in membrane bioreactors (MBRs), Journal of Membrane Science, 361 (2010) 1-14.

[47] F. Meng, S.-R. Chae, A. Drews, M. Kraume, H.-S. Shin, F. Yang, Recent advances in membrane bioreactors (MBRs): membrane fouling and membrane material, Water research, 43 (2009) 1489-1512.

[48] D. Jeison, J.B. van Lier, Cake formation and consolidation: main factors governing the applicable flux in anaerobic submerged membrane bioreactors (AnSMBR) treating acidified wastewaters, Separation and Purification Technology, 56 (2007) 71-78.

[49] B.-K. Hwang, W.-N. Lee, K.-M. Yeon, P.-K. Park, C.-H. Lee, i.-S. Chang, A. Drews, M. Kraume, Correlating TMP increases with microbial characteristics in the bio-cake on the membrane surface in a membrane bioreactor, Environmental science & technology, 42 (2008) 3963-3968.

[50] I.-S. Chang, P. Le Clech, B. Jefferson, S. Judd, Membrane fouling in membrane bioreactors for wastewater treatment, Journal of environmental engineering, 128 (2002) 1018-1029.

[51] S. Chang, A.G. Fane, S. Vigneswaran, Modeling and optimizing submerged hollow fiber membrane modules, AIChE journal, 48 (2002) 2203-2212.

[52] K. Li, X. Tan, Y. Liu, Single-step fabrication of ceramic hollow fibers for oxygen permeation, Journal of membrane science, 272 (2006) 1-5.

[53] P. Le Clech, B. Jefferson, I.S. Chang, S.J. Judd, Critical flux determination by the flux-step method in a submerged membrane bioreactor, Journal of membrane science, 227 (2003) 81-93.

[54] A. Brookes, B. Jefferson, G. Guglielmi, S.J. Judd, Sustainable flux fouling in a membrane bioreactor: impact of flux and MLSS, Separation science and technology, 41 (2006) 1279-1291.

[55] H. Lin, B.-Q. Liao, J. Chen, W. Gao, L. Wang, F. Wang, X. Lu, New insights into membrane fouling in a submerged anaerobic membrane bioreactor based on

characterization of cake sludge and bulk sludge, Bioresource technology, 102 (2011) 2373-2379.

[56] J. Grundestam, D. Hellström, Wastewater treatment with anaerobic membrane bioreactor and reverse osmosis, Water Science and Technology, 56 (2007) 211-217.

[57] H.J. Lin, K. Xie, B. Mahendran, D.M. Bagley, K.T. Leung, S.N. Liss, B.Q. Liao, Sludge properties and their effects on membrane fouling in submerged anaerobic membrane bioreactors (SAnMBRs), Water Research, 43 (2009) 3827-3837.

[58] A. Drews, Membrane fouling in membrane bioreactors—characterisation, contradictions, cause and cures, Journal of membrane science, 363 (2010) 1-28.

[59] G. Kang, M. Liu, B. Lin, Y. Cao, Q. Yuan, A novel method of surface modification on thin-film composite reverse osmosis membrane by grafting poly (ethylene glycol), Polymer, 48 (2007) 1165-1170.

[60] A. Asatekin, A. Menniti, S. Kang, M. Elimelech, E. Morgenroth, A.M. Mayes, Antifouling nanofiltration membranes for membrane bioreactors from self-assembling graft copolymers, Journal of Membrane Science, 285 (2006) 81-89.

[61] T.-H. Bae, T.-M. Tak, Preparation of TiO 2 self-assembled polymeric nanocomposite membranes and examination of their fouling mitigation effects in a membrane bioreactor system, Journal of membrane science, 266 (2005) 1-5.

[62] H.F. Zhang, H.P. Liu, L.H. Zhang, Applied research of nanocomposite membrane on fouling mitigation in membrane bioreactor, in, Trans Tech Publ, pp. 2019-2023.

[63] K. Li, Ceramic membranes for separation and reaction, John Wiley & Sons, 2007.

[64] H.P. Hsieh, R.R. Bhave, H.L. Fleming, Microporous alumina membranes, Journal of membrane science, 39 (1988) 221-241.

[65] H.P. Hsieh, Inorganic membranes for separation and reaction, Elsevier, 1996.

[66] E. Meabe, J. Lopetegui, J. Ollo, S. Lardies, Ceramic Membrane Bioreactor: potential applications and challenges for the future, Spain: CEIT Technological Center, (2013) 1-9.

[67] F.M. Tiller, C.D. Tsai, Theory of filtration of ceramics: I, slip casting, Journal of the American Ceramic Society, 69 (1986) 882-887.

[68] A. Larbot, Ceramic processing techniques of support systems for membranes synthesis, Membrane Science and Technology, 4 (1996) 119-139.

[69] M. Sahibzada, B.C.H. Steele, K. Hellgardt, D. Barth, A. Effendi, D. Mantzavinos, I.S. Metcalfe, Intermediate temperature solid oxide fuel cells operated with methanol fuels, Chemical Engineering Science, 55 (2000) 3077-3083.

[70] A.F.M. Leenaars, K. Keizer, A.J. Burggraaf, The preparation and characterization of alumina membranes with ultra-fine pores, Journal of Materials Science, 19 (1984) 1077-1088.

[71] A. Leenaars, A.J. Burggraaf, The preparation and characterization of alumina membranes with ultra-fine pores: Part 4. Ultrafiltration and hyperfiltration experiments, Journal of membrane science, 24 (1985) 261-270.

[72] A.F.M. Leenaars, A.J. Burggraaf, The preparation and characterization of alumina membranes with ultra-fine pores: Part 3. The permeability for pure liquids, Journal of membrane science, 24 (1985) 245-260.

[73] A. Larbot, A. Julbe, C. Guizard, L. Cot, Silica membranes by the sol-gel process, Journal of membrane science, 44 (1989) 289-303.

[74] L.C. Klein, D. Gallagher, Pore structures of sol-gel silica membranes, Journal of membrane science, 39 (1988) 213-220.

[75] M.A. Anderson, M.J. Gieselmann, Q. Xu, Titania and alumina ceramic membranes, Journal of Membrane Science, 39 (1988) 243-258.

[76] M.D. Moosemiller, C.G. Hill Jr, M.A. Anderson, Physicochemical properties of supported γ-Al2O3 and TiO2 ceramic membranes, Separation Science and Technology, 24 (1989) 641-657.

[77] A.J. Burggraaf, Fundamentals of membrane top-layer synthesis and processing, Membrane Science and Technology, 4 (1996) 259-329.

[78] I.-J. Kang, S.-H. Yoon, C.-H. Lee, Comparison of the filtration characteristics of organic and inorganic membranes in a membrane-coupled anaerobic bioreactor, Water research, 36 (2002) 1803-1813.

[79] Siemens, Membranes in wastewater treatment; for the oil and gas, rubber processing and palm oil industries, Singapore international water week, (2011).

[80] S.H. Park, Y.G. Park, J.-L. Lim, S. Kim, Evaluation of ceramic membrane applications for water treatment plants with a life cycle cost analysis, Desalination and Water Treatment, 54 (2015) 973-979.

[81] C. industry, Water and wastewater treatment continues to drive global nanofiltration ceramic membranes demand, Ceramics international, (2014).

[82] K. Shams Ashaghi, M. Ebrahimi, P. Czermak, Ceramic ultra-and nanofiltration membranes for oilfield produced water treatment: a mini review, Open Environmental Sciences, 1 (2007).

[83] W.a.w. international, TOUGH TALKING: INNOVATION AND APPLICATIONS FOR CERAMIC MEMBRANES, water world, (2014).

[84] V. Kochkodan, N. Hilal, A comprehensive review on surface modified polymer membranes for biofouling mitigation, Desalination, 356 (2015) 187-207.

[85] B. Van der Bruggen, M. Mänttäri, M. Nyström, Drawbacks of applying nanofiltration and how to avoid them: a review, Separation and Purification Technology, 63 (2008) 251-263.

[86] M. Ulbricht, K. Richau, H. Kamusewitz, Chemically and morphologically defined ultrafiltration membrane surfaces prepared by heterogeneous photo-initiated graft polymerization, Colloids and Surfaces A: Physicochemical and Engineering Aspects, 138 (1998) 353-366.

[87] D. Rana, T. Matsuura, Surface Modifications for Antifouling Membranes, Chemical Reviews, 110 (2010) 2448-2471.

[88] K. Sunada, Y. Kikuchi, K. Hashimoto, A. Fujishima, Bactericidal and detoxification effects of TiO2 thin film photocatalysts, Environmental Science & Technology, 32 (1998) 726-728.

[89] S.-Y. Kwak, S.H. Kim, S.S. Kim, Hybrid organic/inorganic reverse osmosis (RO) membrane for bactericidal anti-fouling. 1. Preparation and characterization of TiO2 nanoparticle self-assembled aromatic polyamide thin-film-composite (TFC) membrane, Environmental science & technology, 35 (2001) 2388-2394.

[90] S.H. Kim, S.-Y. Kwak, B.-H. Sohn, T.H. Park, Design of TiO< sub> 2</sub> nanoparticle self-assembled aromatic polyamide thin-film-composite (TFC) membrane as an approach to solve biofouling problem, Journal of Membrane Science, 211 (2003) 157-165.

[91] V.K.K. Upadhyayula, V. Gadhamshetty, Appreciating the role of carbon nanotube composites in preventing biofouling and promoting biofilms on material surfaces in environmental engineering: a review, Biotechnology advances, 28 (2010) 802-816.

[92] S. Kang, M. Herzberg, D.F. Rodrigues, M. Elimelech, Antibacterial effects of carbon nanotubes: size does matter!, Langmuir, 24 (2008) 6409-6413.

[93] B.-H. Jeong, E.M.V. Hoek, Y. Yan, A. Subramani, X. Huang, G. Hurwitz, A.K. Ghosh, A. Jawor, Interfacial polymerization of thin film nanocomposites: a new concept for reverse osmosis membranes, Journal of Membrane Science, 294 (2007) 1-7.

[94] A.K. Ghosh, E.M.V. Hoek, Impacts of support membrane structure and chemistry on polyamide–polysulfone interfacial composite membranes, Journal of Membrane Science, 336 (2009) 140-148.

[95] H.S. Lee, S.J. Im, J.H. Kim, H.J. Kim, J.P. Kim, B.R. Min, Polyamide thin-film nanofiltration membranes containing TiO< sub> 2</sub> nanoparticles, Desalination, 219 (2008) 48-56.

[96] B.-H. Jeong, E. Hoek, Y. Yan, A. Subramani, X. Huang, G. Hurwitz, A.K. Ghosh, A. Jawor, Interfacial polymerization of thin film nanocomposites: a new concept for reverse osmosis membranes, Journal of Membrane Science, 294 (2007) 1-7.

[97] T. Ishigami, K. Amano, A. Fujii, Y. Ohmukai, E. Kamio, T. Maruyama, H. Matsuyama, Fouling reduction of reverse osmosis membrane by surface modification via layer-by-layer assembly, Separation and purification technology, 99 (2012) 1-7.

[98] W. Kern, Thin film processes II, Academic press, 2012.

[99] K. Seshan, Handbook of thin film deposition, William Andrew, 2012.

[100] M. Bouman, F. Zaera, (Invited) The Surface Chemistry of Atomic Layer Deposition (ALD) Processes for Metal Nitride and Metal Oxide Film Growth, ECS Transactions, 33 (2010) 291-305.

[101] S.M. George, Atomic layer deposition: an overview, Chemical reviews, 110 (2010) 111-131.

[102] V. Miikkulainen, T. Rasilainen, E. Puukilainen, M. Suvanto, T.A. Pakkanen, Atomic layer deposition as pore diameter adjustment tool for nanoporous aluminum oxide injection molding masks, Langmuir, 24 (2008) 4473-4477.

[103] K. Grigoras, V.M. Airaksinen, S. Franssila, Coating of Nanoporous Membranes: Atomic Layer Deposition versus Sputtering, Journal of Nanoscience and Nanotechnology, 9 (2009) 3763-3770.

[104] S.M. George, B. Yoon, A.A. Dameron, Surface Chemistry for Molecular Layer Deposition of Organic and Hybrid Organic-Inorganic Polymers, Accounts of Chemical Research, 42 (2009) 498-508.

[105] Y.-B. Jiang, G. Xomeritakis, Z. Chen, D. Dunphy, D.J. Kissel, J.L. Cecchi, C.J. Brinkertt, Sub-10 nm thick microporous membranes made by plasma-defined atomic layer deposition of a bridged silsesquioxane precursor, Journal of the American Chemical Society, 129 (2007) 15446-+.

[106] S. Ghosal, T.F. Baumann, J.S. King, S.O. Kucheyev, Y. Wang, M.A. Worsley, J. Biener, S.F. Bent, A.V. Hamza, Controlling atomic layer deposition of TiO2 in aerogels through surface functionalization, Chemistry of Materials, 21 (2009) 1989-1992.

[107] S.O. Kucheyev, J. Biener, T.F. Baumann, Y.M. Wang, A.V. Hamza, Z. Li, D.K. Lee, R.G. Gordon, Mechanisms of atomic layer deposition on substrates with ultkahigh aspect ratios, Langmuir, 24 (2008) 943-948.

[108] B. Ahmed, M. Shahid, D.H. Nagaraju, D.H. Anjum, M.N. Hedhili, H.N. Alshareef, Surface Passivation of MoO3 Nanorods by Atomic Layer Deposition toward High Rate Durable Li Ion Battery Anodes, Acs Applied Materials & Interfaces, 7 (2015) 13154-13163.

[109] B. Ahmed, D.H. Anjum, M.N. Hedhili, H.N. Alshareef, Mechanistic Insight into the Stability of HfO2-Coated MoS2 Nanosheet Anodes for Sodium Ion Batteries, Small, 11 (2015) 4341-4350.

[110] F. Li, Y. Yang, Y. Fan, W. Xing, Y. Wang, Modification of ceramic membranes for pore structure tailoring: The atomic layer deposition route, Journal of membrane science, 397 (2012) 17-23.

[111] E. Kim, ELECTRON BEAM DEPOSITION.

[112] R. Behrisch, K. Wittmaack, Sputtering by particle bombardment, Springer Berlin, 1981.

[113] D.B. Chrisey, G.K. Hubler, Pulsed laser deposition of thin films, (1994).

[114] U.o. freiburg, Atomic layer deposition, Department of MIcrosystems engineering - IMTEK, (2015).

[115] A. materials, ALB technology, (2015).

[116] Mattopia, Sputter deposition, Wikipedia, (2004).

[117] IST, Pulsed laser deposition-Abstract, (2004).

[118] Y. Zhuan, Z. Li-Ping, X. You-Yi, L. Xiao-Lin, Y. Jing-Zhen, Z. Bao-Ku, F127-based multi-block copolymer additives with poly(N,N-dimethylamino-2-ethyl methacrylate) end chains: The hydrophilicity and stimuli-responsive behavior

investigation in polyethersulfone membranes modification, Journal of Membrane Science, 364 (2010) 34-42.

[119] Y.-H. Zhao, B.-K. Zhu, L. Kong, Y.-Y. Xu, Improving hydrophilicity and protein resistance of poly(vinylidene fluoride) membranes by blending with amphiphilic hyperbranched-star polymer, Langmuir, 23 (2007) 5779-5786.

[120] C.-H. Wei, M. Harb, G. Amy, P.-Y. Hong, T. Leiknes, Sustainable organic loading rate and energy recovery potential of mesophilic anaerobic membrane bioreactor for municipal wastewater treatment, Bioresource Technology, 166 (2014) 326-334.

[121] A. American Public Health, A. American Water Works, F. Water Pollution Control, F. Water Environment, Standard methods for the examination of water and wastewater, American Public Health Association., 1998.

[122] O.H. Lowry, N.J. Rosebrough, A.L. Farr, R.J. Randall, PROTEIN MEASUREMENT WITH THE FOLIN PHENOL REAGENT, Journal of Biological Chemistry, 193 (1951) 265-275.

[123] M. Dubois, K.A. Gilles, J.K. Hamilton, P.A. Rebers, F. Smith, COLORIMETRIC METHOD FOR DETERMINATION OF SUGARS AND RELATED SUBSTANCES, Analytical Chemistry, 28 (1956) 350-356.

[124] B.D. McCloskey, H.B. Park, H. Ju, B.W. Rowe, D.J. Miller, B.D. Freeman, A bioinspired fouling-resistant surface modification for water purification membranes, Journal of membrane science, 413 (2012) 82-90.

[125] J.T. Arena, B. McCloskey, B.D. Freeman, J.R. McCutcheon, Surface modification of thin film composite membrane support layers with polydopamine: Enabling use of reverse osmosis membranes in pressure retarded osmosis, Journal of Membrane Science, 375 (2011) 55-62.

[126] O.H. Lowry, N.J. Rosebrough, A.L. Farr, R.J. Randall, Protein measurement with the Folin phenol reagent, J biol Chem, 193 (1951) 265-275.

[127] M. DuBois, K.A. Gilles, J.K. Hamilton, P.A.T. Rebers, F. Smith, Colorimetric method for determination of sugars and related substances, Analytical chemistry, 28 (1956) 350-356.

[128] P.J. Evans, M.R. Bird, A. Pihlajamäki, M. Nyström, The influence of hydrophobicity, roughness and charge upon ultrafiltration membranes for black tea liquor clarification, Journal of Membrane Science, 313 (2008) 250-262.

[129] H.H.P. Fang, X.L. Shi, Pore fouling of microfiltration membranes by activated, Journal of Membrane Science, 264 (2005) 161-166.

[130] Y.L. He, P. Xu, C.J. Li, B. Zhang, High-concentration food wastewater treatment by an anaerobic membrane bioreactor, Water Research, 39 (2005) 4110-4118.

[131] L. Jin, S.L. Ong, H.Y. Ng, Comparison of fouling characteristics in different pore-sized submerged ceramic membrane bioreactors, Water research, 44 (2010) 5907-5918.

[132] S. Lee, C. Boo, M. Elimelech, S. Hong, Comparison of fouling behavior in forward osmosis (FO) and reverse osmosis (RO), Journal of Membrane Science, 365 (2010) 34-39.

[133] S. Rosenberger, C. Laabs, B. Lesjean, R. Gnirss, G. Amy, M. Jekel, J.C. Schrotter, Impact of colloidal and soluble organic material on membrane performance in membrane bioreactors for municipal wastewater treatment, Water Research, 40 (2006) 710-720.

[134] F. Meng, F. Yang, B. Shi, H. Zhang, A comprehensive study on membrane fouling in submerged membrane bioreactors operated under different aeration intensities, Separation and Purification Technology, 59 (2008) 91-100.

[135] I.J. Kang, S.H. Yoon, C.H. Lee, Comparison of the filtration characteristics of organic and inorganic membranes in a membrane-coupled anaerobic bioreactor, Water Research, 36 (2002) 1803-1813.

[136] L. Fu, N.A. Hashim, Y. Liu, M.R.M. Abed, K. Li, Progress in the production and modification of PVDF membranes, Journal of Membrane Science, 375 (2011) 1-27.

[137] N. Pezeshk, R.M. Narbaitz, More fouling resistant modified PVDF ultrafiltration membranes for water treatment, Desalination, 287 (2012) 247-254.

[138] J. Xiao, W. Xu, D.Y. Wang, D.W. Choi, W. Wang, X.L. Li, G.L. Graff, J. Liu, J.G. Zhang, Stabilization of Silicon Anode for Li-Ion Batteries, J Electrochem Soc, 157 (2010) A1047-A1051.

[139] F. Li, L. Li, X. Liao, Y. Wang, Precise pore size tuning and surface modifications of polymeric membranes using the atomic layer deposition technique, Journal of membrane science, 385 (2011) 1-9.

[140] T.H. Bae, T.M. Tak, Effect of TiO2 nanoparticles on fouling mitigation of ultrafiltration membranes for activated sludge filtration, Journal of Membrane Science, 249 (2005) 1-8.

[141] D.J. Miller, S. Kasemset, L. Wang, D.R. Paul, B.D. Freeman, Constant flux crossflow filtration evaluation of surface-modified fouling-resistant membranes, Journal of Membrane Science, 452 (2014) 171-183.

[142] Y. Masuda, T. Ohji, K. Kato, Tin oxide nanosheet assembly for hydrophobic/hydrophilic coating and cancer sensing, ACS applied materials & interfaces, 4 (2012) 1666-1674.

[143] Q. Liu, X. Wu, B. Wang, Q. Liu, Preparation and super-hydrophilic properties of TiO 2/SnO 2 composite thin films, Materials Research Bulletin, 37 (2002) 2255-2262.

[144] S. Nataraj, R. Schomäcker, M. Kraume, I.M. Mishra, A. Drews, Analyses of polysaccharide fouling mechanisms during crossflow membrane filtration, Journal of Membrane Science, 308 (2008) 152-161.

[145] X.-M. Wang, T.D. Waite, Impact of gel layer formation on colloid retention in membrane filtration processes, Journal of Membrane Science, 325 (2008) 486-494.

[146] W.J.C. Van de Ven, K. van't Sant, I.G.M. Pünt, A. Zwijnenburg, A.J.B. Kemperman, W.G.J. Van der Meer, M. Wessling, Hollow fiber dead-end ultrafiltration: Influence of ionic environment on filtration of alginates, Journal of Membrane Science, 308 (2008) 218-229.

[147] K.S. Katsoufidou, D.C. Sioutopoulos, S.G. Yiantsios, A.J. Karabelas, UF membrane fouling by mixtures of humic acids and sodium alginate: fouling mechanisms and reversibility, Desalination, 264 (2010) 220-227.

[148] K. Listiarini, L. Tan, D.D. Sun, J.O. Leckie, Systematic study on calcium–alginate interaction in a hybrid coagulation-nanofiltration system, Journal of membrane science, 370 (2011) 109-115.

[149] Y. Mo, K. Xiao, Y. Shen, X. Huang, A new perspective on the effect of complexation between calcium and alginate on fouling during nanofiltration, Separation and purification technology, 82 (2011) 121-127.

[150] H.H.P. Fang, X. Shi, Pore fouling of microfiltration membranes by activated sludge, Journal of Membrane Science, 264 (2005) 161-166.